USE OF WIRE MESH-EPOXY COMPOSITE FOR STRENGTHENING CONCRETE BEAMS

ISMAIL M. I. QESHTA

FACULTY OF ENGINEERING

UNIVERSITY OF MALAYA

2014

USE OF WIRE MESH-EPOXY COMPOSITE FOR
STRENGTHENING CONCRETE BEAMS

ISMAIL M. I. QESHTA

DISSERTATION SUBMITTED IN FULFILMENT OF THE

REQUIREMENTS FOR THE DEGREE OF MASTER OF

ENGINEERING SCIENCE

FACULTY OF ENGINEERING

UNIVERSITY OF MALAYA

KUALA LUMPUR

2014

UNIVERSITY OF MALAYA
ORIGINAL LITERARY WORK DECLARATION

Name of Candidate: ISMAIL M. I. QESHTA
Registration/Matrix No: KGA120021
Name of Degree: Master of Engineering Science
Title of Project Paper/Research Report/Dissertation/Thesis ("this Work"):
USE OF WIRE MESH-EPOXY COMPOSITE FOR STRENGTHENING CONCRETE BEAMS

Field of Study: Structural Engineering & Materials
I do solemnly and sincerely declare that:

1) I am the sole author/writer of this Work;
2) This Work is original;
3) Any use of any work in which copyright exists was done by way of fair dealing and for permitted purposes and any excerpt or extract from, or reference to or reproduction of any copyright work has been disclosed expressly and sufficiently and the title of the Work and its authorship have been acknowledged in this Work;
4) I do not have any actual knowledge nor do I ought reasonably to know that the making of this work constitutes an infringement of any copyright work;
5) I hereby assign all and every rights in the copyright to this Work to the University of Malaya ("UM"), who henceforth shall be owner of the copyright in this Work and that any reproduction or use in any form or by any means whatsoever is prohibited without the written consent of UM having been first had and obtained;
6) I am fully aware that if in the course of making this Work I have infringed any copyright whether intentionally or otherwise, I may be subject to legal action or any other action as may be determined by UM.

Candidate's Signature   Date 29.December.2014

Subscribed and solemnly declared before,

Witness's Signature   Date 29.December.2014
Name:
Designation:

ABSTRAK

Ada beberapa jenis teknik yang telah dicadangkan untuk menguatkan struktur konkrit. Namun, masalah utama yang dihadapi oleh jurutera awam dan penyelidik adalah menghasilkan teknik penguatan yang kos efektif, tahan lama dan bertindak dengan berkesan.

Tujuan kajian ini adalah untuk mengkaji keberkesanan penggunaan jaringan wayar-epoxy untuk menguatkan rasuk konkrit. Komposit ini terdiri daripada jaringan wayar dan resin epoxy. Pada peringkat awal kajian ini, rasuk konkrit biasa telah dikuatkan dengan dua matriks ujikaji. Tujuan utama kajian pada peringkat ini adalah untuk mengkaji kesan bilangan lapisan jarngan wayar ke atas sifat rasuk konkrit. Sebagai perbandingan rasuk konkrit juga telah dikuatkan dengan lapisan karbon fibre dan juga hybrid Antara jaringan wayar –epoxy dan karbon fibre. Hasil kajian menunjukkan penggunaan komposit jaringan wayar-epoxy adalah cara yang berkesan untuk meningkatkan kekuatan fleksur rasuk konkrit. Menambahkan lapisan jaringan wayar memberi kesan peningkatan kekuatan fleksur, sifat retakan dan juga penyerapan tenaga. Penggunaan empat lapisan jaringan wayar didapati adalah optimum. Berdanding dengan karbon fibre, komposit jaringan wayar-epoxy adalah lebih efisien dari segi kekuatan fleksur dan lebih duktil. Tambahan lagi, didapati bahawa rasuk konkrit digabungkan dengan hybrid wayar-epoxy dan karbon fibre memberikan kadar penyerapan tenaga yang lebih tinggi berbanding hanya menggunakan karbon fibre.

Kajian terhadap kesan konfigurasi jaringan wayar-epoxy menunjukkan bahawa semua jenis konfigurasi memberi peningkatan kekuatan fleksur. Namun peningkatan dalam penyerapan tenaga bagi rasuk bergabung adalah tinggi. Di samping itu, spesimen dengan kelebaran komposit yang lebih besar menunjukkan sifat yang lebih baik dari segi penyerapan tenaga.

Teknik penguatan ini juga telah digunakan pada rasuk konkrit bertetulang. Matriks kajian terdiri daripada lima rasuk. Satu rasuk telah dijadikan spesimen kawalan. Empat lagi rasuk telah dikuatkan dengan komposit wayar-epoxy, laminat wayar-epoxy dan juga hibrid wayar-epoxy dan karbon fibre. Empat lapisan wayar digunakan wayar-epoxy dalam semua spesimen. Kajian menunjukkan semua rasuk menunjukkan peningkatan dari segi ketegangan, beban untuk retakan pertama dan kebolehan menampung beban. Secara amnya, kesimpulan boleh dibuat bahawa wayar-epoxy adalah satu bahan baru yang boleh digunakan untuk tujuan menambah kekuatan dan pembaik pulihan.

ABSTRACT

A number of techniques and materials have been proposed for strengthening reinforced concrete (RC) structures. However, the main concern of civil engineers and researchers is to develop an optimum strengthening scheme with materials that are cost effective, durable, and that behave satisfactorily.

This study aims to investigate the effectiveness of using a wire mesh-epoxy composite for strengthening concrete beams. This composite consists of wire mesh layers and epoxy resin. In the first step of this study, plain concrete beams were bonded with a different number of wire mesh layers and epoxy resin. As a comparison, the concrete beams were also bonded with a carbon fibre sheet as well as a hybrid of wire mesh-epoxy and carbon fibre. The test results show that the use of wire mesh with epoxy is an efficient way to improve the flexural performance of concrete beam specimens. The increase in wire mesh layers significantly enhances the flexural strength, cracking behaviour and energy absorption capability. Using four layers of wire mesh was found to be optimum in the composite. In comparison with carbon fibre, wire mesh-epoxy composite is more efficient in flexural strength and ductility. In addition, it was found that a concrete beam bonded with a hybrid wire mesh-epoxy-carbon fibre composite has significantly more energy absorption capability compared to specimens bonded with only carbon fibre.

A study on the effect of different configurations of wire mesh-epoxy composite (different wire mesh-epoxy widths) on the flexural behaviour of concrete beams also showed that the wire mesh-epoxy composite for all types of configuration increases the flexural strength. However, the increase in energy absorption of the bonded beams was remarkable. In addition, specimens with large composite width showed better behaviour with respect to the energy absorption capability.

The flexural behaviour of RC beams strengthened with wire mesh-epoxy composite was also investigated in this study and was compared with RC beams strengthened with a carbon fibre sheet. In addition, the structural performance of a beam strengthened using a hybrid of wire mesh-epoxy and carbon fibre sheet was investigated. The results showed that the use of wire mesh-epoxy composite provides considerable enhancement in the performance of the strengthened beams. Compared to carbon fibre, the strengthened beams showed more improvement in the first crack load, stiffness and yield strength. In addition, the use of hybrid wire mesh-epoxy-carbon fibre composite indicated better post-yield behaviour and prevented the debonding of the carbon fibre sheet. In general, it can be concluded that wire mesh-epoxy composite could be a new material for the strengthening and retrofitting purposes.

ACKNOWLEDGEMENTS

DEDICATION

To my loving Mum and Dad

To my dear brothers and sisters

TABLE OF CONTENTS

Title	Page

CHAPTER 1 INTRODUCTION

CHAPTER 2 LITERATURE REVIEW

CHAPTER 3 EXPERIMENTAL PROGRAMME

CHAPTER 4 RESULTS AND DISCUSSION

APPENDIX B ANCILLARY TEST RESULTS

**APPENDIX C STRAINS IN STEEL, WIRE MESH-EPOXY
AND CFRP OF RC BEAMS**

LIST OF TABLES

LIST OF FIGURES

LIST OF ABBREVIATIONS AND SYMBOLS

Abbreviation/Symbol	Phrase
E_{frp}	Elastic modulus of FRP material
E_m	Elastic modulus of matrix
V_m	Volume fraction of matrix
E_f	Elastic modulus of fibres
V_f	Volume fraction of fibres
ε_{fd}	Debonding strain of externally bonded FRP
$f_c{'}$	Specified compressive strength of concrete
n	Number of plies of FRP reinforcement
E_f	Tensile modulus of elasticity of FRP
t_f	Nominal thickness of one ply of FRP reinforcement
ε_{fu}	Design rupture strain of FRP reinforcement
l_{df}	Development length of FRP system

CHAPTER 1

INTRODUCTION

1.1 General

Existing reinforced concrete (RC) structures are in need of upgrading and retrofitting for many different reasons, such as an increase in the vehicular load, corrosion of internal steel reinforcement and to fulfil the current design standards for serviceability requirements. Performing a strengthening and retrofitting programme is more reasonable compared to the demolition and rebuilding of structures when considering the disruption of services, labour and cost of materials as well as the effect on other facilities.

Different strengthening materials have been proposed and used for the strengthening of RC structures. A number of strengthening materials have been used for strengthening, such as steel, fibre reinforced polymer (FRP) and ferrocement laminates (Al-Kubaisy and Jumaat, 2000; Bakis et al., 2002; Jones et al., 1988). Despite the numerous reported studies investigating the behaviour of RC members using different materials, the strengthened members still have undesirable performance compared to unstrengthened members. These problems include the brittle and premature failure modes, loss of ductility and corrosion of the strengthening materials (Grace et al., 1999; Saadatmanesh and Ehsani, 1991). Therefore, further investigation for new or modified materials is necessary for achieving the optimum behaviour of strengthened RC members. This study presents a new composite of wire mesh and epoxy as well as carbon fibre reinforced polymer (CFRP) for strengthening RC beams. The following sections discuss the different strengthening techniques as well as the problems and concerns. Finally, the objectives, scope of work and content of the thesis are described.

1.2 Strengthening techniques and materials

The two main strengthening techniques are external bonding of reinforcement (EBR) and near surface mounted (NSM) (Yost et al., 2007). The EBR technique involves bonding the material (sheet or plate) to the soffit of the beams using a strong adhesive. The EBR technique has a number of advantages, such as ease of application and inspection during service life and significant improvement in flexural capacity and cracking behaviour. The NSM technique involves making grooves in the soffits of beams and embedding the reinforcement (rods or strips) in the grooves with adhesives. The NSM has some advantages over the EBR technique, such as good durability performance and a lower possibility of debonding. In addition, different materials for strengthening are currently used. Although, initially, steel plates were used for strengthening, in the last 20 years, the behaviour of FRP strengthened RC members has been extensively investigated. Despite the high cost of FRP material compared to steel, the most attractive advantage is its high strength to weight ratio and good durability properties. In addition, ferrocement laminates have been used for the strengthening of RC members. The ferrocement laminate has a relatively lower cost than the steel and FRP materials. Beams strengthened using ferrocement laminates have shown a significant improvement in flexural capacity and cracking behaviour.

1.3 Problems and concerns

FRP is currently the most widely used material for strengthening. However, beams strengthened using FRP suffer a loss of ductility (Grace et al., 1999; Ritchie et al., 1991; Saadatmanesh and Ehsani, 1991). This reduction in ductility is attributed to the mechanical properties of the FRP materials. The FRP material has a linear stress-strain relationship up to failure. It does not have a yield plateau as in the case of ductile

materials (e.g. steel). Attempts to overcome the ductility issue have recently been performed by introducing the hybrid FRP strengthening material (Attari et al., 2012; Grace et al., 2002; Grace et al., 2003; Wu et al., 2007). The major drawback of hybrid FRP strengthening is the high cost of the different FRP materials and the fact that hybrid strengthening is still not included in the design standards due to the lack of reported studies (Hawileh et al., 2014).

However, by comparing the advantages of FRP material with the other materials, such as steel and ferrocement laminates, it is found that they also have some drawbacks. The involvement of wire mesh in the form of ferrocement laminates has shown its potential use for enhancing the performance of RC members (Al-Kubaisy and Jumaat, 2000; Paramasivam et al., 1994, 1998). However, ferrocement laminates are relatively thick. Thus, maintaining the composite action and preventing debonding of the laminate is also a concern. As a result, engineers and researchers need to seek alternative materials for achieving the optimum behaviour of strengthened beams. Therefore, for compensating the drawbacks for ductility performance, cost, debonding and weight of strengthening materials, in this study, a new composite of wire mesh and epoxy was studied.

1.4 Objectives

The main aim of this study is to provide a new type of strengthening material and to investigate its performance for the strengthening of plain and RC beams. In this research work, a composite of welded wire mesh and epoxy resin was used as a composite laminate.

An extensive experimental study is conducted using this type of new strengthening material. The sub-objectives of the study are as follows:

1. To develop a composite laminate of wire mesh and epoxy resin.

2. To study the flexural behaviour of concrete beams bonded with wire mesh-epoxy composite.

3. To compare the performance of wire mesh-epoxy composite and CFRP in the strengthening of concrete beams.

4. To develop a new method for strengthening purposes using a hybrid of wire mesh-epoxy and CFRP.

1.5 Scope of work

The experimental investigation consisted of conducting flexural tests of plain concrete beams bonded with composite materials and strengthening and testing of RC beams. The plain concrete beams were bonded with a wire mesh-epoxy composite, CFRP and hybrid wire mesh-epoxy-carbon fibre composite. The aim of this study was to establish the method of preparation and application of new composites to the concrete surface, to ensure that the type of epoxy used was compatible with the wire mesh and to investigate the behaviour of the concrete specimens bonded with the composite. The number of wire mesh layers in the composite varied from 1 to 5. The specimens were tested in flexure until failure. The percentage increase in flexural capacity and energy absorption related to the plain concrete control beam specimen is discussed. The behaviour of specimens bonded with the new composite was compared with the specimens bonded with CFRP sheet. Five RC beams were prepared in the testing matrix. Strengthening using wire mesh-epoxy composite, CFRP and hybrid wire mesh-epoxy-carbon fibre composite was performed on beams. The load-deflection behaviour, stiffness, energy absorption, and strain and cracking behaviour of the strengthened beams are discussed.

1.6 Thesis content

This thesis is divided into five chapters. Chapter 1 provides an introduction and specifies the research needs, objectives and scope of work. A comprehensive literature review of the research studies performed on the behaviour of RC beams strengthened with different materials is presented in chapter 2. Also, an overview of the three main strengthening materials (i.e. steel, FRP and wire mesh) is given. The experimental preparation, specimens fabrication and testing is presented in chapter 3. Chapter 4 presents the discussion of the test results. The discussion of the results is divided into two main sections, the first section is for the flexural test of the plain concrete beams and section two is for the RC beam test results. Finally, chapter 5 presents the conclusion and recommendations.

CHAPTER 2

LITERATURE REVIEW

2.1 General

Several strengthening schemes are reported in literature for strengthening and rehabilitation of RC structures. The two main strengthening techniques currently used for strengthening are the external bonding (EB) and near surface mounting (NSM). In addition, several strengthening materials have been used. The three main materials are the steel, fibre reinforced polymer (FRP) and wire mesh in the form of ferrocement laminate. This chapter provides a brief summary of the existing information of strengthening materials and their effect on the performance of RC beams. First, a general explanation of the properties of each strengthening material (i.e. steel, FRP and wire mesh) is presented. Then the behaviour of RC beams externally bonded using each material is discussed. The advantages and drawbacks found in literature for each strengthening material are also discussed.

2.2 Materials used for strengthening

2.2.1 General

The properties of different materials used for strengthening have a significant effect on the behaviour of strengthened beams. There are three main strengthening materials; namely, steel, FRP and ferrocement. In the following sections, a description of the characteristics of these materials is presented.

2.2.2 Steel

Steel is a primary constituent of RC structures. Steel alloy mainly consists of iron and carbon. Other elements, which may exist in small amounts, are manganese, phosphorous, silicon and copper. Depending on the percentage of carbon, steel is classified into different categories in RC design. The two main categories are mild steel and high yield steel (hot rolled or cold worked) (Mosley et al., 2007). The stress-strain curve of steel has two main stages, linear elastic and plastic. The steel sample behaves linearly under tensile load until reaching a point where the material becomes plastic and the strain rapidly increases until the final failure. The point at which the steel becomes no more elastic is called the yield point. Figure 2.1 shows a typical stress-strain relationship for steel. It should be noted that the curve might slightly vary depending on the manufacturing process and carbon content. Steel has a modulus of elasticity value of approximately 200 GPa. The use of steel in structural strengthening and retrofitting is in the form of steel plates of different thicknesses. The thickness of the steel plates usually used for strengthening is in the range of 1.5–10 mm (Adhikary and Mutsuyoshi, 2002; Grace et al., 2003; Jones et al., 1988; Jumaat and Alam, 2009; MacDonald and Calder, 1982; Raithby, 1982; Swamy et al.,1987). The steel plates are usually attached to the soffits of the beams using epoxy adhesive, bolts (or screws), or epoxy and bolts together (Grace et al., 2003; Jones et al., 1988; Swamy et al., 1987). Figure 2.2 shows a reinforced concrete bridge strengthened using a steel plate. In addition, the strengthening of RC beams using near surface mounted (NSM) steel bars was recently reported by Almusallam et al. (2013).
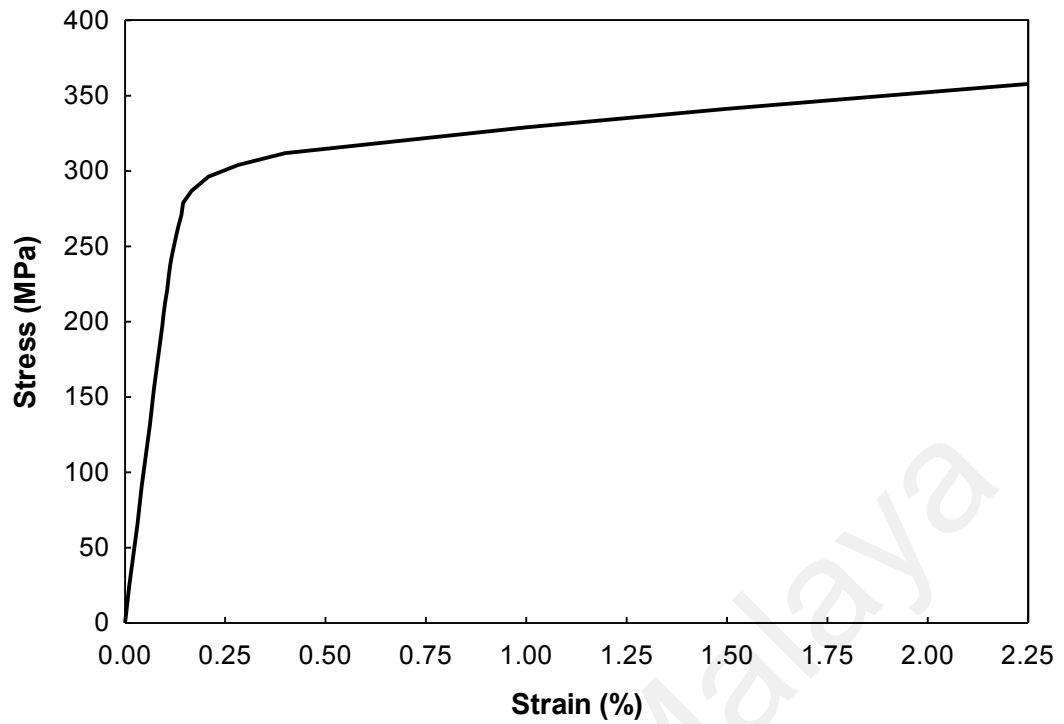
Figure 2.1: Typical stress-strain relationship of steel (Grace et al., 2003)

Figure 2.2: RC bridge strengthened using steel plate (Roads & Maritime- New South Wales, 2014)

2.2.3 Fibre Reinforced Polymer (FRP)

Fibre reinforced polymer (FRP) is a composite material. In concept, a composite material is a material that consists of a combination of two or more materials to form a new material with excellent and useful properties compared to the individual constituent materials alone (Campbell, 2010). The two main constituents of composite material are the reinforcement and the matrix. The reinforcement usually provides the strength and stiffness, whereas the matrix provides a transmission of the load between fibres by the shear stresses and protects the fibres from abrasion and other environmental effects. In FRP, the reinforcement is the fibres with high strength and the matrix is a polymeric material. Figure 2.3 shows the basic components of FRP materials.

FIBRES   POLYMER   FRP
            MATRIX
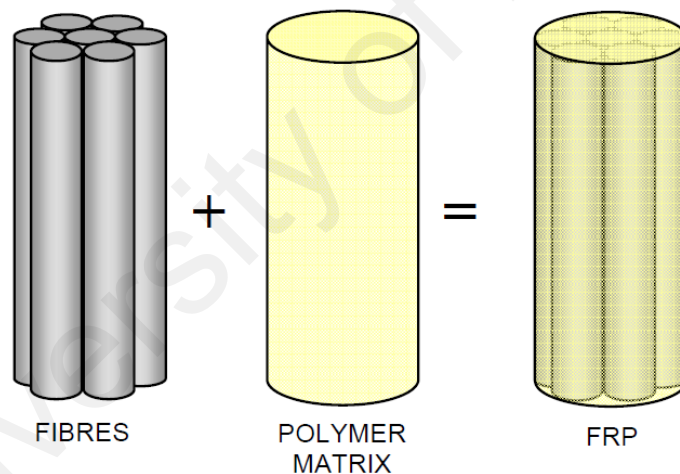
Figure 2.3: Basic components of FRP material (ISIS Canada Educational Module, 2006)

2.2.3.1 Fibres

In civil engineering applications, fibres with a high length to diameter ratio are used. The most common types of FRP used in civil engineering are the glass (GFRP), aramid (AFRP) and carbon (CFRP). The selection criteria of the types of fibre depend on the target strength, stiffness, cost and availability of materials. Figure 2.4 shows carbon

fibre fabric used for strengthening RC structures. The common FRP systems available on the market and suitable for strengthening are wet layup, prepreg, and procured (ACI Committee 440, 2008). The wet layup systems consist of dry fibres impregnated with resin. The dry fibres are either unidirectional or multidirectional. The processes of curing the dry fibres in resin and bonding the fibres to the concrete surface are both performed in place. Prepreg systems are saturated at the manufacturer's factory. The pre-impregnated fibres are applied to the concrete surface with or without additional adhesive. The procured systems are prepared at the manufacturer's factory away from the construction site. An adhesive is used for bonding the FRP material to the concrete surface.
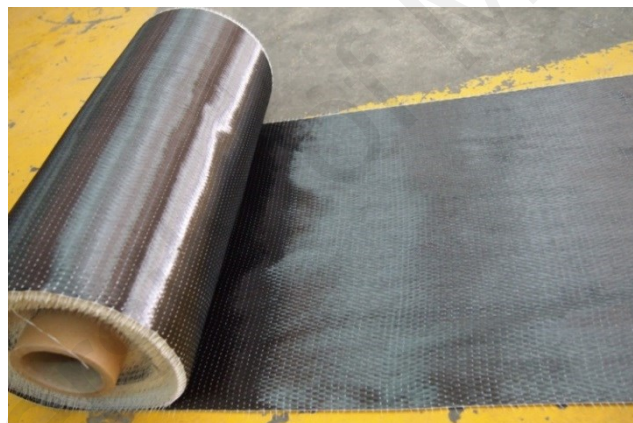
Figure 2.4: CFRP used for strengthening

2.2.3.2 Resins

Resins are generally grouped into two major categories, thermoplastics and thermosetting. Thermoplastics have the ability to soften and harden with an increase or decrease in temperature. Thermosets do not have the ability to melt and reshape at high temperatures and pressure (GangaRao et al., 2007). Thermosets are used in most current civil engineering applications since they have good chemical resistance, good creep

resistance and thermal stability. Many different types of resins are used for FRP strengthening systems. The two main resin types are the saturating resins and adhesives (ACI Committee 440, 2008). Saturating resins are used for the wet layup FRP systems while adhesives are usually used for bonding precured FRP systems.

2.2.3.3 FRP mechanical properties

FRP materials have a linear stress-strain behaviour up to failure. They do not exhibit any plastic behaviour as in the case of steel. The properties of FRP depend on certain factors, such as fibres and matrix proportions, properties of the individual constituents, fibre orientation in the matrix and manufacturing method. Figure 2.5 shows the typical stress-strain relationships of different types of FRP and steel. The modulus of elasticity of aramid and glass fibre is less than that of steel, whereas carbon fibre has a modulus value equal or more than the steel. The tensile elastic modulus of unidirectional FRP can be predicted using the equation called the "rule of mixtures", which is expressed as follows (Campbell, 2010):

$$E_{frp} = E_m \, . \, V_m + E_f \, . \, V_f \qquad\qquad \text{Equation 2.1}$$

Where V_m and V_f are the volume fractions of the matrix and the fibres, respectively. The volume fraction is defined as the volume of fibres or matrix divided by the total volume of FRP. E_m is the elastic modulus of the matrix and E_f is the elastic modulus of the fibres.

The FRP response under tensile load depends on the strain at failure of the fibres and matrix, as well as their volume fractions. The four cases of failure of FRP can be explained as follows (ISIS Canada Educational Module, 2006):

- The failure strain of the matrix is less than the failure strain of the fibres and the volume fraction of the fibres is small (less than 0.1). The failure of the matrix controls the failure of the FRP.

- When the failure strain of the matrix is less than the failure strain of the fibres and the volume fraction of the fibres is large, the failure of the FRP is governed by the failure of the fibres as the fibres carry most of the load.

- The failure strain of the matrix is greater than the fibres and the volume fraction of the fibres is small. The failure of the matrix controls the failure of the FRP.

- When the failure strain of the matrix is greater than the fibres and the fibre volume fraction is large, the failure of the FRP is governed by the failure of the fibres.

It should be noted that in most civil engineering applications, the volume fraction of fibres is usually large (greater than 0.1), and, hence, the effect of the matrix (or resin) on the failure of the FRP is insignificant.
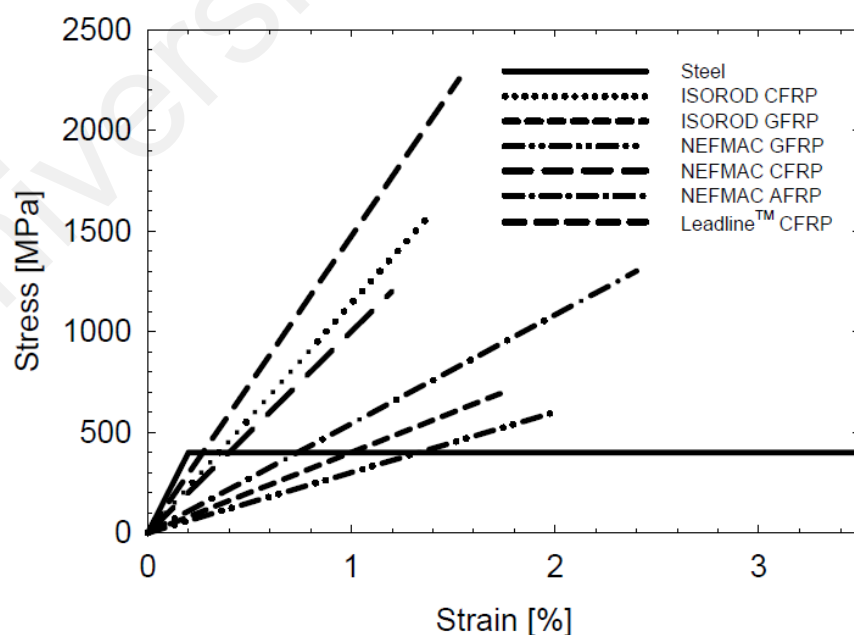
Figure 2.5: Typical stress-strain relationships of different FRP materials and steel (ISIS Canada Educational Module, 2006)

2.2.4 Hybrid FRP

The concept of hybrid composite was first introduced by Hayashi (1972). Since then, the concept has been extensively investigated in the material science field and has been widely applied in aerospace, and, recently, in the upgrading of civil structures. Many advantages are obtained by using the hybrid composites. These advantages include a significant enhancement in the initial stiffness, compressive strength, post-yield ductility and energy absorption. The hybrid composite materials consist primarily of low elongation (LE) and high elongation (HE) materials. As the hybrid is subjected to uniaxial force, the low elongation fibres fracture earlier, followed by load transfer to the high elongation fibres, which continue carrying the load until reaching their ultimate failure strain (Fukuda andChou, 1982). Figure 2.6 shows the normalized stress-strain relationship of a hybrid composite.

Hayashi (1972) proposed that the properties of the hybrid can be obtained by doing a simple summation of the separate properties of the hybrid components. This idea was then extensively studied by Bunsell and Harris (1974). Two sets of samples were performed, unbonded and bonded samples. It was found by the researchers that, initially, the hybrid composite behaved similar to the behaviour proposed by Hayashi (1972) and predicted by the "rule of mixtures" until the first fracture of high modulus fibres. In addition, the first fracture was observed to occur at a larger extension than the fracture of carbon fibres when tested alone due to the residual stresses being induced in the carbon fibre. In the hybrid, which has unbonded layers, the load-strain curve displayed a load drop at the point of first fracture of the fibres. The curve then showed an increase in load, which is attributed to the load being transferred to the glass fibres until its final breaking strain. The load-strain curve in the bonded fibres showed the load

sharing mechanism from the beginning of the test. It was concluded by the researchers that designing a hybrid composite with different ratios can be done in order to obtain targeted characteristics that are important in many manufacturing and civil engineering aspects. Phillips (1976) later extended the investigation to include some other properties of hybrid FRP, such as, impact and fatigue. The results proved the existence of a load sharing mechanism in the hybrid, which was noticed by Hayashi (1972) and Bunsell and Harris (1974). The failure of the hybrid was progressive unlike the sudden breaking of fibres when tested separately. In addition, the fatigue life and impact strength are higher than that of fibres when tested separately. Furthermore, Manders and Bader (1981a, 1981b) investigated the effect of different constituent arrangements and dispersion ratios on the hybrid properties. The authors found that stiffer carbon fibres when finely dispersed with a lower volume in the hybrid give a higher failure strain.

Generally, there are two main methods for making hybrid composites (Bunsell and Harris, 1974). The first method is mingling the fibres while the second method is laminating the fibre sheets from each type to form the hybrid. The arrangement of different fibre sheets or laminates may differ depending on the desired behaviour of the resulted hybrid composite. The second aforementioned method is commonly applied in strengthening structural elements. The hybrid may be a combination of bonded carbon and glass fibres (Bunsell and Harris, 1974), or carbon fibres having different elongation and stiffness values (Wu et al., 2007). In addition, some researchers have successfully used a combination of high elongation, medium elongation and low elongation fibres to form hybrid composites for the strengthening of RC beams (Grace et al., 2002).
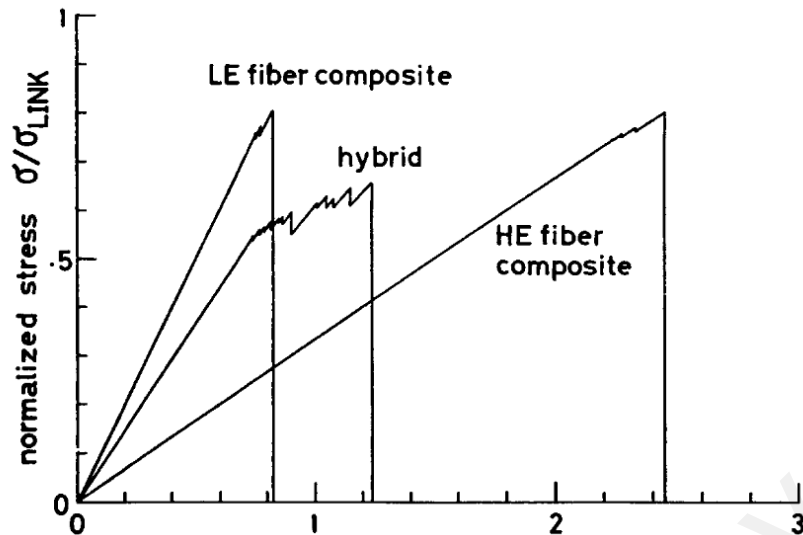
Figure 2.6: Normalized stress-strain relationships of hybrid and non-hybrid composites (Fukuda and Chou, 1982)

2.2.5 Wire mesh for ferrocement laminates

The wire mesh types commonly used in the construction field have square or hexagonal openings. Meshes with hexagonal openings are also called "chicken wire". The square opening meshes are more effective than hexagonal as the wires are oriented in the principal directions of the stresses. However, hexagonal meshes are useful for doubly curved structural elements. The square mesh wires are connected either by welding or weaving. Figure 2.7 shows different types of wire mesh used for ferrocement. The welded meshes consist of longitudinal and transverse wires welded together. The overall thickness of welded wire mesh is equal to the diameters of two single wires. In the woven mesh, the longitudinal wires are woven around the transverse wires. The thickness of woven mesh may vary depending on the weave tightness (may reach up to three wire diameters). The wire meshes are usually galvanized to be protected against rusting. However, galvanization reduces the tensile strength and may make the mesh reinforcement more brittle. The common meshes usually used in the ferrocement industry are made of galvanized steel (ACI Committee 549, 1988).

The mechanical properties of wire mesh vary depending on the types of mesh and the manufacturing process. The welded wire meshes have a larger elastic modulus than the woven meshes. Welding usually reduces the tensile strength of the mesh wires. The ACI Committee 549 (1988) specified the minimum values for the yield strength and elastic modulus of the welded and woven meshes to be used in ferrocement. The yield strength, longitudinal and transverse elastic moduli of mesh should have minimum values of 450 MPa, 200 GPa and 200 GPa, respectively. Whereas, the woven square mesh should have minimum values of yield strength, longitudinal and transverse moduli of 450 MPa, 138 GPa and 165 GPa, respectively. Figure 2.8 shows the stress-strain relationships of the wire mesh samples (welded and woven). The ferrocement laminates are fabricated by embedding the multiple layers of wire mesh in a cement matrix. The matrix consists primarily of Portland cement, water and fine aggregate (ACI Committee 549, 1988). The matrix usually involves 95% of the volume of ferrocement. The behaviour of ferrocement in direct tension and flexure is fully carried by the wire mesh reinforcement (Romualdi, 1987). Therefore, the tensile and flexural strengths are mainly dependent on the mechanical properties and cross-sectional dimensions of the reinforcement. Figure 2.9 shows an RC beam strengthened using ferrocement laminate after failure.
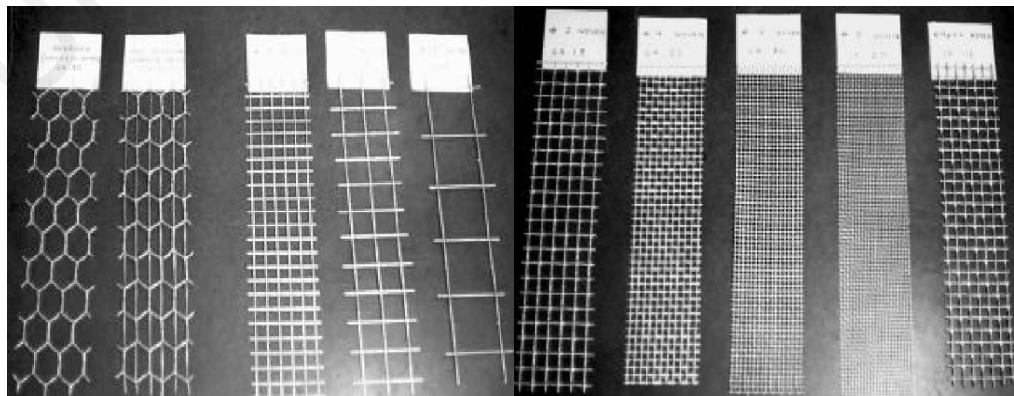
Figure 2.7: Different wire mesh types used in ferrocement (ACI Committee 549, 1988)
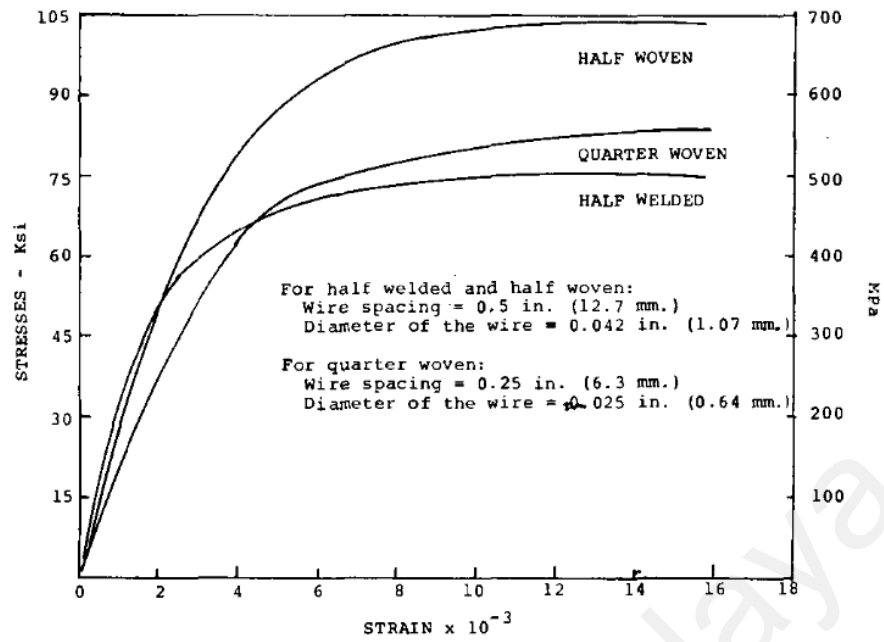
Figure 2.8: Stress-strain relationships of different samples of wire mesh used in ferrocement (ACI Committee 549, 1988)
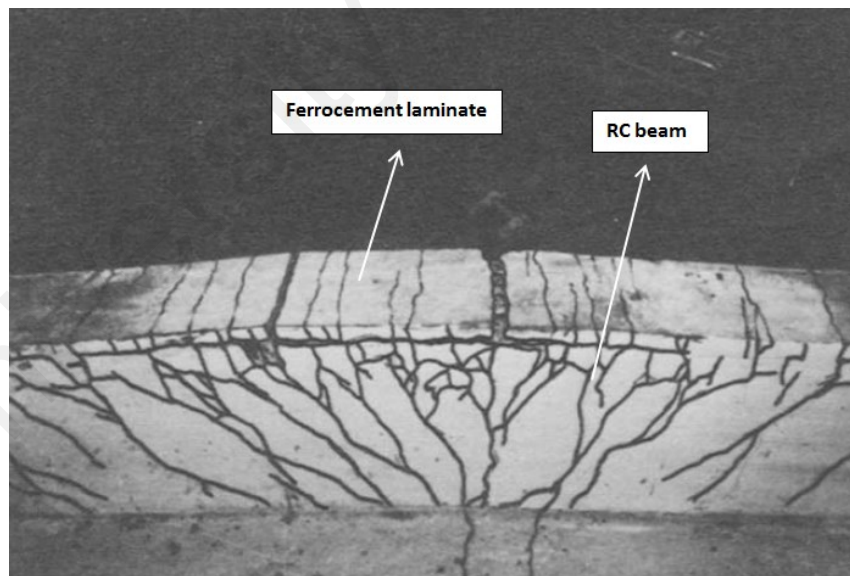
Figure 2.9: RC beam strengthened using ferrocement laminate after failure (Paramasivam et al., 1994)

2.2.6 Other materials for strengthening and repair

In addition to the aforementioned materials investigated extensively for strengthening and retrofitting, a number of other materials have been studied. These materials have shown interesting and valuable results with respect to load carrying capacity, stiffness and ductility.

Diab (1998) used sprayed fibrous concrete for strengthening RC beams. In some beams, steel reinforcement was added to form a larger cross-section of the repaired beams. The researcher found that the use of metallic glass ribbon fibres with the concrete improved the cracking behaviour and ultimate strength of the beams. In addition, the tensile stresses in the internal reinforcement decreased with the addition of fibres with concrete.

A number of studies reported the effectiveness of using sprayed FRP for strengthening and retrofitting (Banthia et al., 2002; Lee, 2004; Lee et al., 2005, 2008; Lee and Hausmann, 2004). The sprayed FRP consists of chopped fibres embedded in a polymeric matrix. The fibres are randomly oriented in the matrix. This material has some advantages, such as its application is easy and quickly, does not require skilful labourers and requires relatively little surface preparation (Lee et al., 2008). Lee and Hausmann (2004) studied the effect of coating thickness, fibre type, fibre length and fibre volume on the ductility and load carrying capacity of sprayed FRP strengthened beams. They found that the thicker coating gives better ductility. In addition, the optimum fibre length and volume were found to be 23 mm and 30%, respectively, for better improvement in strength and energy absorption.

Xing et al. (2010) strengthened RC beams using a U-jacket of steel wire mesh and polymeric mortar. The wire mesh diameter was 3.2 mm. The polymeric mortar has the

capability of hardening within few hours. It was found that all strengthened beams failed in the debonding of the composite after achieving an increase in load carrying capacity and reasonable ductility.

2.3 Behaviour of strengthened RC beams

2.3.1 General

The flexural behaviour of RC beams externally strengthened with different strengthening techniques has been extensively investigated. These techniques involved the use of different materials, such as steel plates, FRP and wire mesh in the form of ferrocement. The following sections present a discussion of the behaviour of RC beams externally strengthened using different materials. In addition, the problems associated with each material are discussed.

2.3.2 Behaviour of RC beams strengthened using steel plates

The use of steel plates for flexural strengthening of RC structures is one of the earliest methods adopted in the last century in the structural upgrading field. The use of steel plates began in the 1960s (Kajfasz, 1967; Lerchental, 1967) and it was adopted in many countries thereafter. The following are some advantages, which increased the tendency to use steel plates in the strengthening and rehabilitation of RC structures (Jones et al., 1986; Swamy et al., 1987):

- The strengthening process can be performed simply and quickly when the structure is in use.

- The resulting changes in member size are small in which only a few millimetres are added.

- Despite the fact that epoxy is expensive compared to other materials, such as concrete and steel, bonding steel can be an economical solution when considering the demolition of the whole structure.

Raithby (1982) described a process of strengthening a RC bridge using steel plates. The full-scale load tests performed on the bridge indicated an increase in stiffness by 11% and a reduction in cracks opening of up to 40%. In addition, laboratory tests were conducted on the RC beams to support the results of full-scale tests. All the beams exhibited an improvement in flexural stiffness of up to 105%. The load associated with 0.1 mm crack width was increased by 100% and the beams gained an increase of 24% in flexural capacity. The laboratory test results by MacDonald and Calder (1982) on RC beams strengthened with steel plates showed that full composite action between the beam and plate could be achieved. The researchers found that for good behaviour under service load, the plate has to be fully bonded with stiff adhesive. Some years later, Swamy et al. (1987) examined the behaviour of RC beams with steel plates bonded to their soffits using proper adhesive. The results showed an increase in the first crack loads by about 57% over the control specimen. The increase in first crack load was a function of the plate and adhesive thicknesses. In general, a thicker adhesive layer gave higher cracking loads in the case of thin plates (1.5 mm). However, the use of thicker plates with an increase in the adhesive thickness indicated a reduction in the first crack load. The improvement in the ultimate load carrying capacity and service loads was about 16% and 17%, respectively. The ratio of the plate width to thickness was investigated to achieve a significant increase in the ultimate capacity and ductile failure. Raithby (1982) specified a plate width to thickness ratio of 60. However, this ratio was reduced by Swamy et al. (1987) to 50. In addition, the researchers recommended that

the neutral axis depth should not be more than 0.4d (Swamy et al., 1987). Where d is the effective depth of the section.

The full composite action and preventing separation or debonding of the external bonded steel plates is important for the utilizing of materials and avoiding sudden brittle failure. The finite element model results by Adhikary and Mutsuyoshi (2002) showed that the steel plate separation occurs in beams with short plate lengths and when the plates cut-off point is far from the support. The different factors related to the end debonding of steel plates were investigated by Jones et al. (1988). They used multiple plates (different number of plates bonded to a beam), different thicknesses of steel plate, tapered plates and different types of end anchorages. It was found that the end debonding of steel plates is due to the high interface stresses at the plate end. In addition, the use of proper anchorage had a considerable effect on preventing the debonding of steel plates. Table 2.1 shows the results of the different configurations of steel plate strengthened beams. As seen from the table, the glued anchor plated showed the best performance. The beam failed by the yielding of steel plates attaining the full theoretical ultimate capacity with an increase of up to 36% over the control specimen. The anchored plates also showed ductile behaviour similar to that of the control beams specimen. Furthermore, Jumaat and Alam (2009, 2010) used end and intermediate anchorages for preventing the debonding of steel plates. They used L-shape intermediate anchorages with a width of 40 mm and spacing of 110 mm centre-to-centre. The results showed that the intermediate anchorage is effective in preventing the premature separation of steel plate. In addition, the optimum length of the end anchorage was found to be 100 mm.

The effect of steel plates bonded to the sides of the beams on the propagation of cracks was studied by Arslan et al. (2008). The results showed that the plate length contributes significantly to the load carrying capacity. In addition, the researchers recommended that the length of side plate should be equal to the bottom plate in order to prevent the propagation of cracks.

Besides the advantages of using steel plates for strengthening purposes, this type of material has shown some disadvantages. Exposure tests performed by Raithby (1982) and MacDonald and Calder (1982) indicated that a considerable amount of corrosion occurs at the steel/epoxy interface, which leads to a decrease in strength and local debonding. A limited improvement was found when applying the chromate primer for protecting the steel from the surrounding environment (MacDonald and Calder, 1982). In addition, the difficulty in handling steel plates on site is one of the major drawbacks of using steel plates for strengthening (Meier, 1995). Usually, the steel plate length cannot exceed 6 to 8 m at the construction site. If the structure to be strengthened requires longer plates, a butt joint has to be welded. However, the high temperature of welding may damage the adhesive used to bond the steel plates.

Table 2.1: The use of different strengthening configuration of beams bonded with steel plates (Jones et al., 1988)

Beam No.	Strengthening configuration	Failure load (kN)	% over beam 1	% increase over control	Mode of failure
Beam 1	1 no. 6mm plate	182	-	-13.3	Plate separation
Beam 2	2 no. 3mm plates, curtailed	208	14.3	-1.0	Plate separation of inner plate
Beam 3	1 no. 6mm plate tapered to 2mm	191	4.9	-9. 1	Plate separation
Beam 4	As beam 1 + bolts at end	221	21.4	+5.2	Debonding followed by concrete crushing
Beam 5	As beam 2 + bolts at end and at curtailment	227	24.7	+8.1	Debonding followed by concrete crushing
Beam 6	As beam 1 + one short and one long anchor plate	285	56.6	+35.8	Plate yield and concrete crushing
Beam 7	As beam 1 + short end anchor plates	283	55.5	+34.8	Plate yield and concrete crushing

2.3.3 Behaviour of RC beams strengthened using FRP

2.3.3.1 Ultimate load capacity

The drawbacks of using steel plates, as discussed in the previous section, have encouraged structural engineers to look for an alternative material for the upgrading and retrofitting of RC structures. FRP materials have been used for a number of years in the automotive and aerospace field due to the need for a high strength and lightweight material (Bakis et al., 2002; ISIS Canada Educational Module, 2006). Strengthening RC structures using FRP materials has recently attracted considerable attention in the civil engineering field from the 1980s onwards. A further decrease in the price of FRP materials increased the number of structures strengthened and retrofitted using FRP

(Meier, 1995). The two common advantages of using FRP in strengthening over the other materials are as follows (Bakis et al., 2002; Teng et al., 2002):

- High strength to weight ratio, which leads to easy installation and reduction of labour cost.

- Good chemical resistance, which leads to excellent durability properties.

The behaviour of RC beams strengthened in flexure has been extensively investigated. The main purpose for using FRP for strengthening RC beams is to increase their ultimate capacity and stiffness. One of the early studies was conducted by Saadatmanesh and Ehsani (1991). They reported that GFRP strengthened beams exhibited an increase in flexural strength and a reduction in crack width. However, all the beams showed a decrease in ductility compared to the corresponding unstrengthened (control) beams. In addition, Ritchie et al. (1991) reported that FRP strengthened beams exhibited an increase in strength and stiffness of up to 97% and 99%, respectively. Figure 2.10 shows the load-deflection relationships of the testing matrix. As seen from the figure, all the strengthened beams exhibited a significant increase in load carrying capacity and stiffness. In addition, the results indicated that the strengthened beams showed cracks with small widths that were closely spaced compared to the control beams which had cracks of large width spaced further apart.
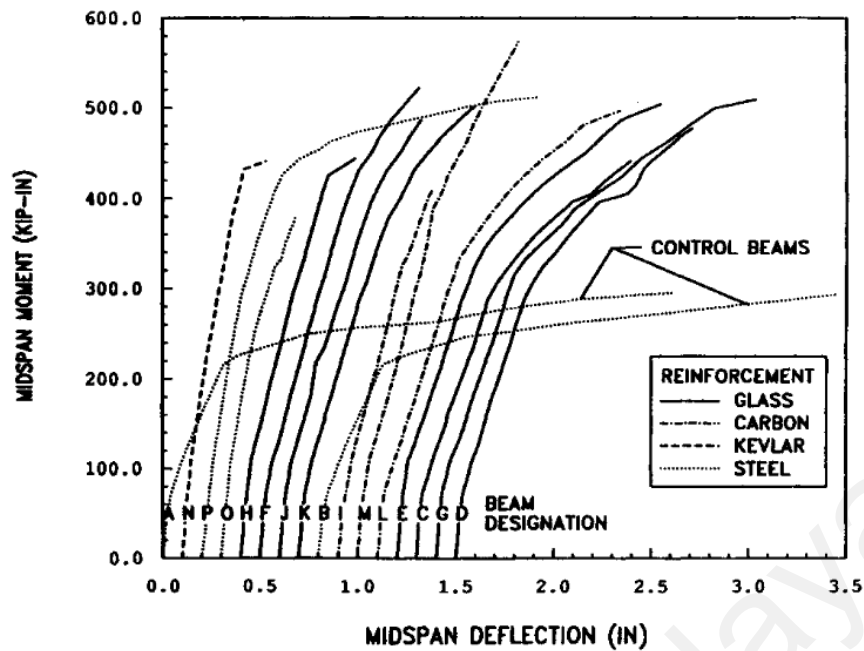
Figure 2.10: Mid-span moment-deflection relationships of FRP strengthened beams with different plates' properties (Ritchie et al., 1991) (In SI units, 1 in = 25.4 mm,1 kip.in = 0.113 kN.m)

2.3.3.2 The effect of FRP thickness

The test results of a number of researchers (Balamuralikrishnan and Jeyasehar, 2009; Chiew et al., 2007; Maalej and Bian, 2001; Maalej and Leong, 2005; Shahawy et al., 1996; Triantafillou and Plevris, 1992) have shown that the thickness of FRP significantly affects the behaviour of strengthened beams. Maalej and Bian (2001) reported that an increase in the thickness of FRP decreased the effectiveness of strengthening for enhancing the structural performance. Table 2.2 shows the results obtained by different researchers for beams strengthened with different FRP thicknesses. As observed from the table, the deflection at failure decreases with the increase in FRP thickness. In addition, the failure mode changes from FRP rupture to debonding with the larger FRP thickness. The value of FRP strain at failure decreases with the thicker FRP due to the premature debonding failure. Triantafillou and Plevris (1992) concluded that beams bonded with thicker plates do not achieve their targeted

strength and ductility due to the premature failure of the plates. The test results of Shahawy et al. (1996) on beams strengthened with different FRP thicknesses indicated an enhancement in the ultimate carrying capacity and stiffness of up to 92% and 78%, respectively. An improvement in serviceability was also observed in the strengthened beams from the cracks with close spacing compared to the large spacing in the control beam. In addition, Maalej and Leong (2005) found that an increase in FRP thickness increases the interfacial shear stresses that cause debonding.

Table 2.2: Test results of beams strengthened with different FRP thicknesses

Beam	FRP thickness (mm)	Ultimate load		Deflection at failure		FRP strain at failure	Failure mode	Researcher
		P_u [a] (kN)	% control	Δ_{fail} [b] (mm)	% control			
Control Beam	-	59.8	-	47.1	-	-	Concrete crushing	Shahawy et al. (1996)
Beam 1	0.1702	66.6	111	33.9	72	0.0032	splitting of CFRP	
Beam 2	0.3404	97.9	164	24.6	52.2	0.0027	splitting of CFRP+ debonding	
Beam 3	0.5105	116.2	194	23.2	49.3	0.0026	splitting of CFRP+ debonding	
Control Beam	-	59	-	23	-	-	Concrete crushing	Maalej and Bian (2001)
Beam 1	0.111	72	122	20.2	87.7	0.0079	FRP rupture	
Beam 2	0.222	86	145.8	17	73.9	0.0075	Ripping of concrete cover	
Beam 3	0.333	82	139	13.2	57.4	0.0061	Ripping of concrete cover	
Beam 4	0.444	79	133.9	10	43.5	0.0037	Ripping of concrete cover	

[a] Value of ultimate load achieved by the beam specimen

[b] Value of deflection at the failure of the beam specimen

2.3.3.3 The effect of FRP length

The effect of the FRP length on the effectiveness of strengthening has also been researched (Arduini and Nanni, 1997; Chiew et al., 2007; Maalej and Bian, 2001; Obaidat et al., 2010, 2011). The study reported by Arduini and Nanni (1997) stated that the length of FRP should be as long as possible to achieve the desirable failure modes (concrete crushing and FRP rupture). Chiew et al. (2007) examined experimentally and analytically the bonded length in the shear span of GFRP strengthened beams. The test results indicated that strengthened beams exhibited an increase in stiffness and strength associated with a reduction in ductility (Figure 2.11). The researchers also found that the strength ratio, SR (which is defined as the ratio of strengthened beam strength to the strength of the control beam (Maalej and Leong, 2005)) increases with the increase in the rigidity of GFRP ($E_{GFRP}.A_{GFRP}$). Up to a ratio of 0.56 of the bonded GFRP length to shear span, the bonded length of the GFRP has little effect on the behaviour of the RC beam.
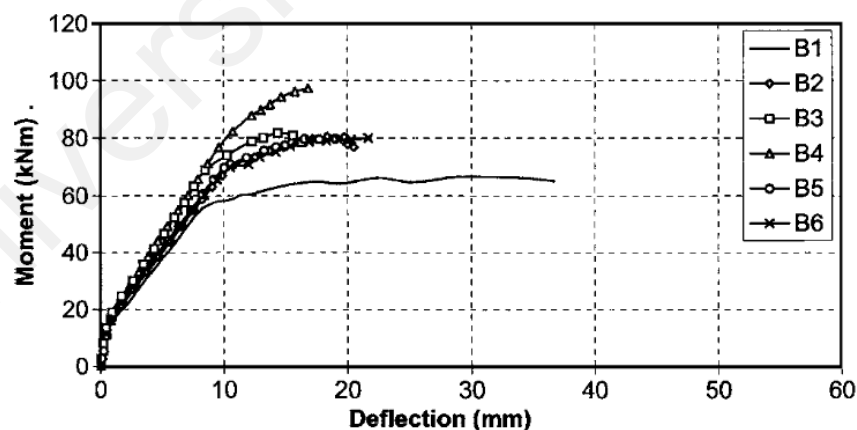
Figure 2.11: Moment-deflection relationships of strengthened beams with different GFRP thickness and length compared to control beam: B1= un-strengthened beam; B2= bonded with laminate thickness 1.7 mm and bonded FRP length to shear span ratio is 0.95; B3= bonded with laminate thickness 3.4 mm and bonded FRP length to shear span ratio is 0.95; B4= bonded with laminate thickness 5.1 mm and bonded FRP length to shear span ratio is 0.95; B5= bonded with laminate thickness 1.7 mm and bonded FRP length to shear span ratio is 0.80; B6= bonded with laminate thickness 1.7 mm and bonded FRP length to shear span ratio is 0.65 (Chiew et al., 2007)

2.3.3.4 Failure modes

With the increasing number of reported research studies, the failure modes of FRP strengthened RC beams could be identified as follows (Smith and Teng, 2002a, 2002b; Teng et al., 2002): FRP rupture, concrete crushing at the compressive zone, FRP end interfacial debonding, concrete cover separation, intermediate cracks interfacial debonding and shear failure. The different failure mechanisms of FRP strengthened beams were also identified by Triantafillou and Plevris (1992) and an equation for each mechanism was proposed. The equations are important for establishing design guidelines for FRP strengthening. Furthermore, Esfahani et al. (2007) studied the effect of the reinforcing bar ratio on the behaviour of FRP strengthened beams. The results showed that specimens strengthened with FRP sheets exhibited more stiffness after the yielding of steel reinforcement than the control beams. It was also found that beams with a large reinforcing bar ratio led to debonding by flexural and shear cracks with a good ductility. Debonding failure is considered the most common failure mode (Bonacci and Maalej, 2001; Maalej and Bian, 2001; Smith and Teng, 2002a, 2002b). The occurrence of FRP debonding starts at the regions where the stress concentration is high (Buyukozturk et al., 2004; Büyüköztürk and Yu, 2006). The high stress concentration is caused due to the discontinuities of materials and the existence of cracks. Hence, a propagation path starts to initiate depending on the properties of bonded material and surface condition of the concrete. The debonding failure mode is generally not desirable as the FRP material, which, generally, has relatively high cost, cannot be fully utilized for the strengthening of the RC beams. In addition, catastrophic brittle failure mode is usually associated with debonding failure. The interfacial shear stresses, which cause the debonding of the FRP sheet, were measured experimentally by Maalej and Bian (2001). The researchers aim of this study was to verify the theoretical predictions done by other researchers (Malek et al., 1998; Roberts, 1989). The results

showed that strengthened beams exhibited a reduction in deflection at failure. The value of interfacial stress was found to be at its maximum at the CFRP tip and decreases exponentially with the increase in distance from the CFRP end. It was also observed that the premature CFRP failure started by the initiation of flexural-shear cracks at the CFRP tips, propagating until reaching the steel reinforcement and separating the concrete cover. The model by Roberts (1989) was found to overestimate the interfacial shear stresses at the CFRP tip, whereas, the model of Malek et al. (1998) was found to be in close agreement with the data reported from the experimental measurements. Moreover, the effect of beam size and thickness of CFRP on the interfacial shear stresses at the CFRP tip were studied by Maalej and Leong (2005). The researchers found that the interfacial shear stresses increase with the increase in beam size and CFRP thickness. The beam size was found to have no effect on the strengthening ratio, deflection or ductility of the strengthened beams.

2.3.3.5 Anchorages

Providing proper clamping at the ends or middle of the FRP sheets/plates are the common solutions to overcome debonding. The mechanical anchorages improve the stress transfer and resist the normal tensile stresses (Khalifa et al., 1999; Quattlebaum et al., 2005). Sharif et al. (1994) examined two types of anchorage system for eliminating the premature failure of FRP. I-FRP jackets and steel-anchored bolts were used at the end of the FRP plates. The results showed that the FRP debonding was prevented by using the end anchorages. However, the I-jacket anchorage system showed better results with respect to failure mode and gain in strength. Garden and Hollaway (1998) found that the end anchorage is necessary for beams with low span/depth ratio where the debonding failure is more probable. Furthermore, Brena et al. (2003) reported that the

use of transverse straps at constant moment region prevented the propagation of flexural cracks and thus prevented local debonding. The tests of Oh and Sim (2004) showed that the use of anchorages increases the ductility. The test results of Siddiqui (2010), Sobuz et al. (2011) and Rasheed et al. (2011) indicated the effectiveness of using U-anchorages for enhancing the flexural capacity and deformability. The use of end anchors prevented the premature debonding of FRP sheets and increased the ductility of the strengthened beams. A combination of external bonding and a mechanical fastening method was recently developed by Guan et al. (2012). The mechanical fastening consists of capping plates and bolts. The mechanical fastener provides higher frictional shear at the FRP and concrete interface and increases the interfacial shear by bonding the plate to the FRP. The proposed system for anchorage of FRP increased the interfacial bonding and prevented debonding of the CFRP sheets. The results also showed that the more closely spaced the mechanical fasteners throughout the longer span the better the results with respect to bonding strength.

ACI Committee 440 (2008) provides a limitation in the FRP material strain (ε_{fd}) for preventing the intermediate induced crack debonding. In addition, transverse clamping using FRP sheets is also recommended. For the concrete cover separation failure, ACI Committee 440 (2008) recommends a U-wrap anchorage when the factored shear force exceeds 0.67 of the concrete shear strength. In general, the FRP sheet should be terminated at a distance l_{df} exceeding the point corresponding to the cracking moment in the bending moment diagram in order to avoid end debonding failure.

where,

$$\varepsilon_{fd} = 0.41\sqrt{\frac{f_c{}'}{nE_f t_f}} \leq 0.9\,\varepsilon_{fu} \qquad\qquad \text{Equation 2.2}$$

$$l_{df} = \sqrt{\frac{nE_f t_f}{\sqrt{f_c'}}}$$
$\hspace{6cm}$ Equation 2.3

where, f_c' is the concrete compressive strength, n is the number of plies of FRP reinforcement, E_f is the elastic modulus of fibres, t_f is the nominal thickness of one ply of FRP reinforcement and ε_{fu} is the design rupture strain of FRP reinforcement.

2.3.3.6 Epoxy adhesive

The use of proper epoxy adhesive was found to improve the behaviour of strengthened beams. Arduini and Nanni (1997) used two types of adhesive with different stiffness. They concluded that the adhesive with larger elongation at failure gives the desirable failure modes, such as concrete crushing and FRP rupture. In addition, Toutanji et al. (2006) bonded RC beams with FRP sheets using inorganic resin. Inorganic resin has a number of advantages over the organic resin, such as, good fire resistance, UV radiation resistance, and ease of mixing and application. They found that the behaviour of strengthened beams differed between the organic and inorganic resin in the load transfer mechanism and failure modes. The inorganic resin showed more desirable failure modes (e.g. FRP rupture) compared to the organic resin.

2.3.3.7 Ductility performance

Ductility is a very important characteristic in RC design. It gives a measure of the ability of structure to undergo a large amount of deflection at or near the ultimate load (Park and Paulay, 1975). This can give proper warning and prevent total failure of the structure. The ductility of the RC structure can be determined through two methods. The first method is based on the moment-curvature diagram. In this method, the ductility is

calculated as the ratio of curvature at the ultimate load to the curvature at the yield load ($\mu_\varphi = \dfrac{\varphi_u}{\varphi_y}$). The second method is based on the load-deflection curve. In this method, the ductility is calculated as the ratio of the deflection at the ultimate load to the deflection at the yield load ($\mu_\Delta = \dfrac{\Delta_u}{\Delta_y}$). Recently, Oudah and El-Hacha (2012) proposed a new expression for ductility of FRP strengthened RC beams taking into consideration the relationship between the deformability and energy dissipation of the strengthened beam. Despite the many advantages of FRP over the other materials in terms of high strength to weight ratio, good durability properties and ease of handling and transportation, the test results of FRP strengthened beams have shown that the beams suffer from a loss of ductility (Chiew et al., 2007; Ritchie et al., 1991; Toutanji et al., 2006; Triantafillou and Plevris, 1992). Figure 2.11 shows the load-deflection relationships of beams tested by Chiew et al. (2007). It is clearly seen from the figure that the strengthened beams (B2 to B6) did not undergo a large amount of plastic deformation like the control specimen (B1). Grace et al. (1999) investigated the behaviour of RC beams bonded with different configurations of GFRP and CFRP. Although all strengthened beams achieved an increase in the load carrying capacity and stiffness, they showed a reduction in ductility. Figure 2.12 shows the load-deflection relationships of the FRP strengthened beams and the control specimen. As can be seen from the figure, the strengthened beams did not show a clear yield plateau, which is seen in the normal under-reinforced RC beams. Although the use of anchorages prevented the premature debonding of the FRP, there is not much enhancement in the ductility of the strengthened beams (Buyukozturk et al., 2004; Oh and Sim, 2004; Rasheed et al., 2011; Siddiqui, 2010; Sobuz et al., 2011). The main reason for the reduction in ductility is that the FRP is a brittle material. Brittle materials have a linear stress-strain relationship up to failure. They do not show a yield plateau as in the case of ductile materials (e.g. steel) (Hinton et al., 2004).
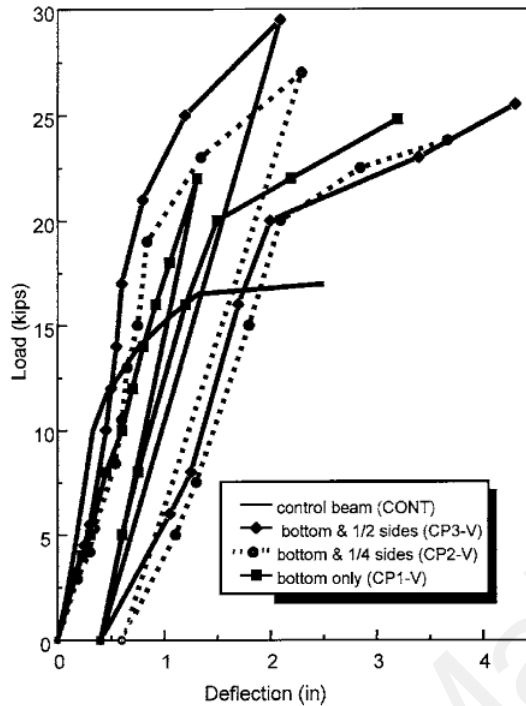
Figure 2.12: Load-deflection relationships of beams strengthened with different FRP configurations and control beam (Grace et al., 1999) (In SI units, 1 in = 25.4 mm and 1 kip = 4.448 kN)

2.3.4 Behaviour of RC beams strengthened using hybrid FRP

Hybrid FRP material is used in an attempt to achieve ductile performance of FRP strengthened RC structures. Initially, the hybrid FRP was used as internal reinforcement to obtain post peak performance similar to steel (Harris et al., 1998; Razaqpur and Ali, 1996). In later years, the hybrid FRP was applied to RC structures for strengthening and retrofitting purposes (Attari et al., 2012; Grace et al., 2002; Grace et al., 2003; Grace et al., 2004; Yi and Cho, 2012). Two main advantages of using hybrid FRP material in strengthening of RC structures have been reported (Bank, 2013; Grace et al., 2002; Wu et al., 2006; Wu et al., 2007):

- The sequential rupture of fibres with different failure strain provides a pseudo ductile behaviour that is similar to that seen in under-reinforced RC structures.

- Hybrid FRPs containing high modulus fibres provide the desired flexural stiffness and improve the yield load of RC structures.

The considerable decrease in the ductility of FRP strengthened beams has encouraged engineers and researchers to explore the hybrid FRP materials in order to achieve progressive failure in the strengthened beams. Grace et al (2002) proposed a new hybrid FRP for strengthening RC beams. The hybrid FRP contains high elongation (HE) fibres, medium elongation (ME) fibres and low elongation (LE) fibres. The developed hybrid composite was made to have a yield pattern similar to that of steel. The low elongation fibres were selected to have a failure strain close to the yield strain of steel, whereas the medium elongation fibres reduced the large drop in load after the failure of low elongation fibres, and, hence, provide gradual strain relaxation. The researchers found that beams strengthened with the hybrid composite showed a yield plateau similar to that in normal under-reinforced concrete. In addition, an improvement in ductility of the hybrid FRP strengthened beams compared to carbon fibre alone was observed. The same researchers later developed an innovative triaxial hybrid fabric (Grace et al., 2003, 2004). The behaviour of beams strengthened with the developed fabric was compared to beams strengthened with steel plates and carbon fibre. The beams strengthened with the hybrid fabric showed better ductility compared to beams with carbon fibre. The measured strain in the hybrid fabric showed that it reached 100% of its theoretical ultimate strain, whereas, carbon fibre only reached 60%. The researchers also found that beams strengthened with the hybrid fabric have similar behaviour to that strengthened with steel plates. Wu et al. (2006, 2007) investigated the effect of hybrid strengthening on the serviceability of RC beams. A considerable increase in the stiffness and load carrying capacity of hybrid strengthened beams was observed. The ductility of hybrid strengthened beams was much better than beams with one type of FRP (Figure 2.13). The researchers related the improvement in ductility to the sequential failure of the high

modulus (low failure strain) fibres, which improved the post peak ductility. It was also found by Wu et al. (2007) that the failure of high modulus CFRP sheets developed high tensile strain, which initiated the failure of high strength carbon fibres and avoided debonding (Figure 2.14).

Furthermore, the effect of hybrid strengthening on preloaded RC beams was recently performed by Kim and Shin (2011). They found that a three layer strengthening scheme gives better results with respect to yield load and stiffness than the two layer scheme. In addition, the combination of one CFRP and two GFRP layers gave the best ductile behaviour. Attari et al. (2012) found that hybrid carbon-glass fibre sheets and hybrid HFRP sheets significantly increased the flexural strength with ductility close to that of the control beam.

However, the use of hybrid FRP is still limited in real field applications for many reasons, such as the high cost of different FRP materials and the small number of reported studies (Bank, 2013). There is no established design guidelines for its use compared to the conventional FRP or ferrocement design standards. A recently reported study by Hawileh et al. (2014) stated that the ACI Committee 440 (2008) prediction for the ultimate capacity of beams strengthened using hybrid FRP is not as accurate as the single type of FRP. Therefore, more studies on hybrid strengthening are still needed to establish design guidelines that can accurately predict the behaviour of strengthened beams and lead to the effective use of the material.
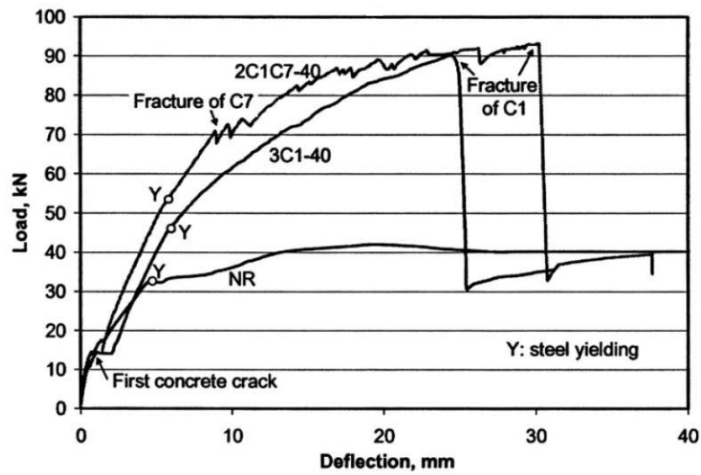
Figure 2.13: Load-deflection relationships of control beam and strengthened beams with hybrid CFRP: NR= control beam; 3C1-40= strengthened with three layers of high strength CFRP sheets; 2C1C7-40= strengthened with two layers of high strength CFRP sheets and one layer of high modulus CFRP sheet (Wu et al., 2007)
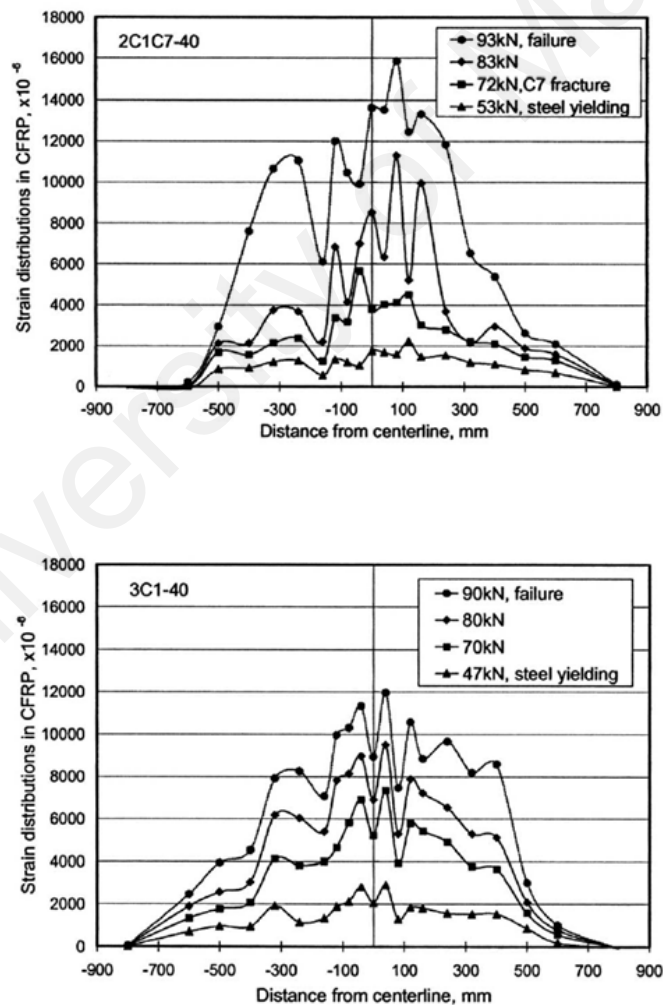
Figure 2.14: Strain distribution of beams strengthened with one type of carbon fibre and hybrid carbon fibres: 2C1C7-40= bonded with two layers of high strength CFRP and one layer of high modulus CFRP; 3C1-40= bonded with three layers of high strength CFRP (Wu et al., 2007)

2.3.5 Behaviour of RC beams strengthened using ferrocement laminates

The incorporation of wire mesh with cement mortar in the form of ferrocement for strengthening and rehabilitation purposes has been widely used since the 1980s (Balaguru, 1989; Iorns, 1987; Reinhorn and Prawel, 1985; Romualdi, 1987). The ferrocement laminate is currently used for strengthening many types of concrete structural elements. This includes confinement of concrete columns (Shannag and Mourad, 2012; Takiguchi, 2003; Xiong et al., 2011) and bonding the laminates to the tension face of beams and slabs (Fahmy et al., 1997; Paramasivam et al., 1994, 1998; Thanoon et al., 2005). The use of ferrocement for retrofitting RC beams has many advantages (ACI Committee 549, 1988; Ahmed and Robles-Austriaco, 1991), such as:

- Ease of handling and low labour cost.

- Good durability properties of ferrocement laminate.

- Cost-effectiveness when considering the low cost of wire mesh and cement mortar compared to FRP and steel materials.

- High tensile strength provided by the multiple layers of wire mesh in the laminate.

Basunbul et al. (1990) used ferrocement laminates for repairing pre-damaged RC beams. The researchers found that the use of ferrocement enhanced the flexural capacity by up to 25%. In addition, the enhancement in the crack load was found to be above 100% with the use of ferrocement and epoxy injection for the repair of specimens. Compared to strengthening using steel plates, ferrocement laminates showed better ductility and durability performance. Later, Paramasivam et al. (1994) tested twelve beams bonded with ferrocement laminates. They used "L" shape mild steel as shear connectors for attaching the ferrocement laminates. In addition, the researchers varied the spacing of the shear connectors, method of surface preparation and volume fraction

of mesh reinforcement. The test results showed that the use of ferrocement laminates with properly spaced shear connectors and a roughened surface can enhance the behaviour of RC beams. Figure 2.15 shows the load-deflection curves of beams bonded with ferrocement laminates and the control specimen. All the strengthened beams exhibited a delay in first crack depending on the volume fraction of mesh reinforcement in the laminate. The same researchers (Paramasivam et al., 1998) later investigated the transfer of forces at the concrete-ferrocement laminate interface. In addition, the effect of pre-damage level on beams behaviour was studied. The composite action between the ferrocement laminate and RC beam was achieved by using shear connectors. The results showed that the ferrocement laminate enhanced the cracking behaviour and stiffness of the beams. A design chart was also proposed, which is useful for the estimation of the volume fraction of mesh reinforcement and the maximum interfacial shear stresses that develop between the ferrocement laminate and the beam surface. Moreover, Al-Kubaisy and Jumaat (2000) found that the use of Hilti bolts, mild steel bars with adhesive and dowel bars can enhance the composite action between the beam and the ferrocement laminate. In addition, a decrease in volume fraction of reinforcement reduces the ultimate capacity. Improvements in the cracking loads of up to 80% were achieved. Recently, Bansal et al (2008) studied the effect of different wire mesh orientation on the performance of ferrocement strengthened beams. Wire mesh orientations of 0º, 45º and 60º were used. The test results showed that all the beams exhibited a remarkable increase in load carrying capacity. However, the orientation of 45º showed the highest increase in energy absorption.

However, due to the increasing use of other materials that have a higher strength to weight ratio, such as FRP, the application of ferrocement laminate is limited. In addition, the difficulty in maintaining the composite action between the ferrocement

laminate and concrete beams is one of the issues that need to be resolved by designers. This difficulty is attributed to the relatively heavy weight of ferrocement laminate due to the high density of cement mortar. Although shear connectors have been proposed to overcome the problem of the loss in composite action, the application of shear connectors on site is limited by the shape and conditions surrounding the structural element.
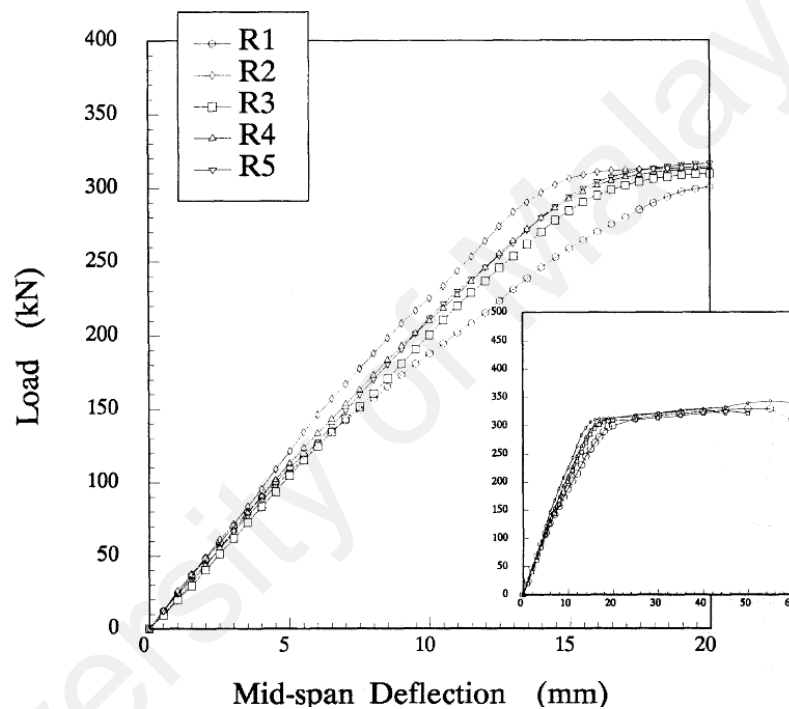
Figure 2.15: Load-deflection relationships of ferrocement strengthened beams: R1= control; R2= 200 mm shear connector spacing and 1.25% reinforcement volume fraction; R3= 300 mm shear connector spacing and 1.25% reinforcement volume fraction, R4= 400 mm shear connector spacing and 1.25% reinforcement volume fraction; R5= 300 mm shear connector spacing and 2.23% reinforcement volume fraction (Paramasivam et al., 1994)

CHAPTER 3

EXPERIMENTAL PROGRAMME

3.1 General

This chapter presents the experimental preparation and tests set-up conducted in this research. The testing programme of each study is first presented. The second section explains the geometry and details of beam specimens used. Then, the materials properties and preparation of specimens are described. Finally, the test set-up and instrumentation are presented.

3.2 Testing programme

This study includes the testing of three groups of beam specimens. First group consisted of ten plain concrete beam specimens bonded with wire mesh-epoxy composites and CFRP. One specimen was considered as a control. Five specimens were bonded with different number of wire mesh layers. Two specimens were bonded with two CFRP sheets with different widths. The remaining two specimens were bonded with a hybrid of two wire mesh layers and a CFRP sheet. The length of all bonded materials was 270 mm. The description of test specimens is shown in Table 3.1.

The second group of plain concrete beam specimens consisted of four specimens. One specimen was considered as a control. The other three specimens were bonded with wire mesh-epoxy composite with widths of 45, 70 and 95 mm. The length of wire mesh-epoxy in all specimens was 270 mm. Table 3.2 shows the summary of test specimens.

The third group includes a total of five RC beams. The experimental work consisted of one control beam and four beams strengthened with wire mesh-epoxy composites and CFRP as well as a hybrid of wire mesh-epoxy and CFRP. The test beams description is

presented in Table 3.3. The width of wire mesh-epoxy composite in specimens A1, A2 and HY was 150 mm. Specimens B and HY were strengthened with 75 mm width CFRP sheet. The length of strengthening materials in all specimens was 2420 mm. The plain concrete test results showed that the use of four layers of wire mesh is optimum for increasing flexural capacity of strengthened specimens. Thus, all wire mesh-epoxy composites used in this study consisted of four wire mesh layers.

Table 3.1: Summary of test specimens of first group of plain concrete beams

Specimen group	Specimen designation	Bonded material
N/A	CP	N/A
Group A	A1	One layer of wire mesh (width=100 mm)
	A2	Two layers of wire mesh (width=100 mm)
	A3	Three layers of wire mesh (width=100 mm)
	A4	Four layers of wire mesh (width=100 mm)
	A5	Five layers of wire mesh (width=100 mm)
Group B	B1	CFRP sheet (width= 10 mm)
	B2	CFRP sheet (width= 20 mm)
Group C	HY1	Hybrid CFRP sheet (width=20 mm) + Two layers of wire mesh (width=20 mm)
	HY2	Hybrid CFRP sheet (width=20 mm) + Two layers of wire mesh (width=100 mm)

Table 3.2: Summary of test specimens of second group of plain concrete beams

Specimen	Bonded material overall width (mm)	Arrangement of wire mesh layers
Control	N/A	N/A
A1	95	Two layers (16 wires/layer)
A2	70	Two layers (10 wires/layer) + one layer (12 wires)
A3	45	Four layers (6 wires/layer) + one layer (8 wires)

Table 3.3: Summary of test specimens of RC beams

Beam Designation	Strengthening material
CB	N/A
A1	Wire mesh-epoxy composite (applied directly on beam surface)
A2	Wire mesh-epoxy composite laminate
B	CFRP sheet
HY	A hybrid of wire mesh-epoxy composite and CFRP

3.3 Geometry and properties of specimens

3.3.1 Plain concrete beams

Concrete beam specimens with 100 mm width, 100 mm depth and 500 mm length were used. The specimen details are shown in Figure 3.1.
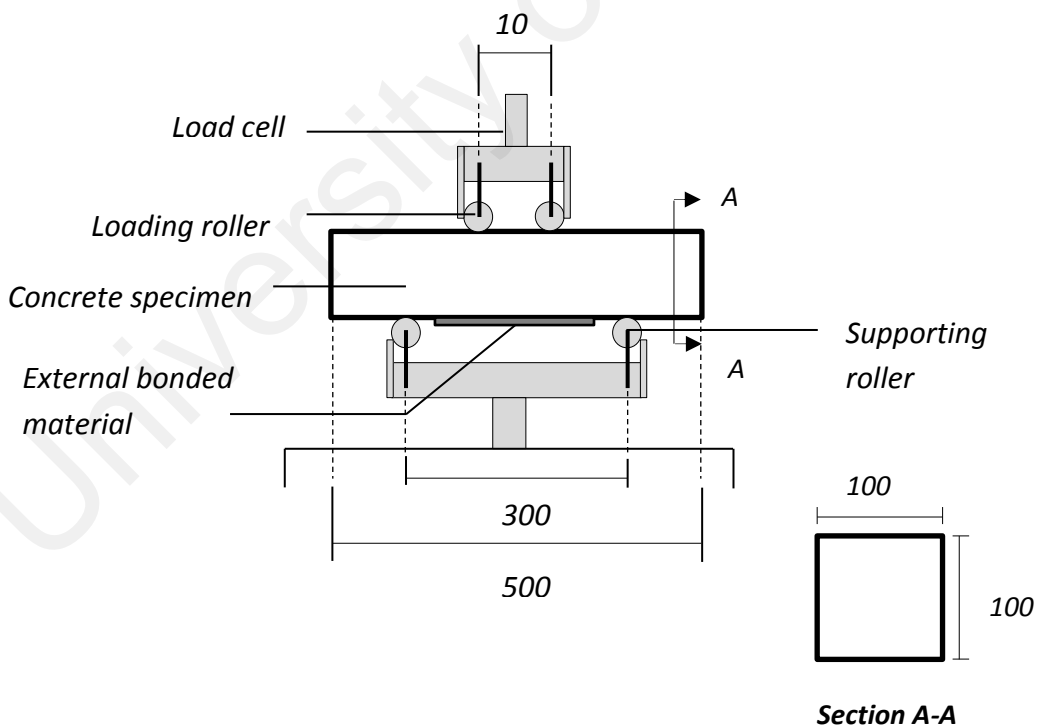
Figure 3.1: Plain concrete beam specimen details (mm)

3.3.2 RC beams

A total of five RC beam specimens with identical dimensions and reinforcement details were fabricated. Figures 3.2 and 3.3 show the RC beams details and sections. The beam total length was 2800 mm. The beam width and depth were 150 and 250 mm, respectively. The beams were singly reinforced with two 12 mm deformed steel bars. The reinforcement ratio was 0.68%. The full design calculation of beam section is presented in Appendix A chapter. Shear links were provided in the shear span at spacing of 75 mm center to center using 8 mm mild steel bars and 10 mm deformed hanger bars.
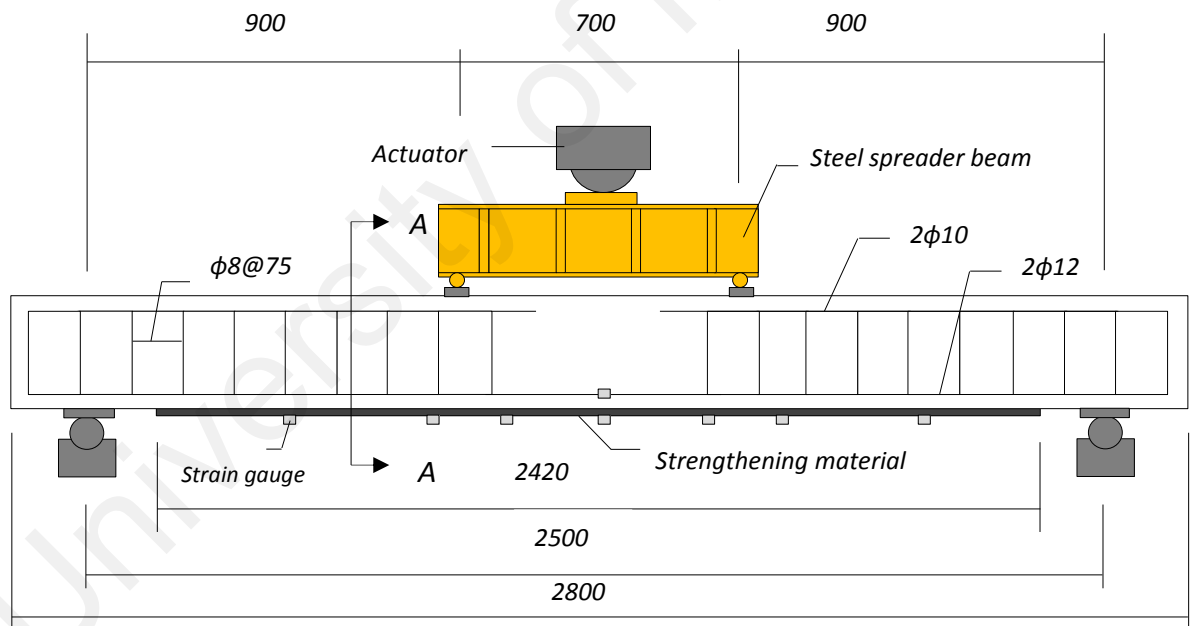
Figure 3.2: RC beam details (mm)
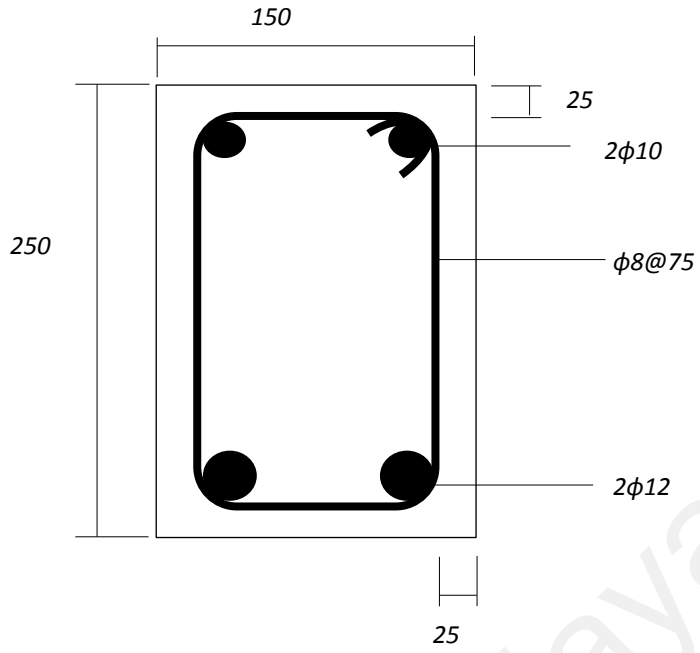
Section A-A

(Control specimen CB)

Wire mesh-epoxy   CFRP sheet

Section A-A

(Specimens A1 and A2)

Section A-A

(Specimen B)

Section A-A

(Specimen HY)
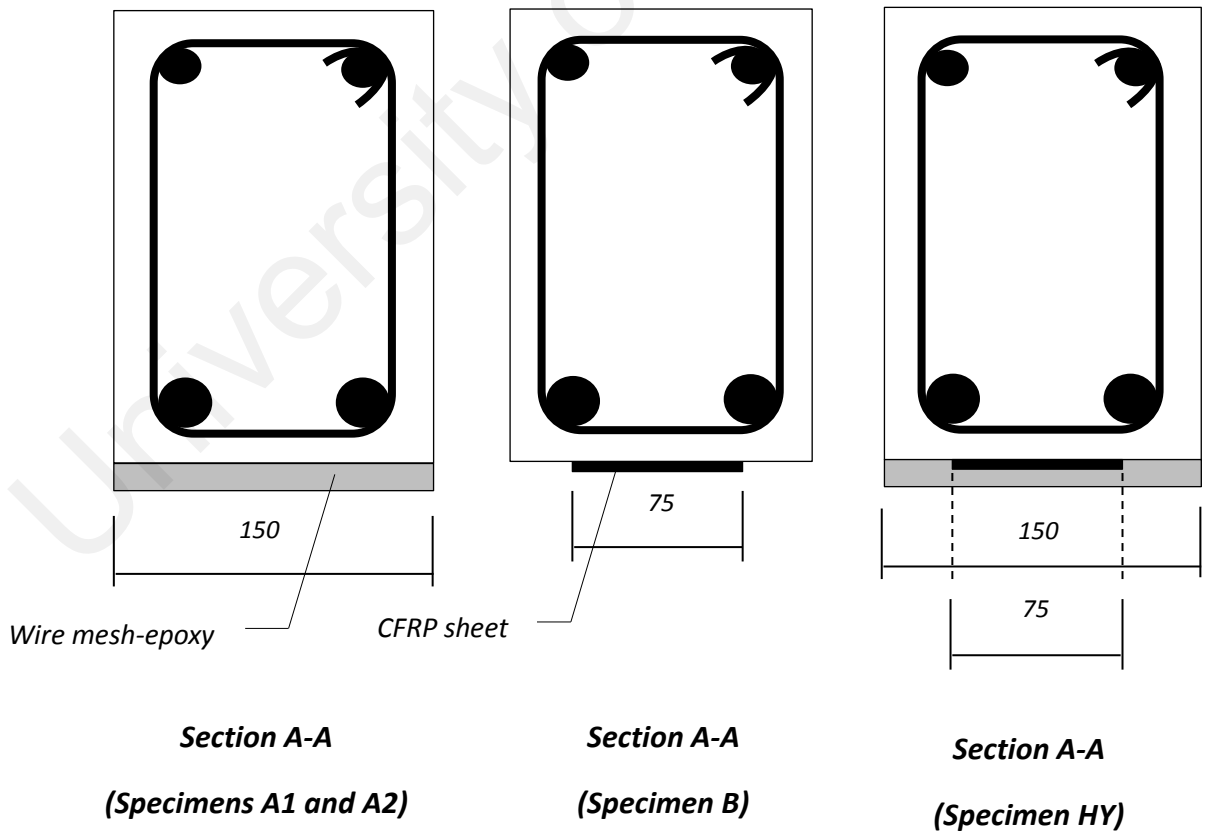
Figure 3.3: RC beams sections (mm)

3.4 Material properties

This section presents the materials properties of concrete, steel, wire mesh, epoxy resin and CFRP. It should be mentioned that the materials properties described in this section are reported from the manufacturer except for the wire mesh and concrete batches of plain concrete specimens. The full description of the testing of each material is explained in detail in Appendix B chapter.

3.4.1 Concrete

The average concrete 28-day compressive strength for the first group of plain concrete beams was 44 MPa, while it was 56 MPa for the second group. The maximum size of aggregate for both batches was 20 mm, and slump ranging from 30 to 60 mm. The specified concrete 28-day compressive strength of RC beams was 40 MPa. The maximum size of aggregate was 20 mm, 2% air content and slump ranging from 75 to 100 mm.

3.4.2 Steel

The yield strengths for 12, 10 and 8 mm bars were 529, 521 and 317 MPa, respectively. The elastic modulus of 12 and 10 mm bars was 200 GPa while 8 mm diameter bars had an elastic modulus of 210 GPa.

3.4.3 Welded wire mesh

Common welded wire mesh with closely spaced wires and square openings was used. The mesh had a wire spacing of 6.35 mm and 0.64 mm wire diameter. Two samples of

wire mesh from two different suppliers were used. The mechanical properties of first sample of wire mesh were as follows: ultimate strength of 572 MPa, yield strength of 440 MPa, strain at failure of 1.5%, and modulus of elasticity of 119.7 GPa. The mechanical properties of the second sample of wire mesh were as follows: ultimate strength of 665 MPa, yield strength of 270 MPa, strain at failure of 1.2%, and modulus of elasticity of 114.2 GPa.

3.4.4 Epoxy resin

The two-part epoxy impregnation resin was used for fabricating the wire mesh-epoxy composites (Sikadure®-330, 2012). In addition, it was used for bonding the CFRP and wire mesh-epoxy laminate to beam surface. The tensile strength, flexural and tensile elastic moduli were 30, 3800 and 4500 MPa, respectively. The elongation at break was 0.9%.

3.4.5 CFRP sheet

A unidirectional carbon fibre sheet with a thickness of 0.17 mm was used. The mechanical properties of the CFRP sheet were as follows: ultimate strength of 4900 MPa, ultimate strain of 2.1%, and elastic modulus of 230 GPa.

3.5 Specimens preparation and strengthening

In this section, the methods of preparation and bonding of strengthening materials to beams soffits are described in details.

3.5.1 Plain concrete specimens

The method of applying the wire mesh-epoxy composite to the plain concrete beam specimen soffit was carried out using the following procedure:

(1) Preparation of wire mesh: The wire mesh was cut into layers with specified dimensions. The individual layers were first tied together using a thin fabric thread or metal wire to prevent any slippage at the time of placing the wire mesh on the surface of the specimen and to ensure that all the wires had the same alignment. Figure 3.4 shows a wire mesh sample used in this study.

(2) Concrete surface preparation: The surface preparation was done based on the manufacturer's instructions for the application of epoxy resin (Sikadure®-330, 2012). The surface was abraded to remove the loose material and weak cement layer to expose the textured smooth surface of the concrete. The surface was then cleaned to remove the dust and remaining loose material using a brush and vacuum cleaner. A thinner was used to ensure the surface was completely clean of dust and any other material that might affect the bonding. Figure 3.5 shows the surface preparation of the concrete specimen.

(3) Spreading epoxy on the concrete surface: A thin layer of epoxy was spread on the concrete surface in order to make sure that the epoxy completely covered the concrete surface and filled some surface voids for perfect bonding.

(4) Placement of wire mesh: The wire mesh layers were laid on the soffit of the specimen and covered with epoxy.

(5) Applying epoxy resin: The amount of epoxy used to ensure perfect bonding between the wire mesh and the concrete was 1.5 kg/m^2 for each layer. Care should be taken concerning the amount of epoxy for cost effectiveness and the overall thickness of the composite. Figure 3.6 shows the preparation of a

specimen with multiple layers of wire mesh and the application of the epoxy on the wire mesh layers.

(6) Curing of epoxy: A polymeric release acetate film was placed on top of the wire mesh and epoxy matrix in order to ensure a smooth surface. A piece of plywood was then placed on top of the acetate sheet and clamped to compress the composite and provide perfect bonding with the concrete surface (Figure 3.7). The composite was left for one week for curing of the epoxy according to the manufacturer's recommendations (Sikadure®-330, 2012). The clamping was then opened and the acetate sheet was removed.

For carbon fibre, the sheet was applied on the thin layer of epoxy on the surface of the specimen. A roller was then used to squeeze out the epoxy through the fibre strands and distribute it evenly over the whole sheet. For the specimen with hybrid wire mesh-epoxy-carbon fibre, both procedures mentioned above were implemented. The carbon fibre sheet was placed first, followed by the wire mesh and epoxy placement on the carbon fibre sheet and concrete surface. Figure 3.8 shows a specimen ready for testing.
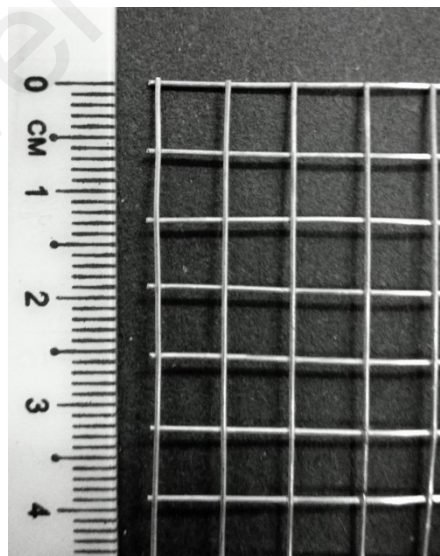
Figure 3.4: Wire mesh sample

Figure 3.5: Surface preparation of concrete specimen

Figure 3.6: Applying of epoxy on multiple layers of wire mesh

Figure 3.7: Compressing the composite

Figure 3.8: A specimen ready for testing

3.5.2 RC beam specimens

A proper concrete surface preparation was done before applying the strengthening materials. The surface preparation was done in accordance with the manufacturer's instructions for the application of epoxy resin (Sikadure®-330, 2012). The surface was first abraded to remove the cement laitance and loose materials that might interfere in the bonding (Figure 3.9). The dust was then removed using a brush and vacuum air cleaner (Figure 3.10). Acetone was used to ensure the cleanness of the surface from any material that can affect the bonding.

Two different methods for the application of the wire mesh-epoxy composite were adopted in this study. The wire mesh-epoxy composite in specimen A1 was applied directly on the beam surface. After the surface preparation was completed, a thin layer of epoxy was spread over the surface. This layer helped to fill the small voids on the prepared surface for perfect bonding. The multiple layers of wire mesh were then placed on the concrete surface and the epoxy resin was applied (Figure 3.11). It should be mentioned that the amount of epoxy sufficient for bonding the wire mesh was 1.5 kg/m^2 per layer. An acetate release film was placed on the composite to obtain a smooth surface after hardening. A piece of plywood was then placed on the acetate film and clamped to provide good bonding with the surface of the concrete. The composite was left for one week for curing according to the manufacturer's recommendations. After one week, the clamp was finally opened and the acetate film was removed.

In specimens A2 and HY, the wire mesh-epoxy composite was applied as a laminate. The laminate was prepared away from the beams and applied to their surface after hardening using the same epoxy resin. The main aim of fabricating the laminate was to study the practical perspective of the application of the wire mesh-epoxy composite on site. It is important to develop the composite, which can be practically acceptable and

less laborious for site application. The laminate was prepared by first applying the epoxy on the layers of the wire mesh placed in a special mould and left one week for curing. After hardening of the composite, the laminate was taken from the mould and prepared for bonding on the soffits of the beams. Figure 3.12 shows the wire mesh-epoxy laminate. After completing the preparation of the concrete surface, the epoxy resin was applied on the beam surface followed by the placement of the laminate. Figure 3.13 shows the placement of the laminate on the beam surface before clamping. A plywood piece was placed between the laminate and clamping to avoid any local damage on the laminate surface and to distribute the pressure evenly over the laminate for perfect bonding. It should be noted that the amount of epoxy found sufficient for bonding the laminate was 0.75 kg/m^2. This amount is similar to that recommended by the manufacturer for bonding one layer of carbon fibre sheet (Sikadure®-330, 2012; SikaWrap®-301 C).

In specimen B, the conventional wet lay-up procedure was used for bonding the CFRP sheet on the beams surface. The epoxy was first spread over the concrete surface followed by placement of the CFRP sheet. A special roller provided by the manufacturer was used to squeeze the resin through the fibres (Figure 3.14). In specimen HY, both procedures mentioned above for bonding the wire mesh-epoxy laminate and CFRP sheet were applied. The CFRP sheet was applied first on the concrete surface, followed by bonding the wire mesh-epoxy laminate using epoxy resin.

Figure 3.9: Surface preparation of RC beam

Figure 3.10: Removing of dust and loose materials by vacuum air cleaner

Figure 3.11: Applying epoxy on multiple layers of wire mesh placed on beam surface

Figure 3.12: Wire mesh-epoxy laminate

Figure 3.13: Placement of the wire mesh-epoxy laminate on beam surface

Figure 3.14: Strengthening of beam with CFRP sheet

3.6 Test set-up and instrumentation

3.6.1 Plain concrete specimens

All specimens were tested in four-point bending until failure at a span of 300 mm. Figure 3.15 shows the test set-up. The two concentrated loads were applied at an equal distance of 100 mm from the supporting rollers. The tests were carried out under displacement control at a constant displacement rate of 0.05 mm/min. The mid-span deflection was monitored by a linear variable displacement transducer (LVDT). The specimen dimensions and test set-up were similar to that recommended by BS EN 12390-5 (2009).
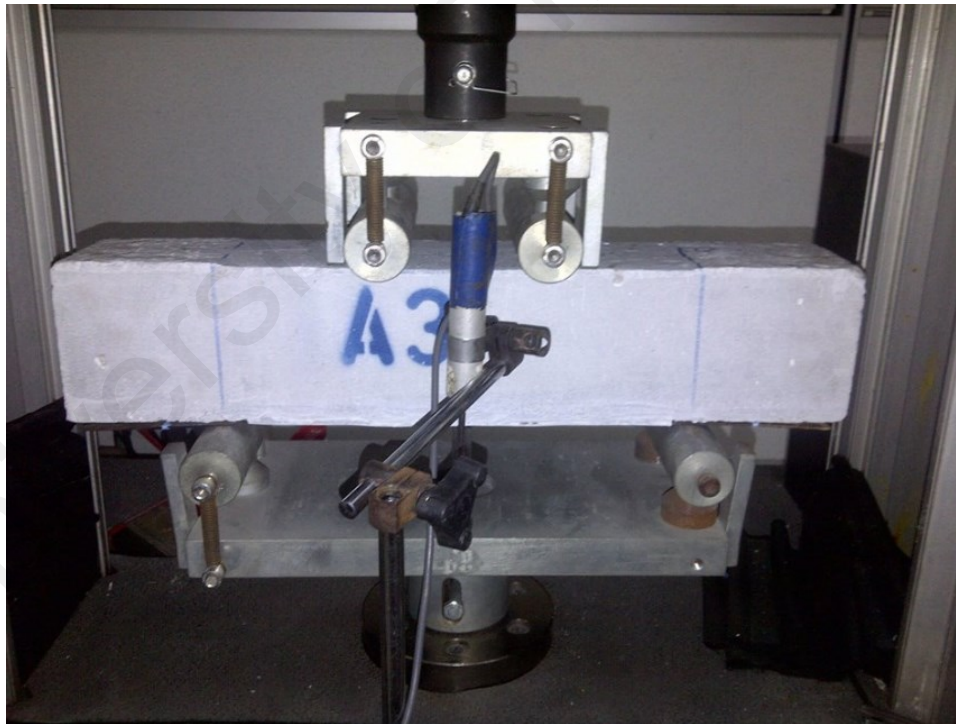
Figure 3.15: Test set-up of plain concrete beams

3.6.2 RC beams

All the beams were tested under four-point bending until failure with an effective span of 2500 mm. Figure 3.16 shows the test set-up of RC beams. The load was applied through a steel spreader beam that distributed the load equally through two point loads. The distance between the two point loads was 700 mm. The load was applied on the beams using a hydraulic actuator through a steel frame fixed on the laboratory floor. The mid-span deflection was monitored during the test using a linear variable displacement transducer (LVDT). Strains of the internal steel reinforcement and strengthening materials were monitored using strain gauges. One strain gauge was placed at the centre of each steel reinforcement bar. The strain gauges were placed at the mid-span of the strengthening material and at distances of 300, 500 and 1000 mm from the centre of beam. The distribution of cracks was observed during the test. In addition, the crack widths at the different levels of load were measured using a microscope.

Figure 3.16: Test set-up of RC beams

CHAPTER 4

RESULTS AND DISCUSSION

4.1 General

In this chapter, the test results of beam specimens bonded with wire mesh-epoxy composite and CFRP as well as a hybrid of wire mesh-epoxy-carbon fibre composite are presented and discussed. The results of each group of plain concrete specimens and RC beams are discussed separately. First, the effect of the different strengthening materials on first crack load, maximum deflection, ultimate load and energy absorption of plain concrete beam specimens is discussed. Then, the performance of strengthened RC beams with respect to load-deflection behaviour, stiffness, energy absorption, measured strains and cracking behaviour is analyzed and discussed.

4.2 Plain concrete beams

4.2.1 First group of plain concrete beams

The experimental programme included groups A, B and C. A plain concrete beam specimen was tested as a control. Group A included five specimens bonded with a different number of wire mesh layers. Group B included two specimens bonded with carbon fibre sheets. The specimens in group C were bonded with a hybrid of wire mesh and carbon fibre sheets. The enhancement in the behaviour of plain concrete specimens bonded with different types of materials is discussed in the following sections.

4.2.1.1 Effect of wire mesh layers

4.2.1.1.1 First crack and ultimate load

The loads at which the first crack occurred are presented in Table 4.1. It should be noted that the first crack of specimens CP, A1 and A2 could not be detected as the crack propagated immediately and caused fracture of the specimen. Ordinarily, a plain concrete specimen fails suddenly when the maximum stresses in concrete reach the modulus of rupture value of the concrete. The micro-crack initiated in the vicinity of the tension face of specimen CP propagated immediately and the specimen broke into two parts. The failure mechanism of the specimen with one layer of wire mesh (A1) was similar to the control specimen (CP). However, the ultimate load of A1 was 35.67% more than CP specimen. Specimen A2 with two layers of wire mesh showed an increase in ultimate load to 24.6 kN. At this load, a small drop in load was detected. The specimen then continued to carry the load constantly with an increase in deflection until final fracture. As an example, Figure 4.1 shows specimen A2 after failure. The considerable increase of ultimate load in specimens A1 and A2 was related to the effect of epoxy and wire mesh. The wire mesh-epoxy composite prevented the propagation of a micro-crack and provided additional tensile strength in the tension face of the specimen. A crack started to appear at a load 22 kN in the specimen with three layers of wire mesh (A3). After the first crack, the load continued to increase and some other cracks were detected at loads 23 kN and 24 kN on the tension face. The specimen broke at a load of 24 kN, which is close to the failure load for specimen A2. In specimen A4, which had four layers of wire mesh, an increase in the first crack load was observed. The first crack load was 25 kN. Similar to specimen A3, the load continued to increase and some other cracks were detected at higher load levels. The specimen failed at a load of 32 kN, which is much higher than the failure load of the A3 specimen. In addition, a good improvement in the first crack and ultimate load was achieved in specimen A5.

The first crack started to appear at a load of 30 kN, which is a considerable delay compared to the A4 specimen. In addition, similar to specimen A4, specimen A5 continued to sustain an increasing load after the first crack. The crack propagated with an increase in load; other cracks were detected at mid span and the edges at loads of 31 kN and 37 kN. Figure 4.2 shows the crack propagation in specimen A5 under increasing load. The specimen could sustain a load until 38.1 kN and then broke after the failure of the wire mesh-epoxy composite. The first crack and ultimate load were generally improved with the increasing number of wire mesh layers. This is attributed to the fact that additional wire mesh provides more resistance to an increasing load and restraint of micro-cracks propagation. The overall results of the first cracks and failure load demonstrate the advantage of using wire mesh as an external method for enhancing the concrete rupture modulus and first crack. The first crack was delayed much better than the other enhancing techniques, such as internal steel fibres (Hassanpour et al., 2012; Padron and Zollo, 1990; Soulioti et al., 2011). These improvements are of major concern when considering the serviceability of concrete structures. In addition, the method used in this study can be easily applied to existing structures for enhancing their properties, unlike internal reinforcing fibres, which need to be added at the time of preparing the mixing of concrete.

Table 4.1: Summary of test results of the first group of plain concrete beams

Specimen	Ultimate load (kN)	Deflection at failure (mm)	Energy absorption (N.m)	First crack load (kN)
CP	17.1	0.95	7.27	17.1
A1	23.2	1.51	13.92	23.2
A2	24.6	1.68	18.31	24.6
A3	24.0	2.13	20.99	22.0
A4	32.2	3.07	41.45	25.0
A5	38.1	2.38	41.97	30.0
B1	22.0	1.73	14.15	22.0
B2	18.0	1.46	8.73	17.0
HY1	20.8	2.21	28.25	20.0
HY2	28.0	2.48	33.12	23.0
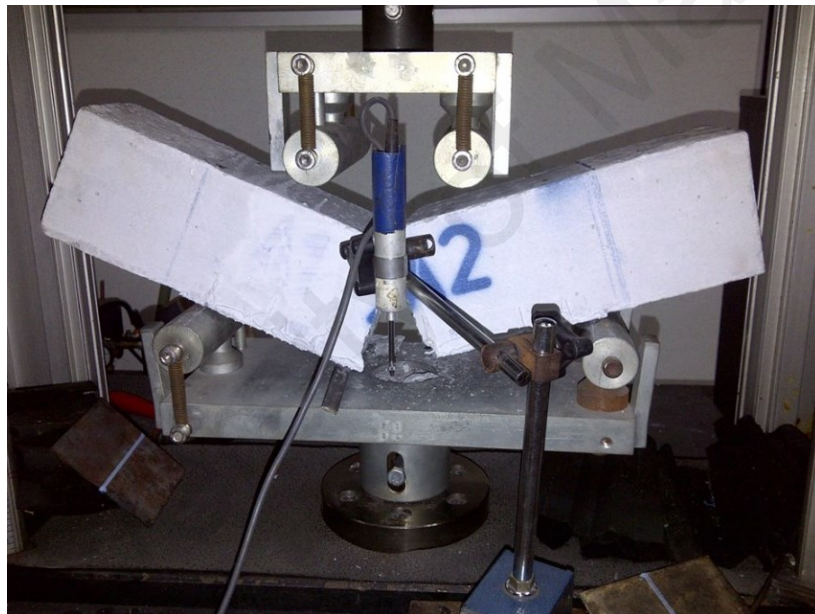
Figure 4.1: Failure of specimen A2

Figure 4.2: Crack propagation in A5 specimen during test

4.2.1.1.2 Deflection and failure modes

The deflection values at failure of all specimens are summarized in Table 4.1. Figure 4.3 also shows the load-deflection relationships for group A specimens and the control specimen CP. The load-deflection curve, which represents the strength and serviceability characteristics, is very important for describing the flexural properties of concrete elements. The load-deflection relationship is affected by the following main parameters; ultimate load, deflection at failure, first crack load and flexural stiffness (slope of load-deflection curve). All load-deflection curves showed a similar trend regardless of the number of wire mesh layers. Compared with the other methods for enhancement of concrete performance (Balaguru et al., 1992; Hassanpour et al., 2012; Soulioti et al., 2011), the load-deflection relationship of the wire mesh-epoxy bonded specimens is totally different. In the internally fibre-reinforced concrete, the plastic stage is much more dominant than the elastic, whereas, in this research, the curve only shows plastic behaviour (reduction in slope) in the late stage. The loading phases of group A specimens can be explained as follows: the first phase represents the elastic

behaviour where there is no crack in the tension face and the specimen maintains its full flexural stiffness and rigidity. The load increases linearly with the deflection. The second phase corresponds to the initiation of cracks and reduction in the slope of the load-deflection curve. In this phase, the bending stiffness of the specimen reduced. The final phase includes the failure of wire mesh-epoxy composite and fracture of the specimen. However, the plain concrete specimen (CP) failed immediately after the occurrence of a crack. The failure was sudden and without any cracks before the final fracture of the specimen. This is, however, expected as the flexural strength of plain concrete is too small and always neglected in design (Neville and Brooks, 2008). Group A specimens failed through the fracture of the wire mesh-epoxy composite. The wire mesh failed first by yielding of the wires and final rupture. All externally wire mesh-epoxy bonded specimens exhibited an increase in deflection at failure compared to plain concrete. The increase in deflection in all specimens, except specimen A5, was associated with the increase in the wire mesh layers. An increase in the number of wire mesh layers from 0 to 1, 2, 3, 4 and 5 increased the deflection of the concrete beam specimen by about 34%, 55%, 89%, 173% and 126%, respectively. Specimen A5 failed at a deflection of 2.15 mm, which is smaller than that of specimen A4 with a deflection of 2.59 mm. It should be mentioned that the further addition of wire mesh may reach an optimum level where the enhancement in overall performance does not improve much. It should be noted that the overall thickness of the five-layer wire mesh-epoxy composite was measured to be only 5 mm. The wire mesh-epoxy composite showed good bonding to the concrete surface as it failed by rupture in all specimens. In addition, the amount of epoxy required for bonding the wire mesh layers was found to be reasonable and within the range specified by the manufacturer. An amount between 0.7 and 1.5 kg/m^2 is required for bonding carbon fibre sheets (Sikadur$^®$-330, 2012) whereas the amount of epoxy used for bonding wire mesh layers was about 1.5 kg/m^2, as

mentioned earlier in this paper. This shows the cost-effectiveness of the wire mesh-epoxy composite, as the price of wire mesh is very low compared to carbon fibre.
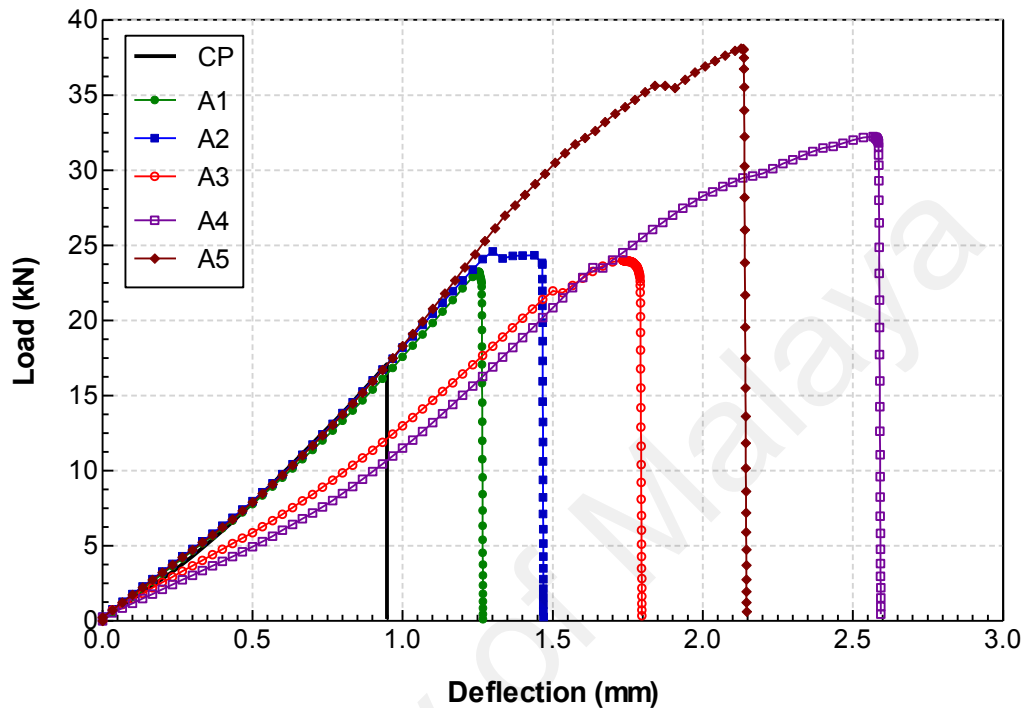
Figure 4.3: Load-deflection curves of group A specimens and control specimen CP

4.2.1.1.3 Energy absorption values

The plain concrete specimen failed suddenly when the deflection exceeded the ultimate strength. On the other hand, the specimens with wire mesh-epoxy composite continued to carry higher loads than the plain concrete and showed greater deflection. Inspection of the fractured specimens showed that the failure took place after the fracture of the wire mesh-epoxy composite. The wire mesh continued to elongate until failure. This shows that, unlike the plain concrete specimen, the specimens with wire mesh-epoxy composite have a higher fracture work or toughness than the plain concrete. The toughness indicates the amount of energy absorption capability of a particular specimen and is measured by the area under the load-deflection curve (Mehta and Monteiro,

2006). The energy absorption values of group A specimens are presented in Table 4.1. In addition, Figure 4.4 shows the percentage increase in the energy absorption values of specimens with wire mesh over that of plain concrete (CP). The figure shows that increasing the amount of wire mesh increased both the flexural strength and energy absorption. However, the increase in energy absorption for all specimens with wire mesh-epoxy composite was much higher than that of the flexural strength. The percentage increase in energy absorption of specimen A4, for example, was five times the increase in flexural strength. In addition, among all the specimens, the specimens with four and five wire mesh layers showed a significant increase in energy absorption. However, the energy absorption of specimen A5 was almost the same as specimen A4.

Specimen A3 had an increase in energy absorption of around 189%, whereas specimens A4 and A5 had an increase of about 470% and 478% over the plain concrete specimen, respectively. A slight increase in energy absorption was observed in specimen A5 over specimen A4. Although it is still higher than A4, it shows that a further increase in the wire mesh layers does not significantly improve the energy absorption and ductility of plain concrete. The energy absorption mechanism of wire mesh-epoxy bonded specimens can be explained as follows: after the occurrence of the first crack in the concrete, the wire mesh-epoxy composite will carry the increasing load if its tensile strength is greater than the load at the crack. The concrete at the cracked section does not carry any tension and the wire mesh resists the load entirely. As the load keeps increasing, the wire mesh layer will transfer the load to the subsequent layers through the shear stresses in the epoxy matrix. The wire mesh will continue carrying the increasing load until its final failure. The wire mesh fails by yielding and fracturing. Figure 4.5 shows the failure of the wire mesh-epoxy composite of specimen A4. The improvement in the energy absorption of specimens bonded with wire mesh layers can be related to the ductility of wire mesh. Ductile materials have greater fracture energy

compared to brittle materials (Lu and Yu, 2003). It can be concluded that specimens with wire mesh-epoxy composite have much better ductility than the plain concrete. The general findings of energy absorption performance of this method can be matched with that of internal fibre reinforcement. The energy absorption improvement in the internal fibre reinforcement is evaluated with respect to the first crack deflection (Balaguru et al., 1992). This makes the close comparison a bit difficult due to the different curves trend and materials used. However, researchers have generally reported the same findings that the enhancement in energy absorption of fibre reinforced concrete is much higher than the flexural capacity (Hassanpour et al., 2012; Mehta and Monteiro, 2006).
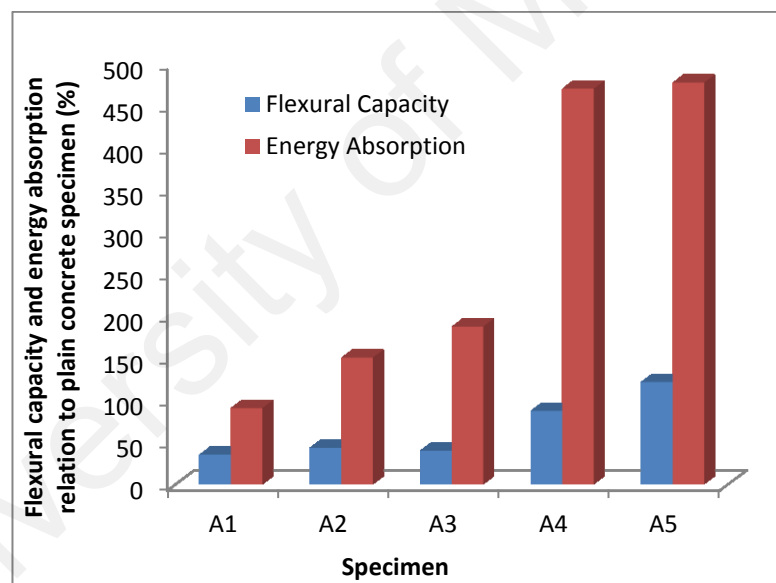
Figure 4.4: Percentage increase in flexural capacity and energy absorption of group A specimens

Figure 4.5: Failure of wire mesh-epoxy composite in specimen A4

4.2.1.2 Effect of CFRP sheet

FRP is currently the most common material used for upgrading existing reinforced concrete structures (Akbarzadeh and Maghsoudi, 2010; Obaidat et al., 2011; Teng et al., 2002; Zhou et al., 2013). Group B contains two specimens bonded with carbon fibre sheets. B1 and B2 were bonded with carbon fibre sheets having two different widths of 10 mm and 20 mm, respectively. Figure 4.6 shows the load-deflection relationships of specimens B1, B2 and CP. The load-deflection curves showed similar trends to the specimens of group A and CP. The group A specimens showed a decrease in the slope of the load-deflection curve prior to failure. For group B specimens, the load-deflection curves at failure showed a sudden drop. This drop is very similar to the plain concrete control specimen CP. Both B1 and B2 failed by premature separation of the carbon fibre and catastrophic fracture of the specimen. Overall, the achievement in deflection of group B specimens was less than for group A specimens. The deflection values at failure of B1 and B2 are presented in Table 4.1. Generally, all bonded specimens

exhibited an increase in deflection at failure over specimen CP. Specimen B1 showed better improvement of deflection at failure. Specimen B2 did not show a meaningful increase in deflection as the separation of the carbon fibre sheet occurred at a lower load than for B1. Even though the width of carbon fibre sheet was doubled in specimen B2, it could not be fully utilized in increasing the flexural performance of the plain concrete and showed premature failure before reaching its rupture strength. Separation of the carbon fibre usually occurs due to high stress concentration in certain regions. Discontinuity of material and the presence of cracks are the two main factors for causing the stress concentrations. The propagation of separation started at the high stress concentration regions. This propagation is dependent on factors, such as the bonding material, surface preparation and fracture properties of adhesion material. The failure mechanism of group B specimens can be described as follows: as the load applied on the specimen increases, the stresses in the concrete increase. When the internal stresses reach the modulus of rupture value of the concrete, micro-cracks start to propagate. The propagation of cracks in the vicinity of concrete tension face initiates the stress concentrations in some regions. A separation path at the carbon fibre-concrete interface thus starts to initiate at the end of the carbon fibre sheet. The separation propagates towards the centre of the beam until it reaches the constant moment region, where the moment is higher than the plain concrete strength and the specimen ruptures. Separation of the FRP from the concrete substrate depends on factors other than the aforementioned, such as the strength and geometry of the concrete element. Separation of the FRP is also termed "debonding". It is a common problem in the structural strengthening and rehabilitation field (Buyukozturk et al., 2004). The separation of carbon fibre sheet can be avoided by many means, such as end clamping and ensuring good surface preparation. Figure 4.7 shows specimen B1 after failure. It is important to compare the behaviour at failure of the bonded materials between the group A and

group B specimens. As explained previously, the wire mesh-epoxy composite failed by rupturing of the wire mesh layers after a significant increase in deflection and ultimate load. In contrast, the carbon fibre failed prematurely before it reached its full strength. This shows that the wire mesh had better behaviour with respect to bonding to concrete and utilizing its full strength in enhancing the properties of concrete.

Enhancement of the first crack load is one of the main purposes of this research. Specimen B1 with a 10 mm wide carbon fibre sheet failed at a load of 22 kN. There was no critical crack observed until failure of the specimen. Specimen B2, which had a carbon fibre sheet width of 20 mm, failed at 18 kN. A critical crack appeared at a load of 17 kN. Compared to group A specimens, the carbon fibre sheets did not show any resistance to crack propagation. Group A specimens increased the first crack to higher load levels. In specimens A4 and A5, for example, the first crack started to appear at a load of 25 kN and 30 kN, respectively. Even though specimen B2 had a wider carbon fibre sheet, it did not show better results with respect to the first crack and ultimate loads. Specimen B1 had better results in terms of ultimate load as it failed at 22 kN with 28.65% increase in flexural capacity over the plain concrete control specimen (Figure 4.8). From the group B test results, it can be concluded that the use of carbon fibre sheets does not significantly improve the first crack and ultimate load.

In order to evaluate the energy absorption capability of group B specimens, the area under the load-deflection curve for each specimen is calculated. As mentioned previously, group B specimens did not exhibit much improvement in ultimate load and deflection. Consequently, the amount of energy absorbed at the fracture was not improved remarkably. The calculated energy absorption values of specimens B1 and B2 are shown in Table 4.1. Figure 4.8 compares the percentage increase in energy absorption with that of flexural capacity enhancement for group B specimens. Specimen

B2 did not exhibit much of an increase in energy absorption compared to the increase in flexural capacity.

The primary objective of using carbon fibre sheets was to compare the enhancement in plain concrete behaviour with different bonded materials having similar ultimate or yield load. For the sake of comparison, Specimens A4 and B1 were bonded with two types of material that have the same load carrying capacity. The effectiveness of each material is evaluated with respect to the increase in the flexural capacity of each specimen. A lower amount of carbon fibre was applied, as it has higher ultimate tensile strength. The calculated yield load of one layer of wire mesh is 2.12 kN. This means that the four wire mesh layers in specimen A4 can carry approximately 8.49 kN. The 10 mm carbon fibre sheet will rupture at 8.33 kN. The increase in ultimate load in B1 was much lower than A4. Specimen A4 exhibited an increase in the flexural capacity of about 88%, whereas specimen B1 exhibited an increase of only 29%. In the other specimen, B2, the width of carbon fibre sheet was doubled to 20 mm. The larger carbon fibre sheet width in specimen B2 was expected to increase the ultimate load more than specimen B1. The specimen failed at a lower load with an increase in flexural capacity of only 5% due to the separation of carbon fibre. This failure is undesirable as the strength of carbon fibre is not fully utilized. Other studies that have used internal polymeric fibres (e.g. polypropylene) to improve the properties of concrete have shown better results compared to the externally bonded carbon fibre sheets (Soroushian and Tlili, 1993; Yap et al., 2014; Yap et al., 2013).
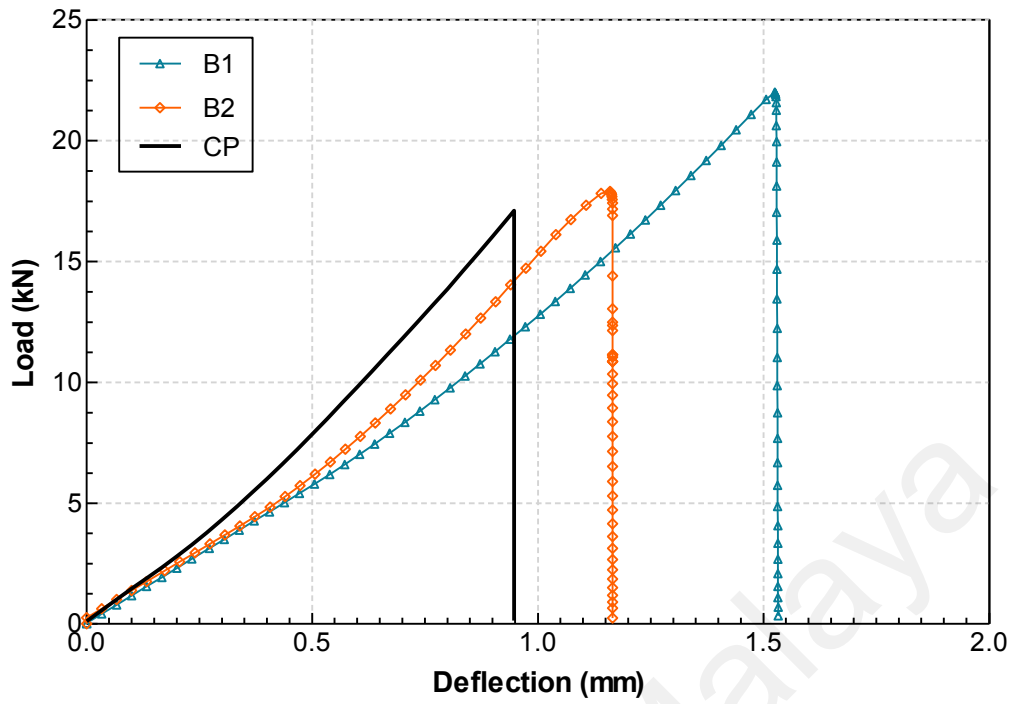
Figure 4.6: Load-deflection curves of group B specimens and control specimen CP

Figure 4.7: Separation of CFRP sheet in specimen B1
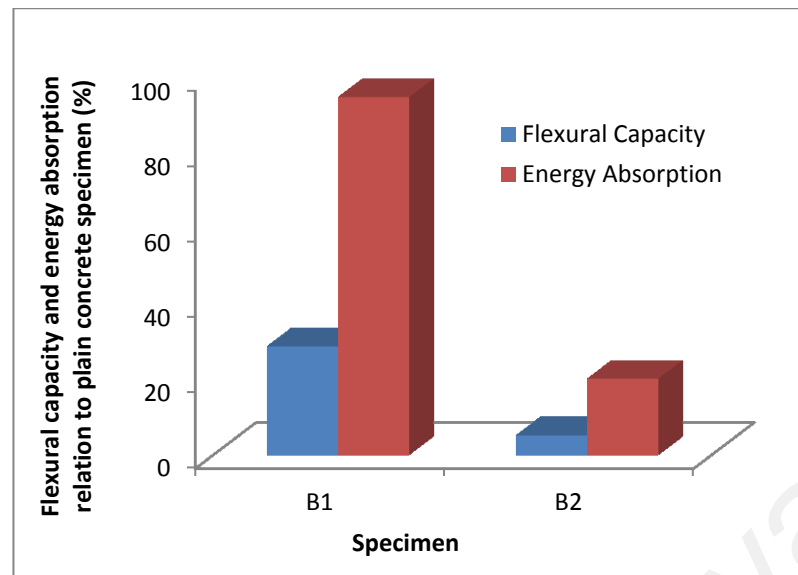
Figure 4.8: Percentage increase in flexural capacity and energy absorption of group B specimens

4.2.1.3 Effect of hybrid wire mesh-epoxy-carbon fibre composite

The use of hybrid materials for enhancing the performance of concrete structures has recently attracted major attention (Attari et al., 2012; Wang et al., 2012; Yi and Cho, 2012). Group C specimens were bonded with a carbon fibre sheet and two layers of wire mesh. The carbon fibre sheet width was the same in this group (20 mm). In specimen HY1, the wire mesh had the same width as the carbon fibre sheet (20 mm). However, the HY2 specimen had 100 mm wide wire mesh layers. The main purpose of the use of this hybrid composite was to study the effect of the addition of wire mesh on the overall behaviour of specimens bonded with carbon fibre. The aim of the bonding configuration of specimen HY1 was to study the contribution of the wire mesh to the carbon fibre without providing any clamping effect. Whereas, in specimen HY2 the additional clamping effect provided by the wire mesh in preventing or delaying separation was studied. The contribution of the wire mesh is evaluated by comparing specimens HY1 and HY2 with B2. The load-deflection relationships of specimens HY1 and HY2 are shown in Figure 4.9. The load increased linearly with deflection until the

occurrence of the first crack. At this stage, a drop in load was observed. The load-deflection curve beyond this point was no longer linear and showed a fluctuation in load. This fluctuation is due to the sequential failure of the wire mesh. The sequential rupture of wire mesh allows additional deflection as it reaches its failure strain and the load is totally transferred to the carbon fibre. The carbon fibre sheet then started to separate at its tip. Specimens HY1 and HY2 failed at a deflection of 2.01 mm and 2.24 mm, respectively. These deflection values are larger than the deflection at failure (1.17 mm) for B2. Figure 4.9 also compares between specimens HY2 and A2. Specimen HY2 failed at a higher ultimate load and deflection. Both specimens had similar behaviour until the occurrence of the first crack. However, specimen HY2 showed much better results in the non-linear part due to the contribution of the carbon fibre and gradual failure of the wire mesh. The carbon fibre sheet delayed the specimen fracture after the failure of the wire mesh. The specimen final failure was by separation of the carbon fibre sheet. Generally, hybrid specimens showed better non-linear deformation compared to both the carbon fibre and wire mesh specimens alone.

The crack opening of group C specimens was also evaluated. Table 4.1 presents the first crack load values of specimens HY1 and HY2. In specimen HY1, the first crack was detected at a load of 20 kN. Compared to specimen B2, there is an improvement in the first crack load. The first crack in specimen HY2 occurred at a load of 23 kN. The improvement in first crack load in specimen HY2 is better than for HY1. The larger width of wire mesh delayed the propagation of micro-cracks. As can be seen in Figure 4.9, the maximum load value of specimen HY1 was about 20 kN, and 28 kN for specimen HY2, which shows an increase of about 40%. The flexural load capacity of the HY2 specimen is also about 13.8% and 55.6% higher than that of specimens A2 and B2, respectively. The increase in ultimate load for specimen HY2 is due to two main

reasons – the additional amount of wire mesh as well as the clamping effect provided by the wide wire mesh layers, which delayed the separation of the carbon fibre sheet.

The energy absorption values of specimens HY1 and HY2 are shown in Table 4.1. The energy absorption ratio between group C specimens and control specimen (CP) is also shown in Figure 4.10. Both specimens showed a remarkable energy absorption capability. The gradual failure of wire mesh caused a 'zig-zag' loading and unloading manner in the non-linear phase of the load-deflection curve. This behaviour increased the deflection and prevented the catastrophic failure of the specimen. After the failure of the wire mesh, the specimen did not fracture immediately like the specimens in group A. It continued carrying the load until the final separation of the carbon fibre sheet. The addition of the wire mesh to specimen B2 proved to have a significant enhancement in ductility of the specimens bonded with carbon fibre sheets. Furthermore, compared to the specimens in groups A and B, the non-linear phase of group C specimens is considerably larger. A study by Wu et al. (2007) revealed that the failure of lower strain material redistributes the strain in the hybrid and thus reduces the stress concentrations and propagation of separation. This explains the delay in separation in specimen HY1 even though it did not have any clamping, as in HY2. Other factors, such as the amount of epoxy associated with the wire mesh and surface preparation might have a minor effect. The increase in flexural capacity in comparison with energy absorption should also be discussed. Figure 4.10 shows that specimen HY1 compared to control specimen gained an increase in flexural capacity of only 22%. However, the enhancement of energy absorption was about 289%. Specimen HY2 had an increase in flexural capacity and energy absorption of about 64% and 356%, respectively. It can be seen that just by using a small width (20 mm) of carbon fibre the flexural capacity and energy absorption of the beam improved significantly. In addition, as can be seen in Figure 4.11, the performance of the HY2 specimen in terms of flexural capacity and energy absorption is

better than the beam with three wire mesh layers (A3), and is close to the beam with four wire mesh layers (A4). Therefore, as a result, the use of a hybrid of carbon fibre and wire mesh significantly improves both flexural capacity and energy absorption. The improvement in energy absorption of specimen HY2 over specimen A2 is also related to the ability of the carbon fibre sheet to carry an increasing load after the failure of the wire mesh. Although the final failure of group C specimens was by separation, it occurred after gaining reasonable ductility. This leads to the conclusion that the use of wire mesh with carbon fibre proved that it could either reduce or even prevent the brittle failure of carbon fibre bonded specimens.
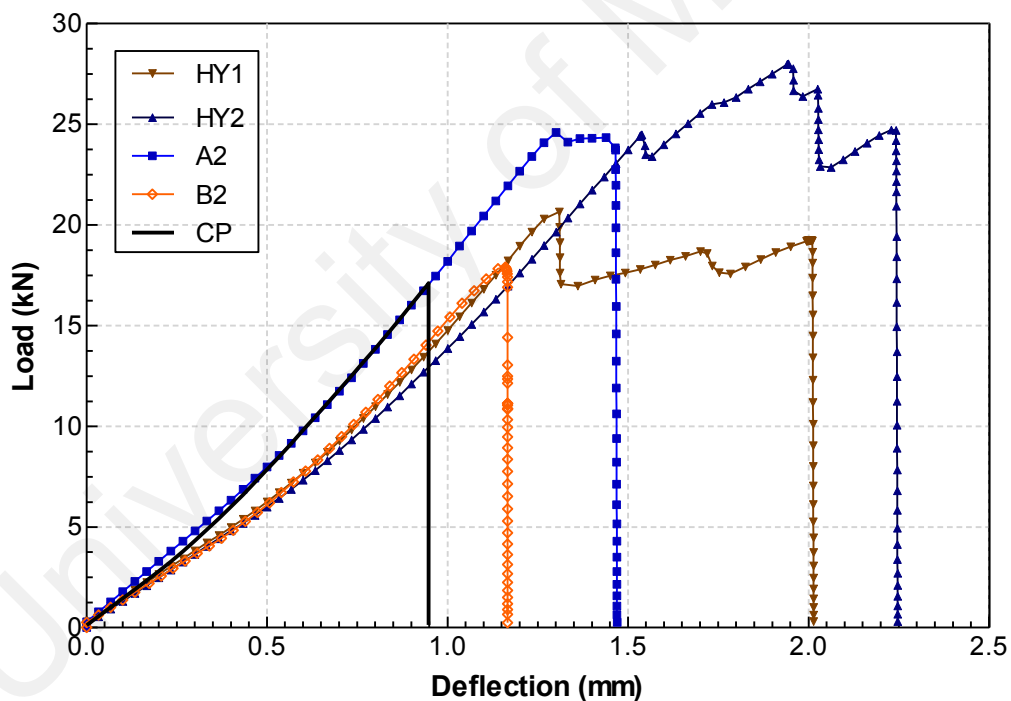

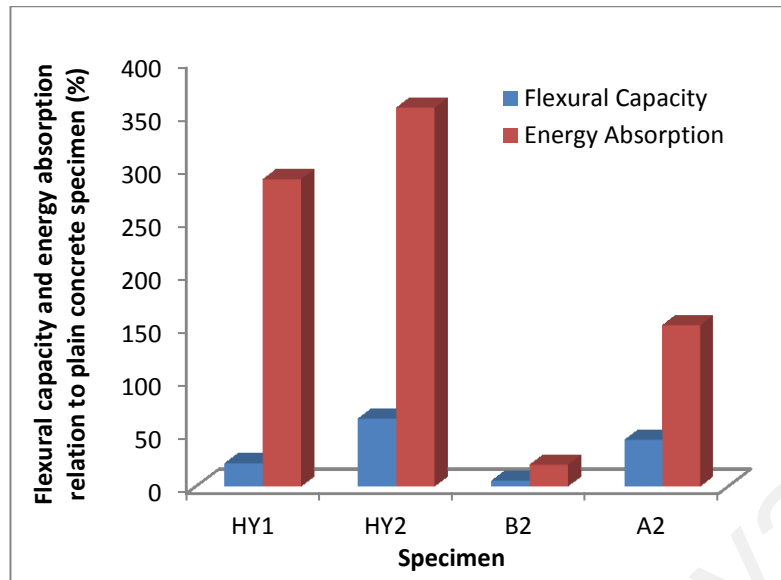Figure 4.9: Load-deflection curves of group C specimens and specimens A2, B2 and CP

Figure 4.10: Percentage increase in flexural capacity and energy absorption of group C specimens, specimen B2 and specimen A2
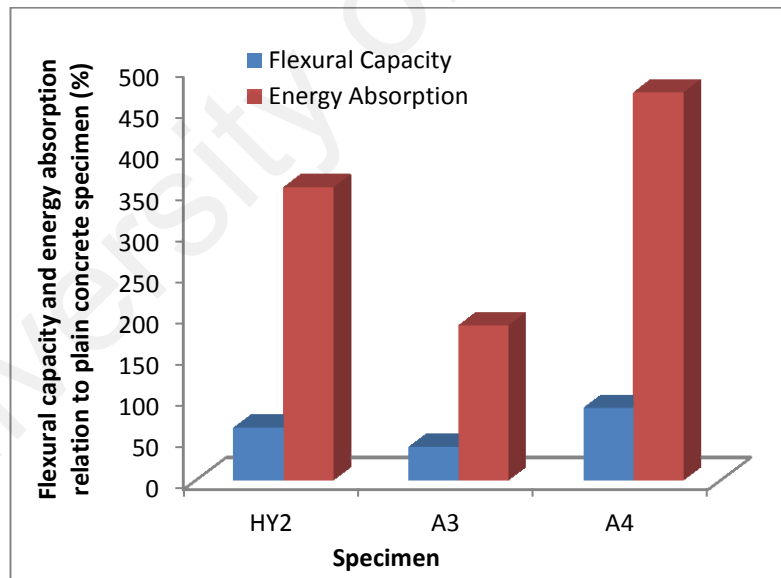

Figure 4.11: Enhancement in flexural capacity and energy absorption of HY2, A3 and A4 specimens

4.2.2 Second group of plain concrete beams

In this study, four concrete beam specimens were tested. One specimen was considered as control. Specimens A1, A2 and A3 had composite widths of 95, 70 and 45 mm, respectively. The amount of wire mesh and epoxy was kept the same in all specimens. The following sections discuss the improvement in performance of concrete beam specimens bonded with different widths of wire mesh-epoxy composite.

4.2.2.1 Flexural capacity and deflection at failure

The test results are summarized in Table 4.2. In addition, Figure 4.12 presents the load-deflection relationships of all specimens. The load-deflection curves have two main stages. The first stage represents the linear increase in load with deflection. At this stage, the specimen maintains its full flexural rigidity. The second stage represents the reduction in slope and non-linear pattern of curve. This stage starts after the occurrence of first crack. All specimens bonded with wire mesh-epoxy composite exhibited increase in their load carrying capacity. This is due to the contribution of wire mesh-epoxy composite in the tension face of specimens. The plain concrete control specimen fails suddenly without showing any cracks. The failure took place immediately after the occurrence of first crack. Specimen A1 had increase in ultimate load of about 24.8 kN. A crack appeared in the specimen mid-span at load 24.0 kN. A small drop in the slope of load-deflection curve was observed at the occurrence of the first crack. The load then showed a small increase with the increase in deflection until the specimen failure. The increase in ultimate load value of specimen A2 was up to 23.2 kN. A crack was observed at load of 21.4 kN and propagated with the increase in load until the final failure. Figure 4.13 shows the failure of specimen A2. Specimen A3 had a linear increase in load with deflection until 25.1 kN. A critical crack was observed at this load

level. In addition, a large drop in load until 22.0 kN occurred. However, at this load level the specimen was able to carry load constantly until final failure. Figure 4.14 shows the propagation of crack in specimen A3. In general, all bonded specimens had similar load carrying capacities. This is expected as the same amount of wire mesh was used for all specimens. In addition, it should be noted that the first crack load values of bonded specimens were higher than the failure load value of control specimen. The results reported in this study can be compared with the previous studies on the use of internal fibres for the improvement of concrete performance (Padron and Zollo, 1990; Soulioti et al., 2011). The cracking behaviour of externally wire mesh-epoxy bonded concrete specimens is different from fibre-reinforced concrete. In the fibre-reinforced concrete, the first crack occurs at very early stage, whereas, in the wire mesh-epoxy bonded specimens the crack is delayed considerably. This is important for concrete under service load. The deflection at failure values of all specimens are shown in Table 4.2. All bonded specimens exhibited increase in deflection at failure compared to the plain concrete control specimen. Specimens A1, A2 and A3 had increase in deflection at failure of about 40%, 11% and 18% over the control specimen, respectively. Furthermore, the amount of epoxy used for bonding the wire mesh layers was found approximately 1.5 kg/m^2. The amount recommended by the manufacturer for bonding the carbon fibre using the same epoxy was in the range of 0.7~1.5 kg/m^2 (Sikadur$^®$-330, 2012). This shows the cost-effectiveness of using wire mesh-epoxy composite for enhancing the performance of concrete structures when considering the high cost of FRP material compared to wire mesh.

Table 4.2: Summary of test results of the second group of plain concrete beams

Specimen	Ultimate load (kN)	Deflection at failure (mm)	Energy absorption (N.m)
Control	21.0	0.91	8.85
A1	24.8	1.57	16.87
A2	23.2	1.08	11.58
A3	25.1	1.20	14.62
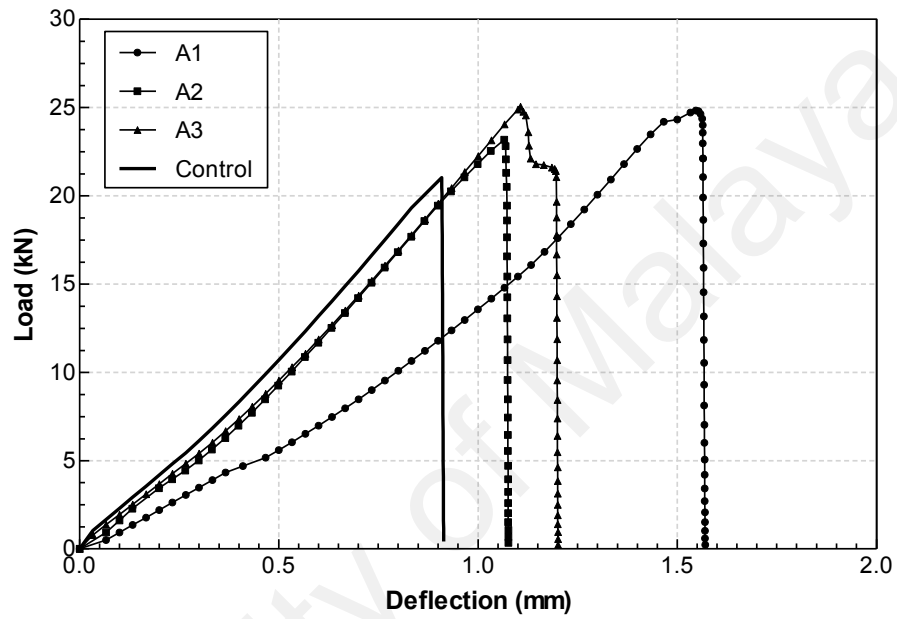
Figure 4.12: Load-deflection relationships of all specimens
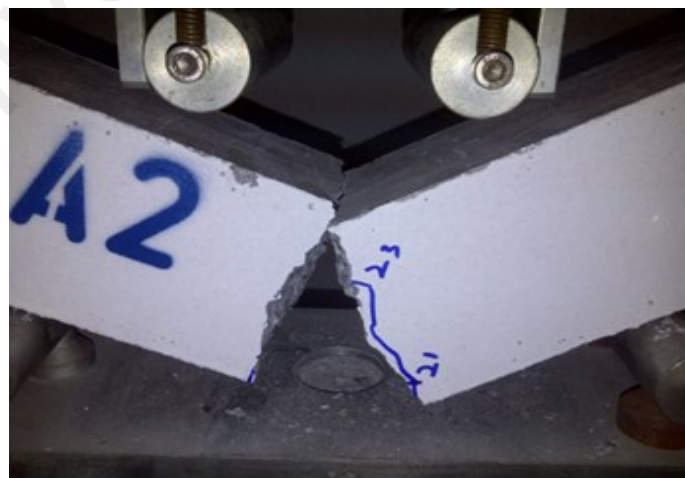
Figure 4.13: Failure of specimen A2

Figure 4.14: Propagation of crack in specimen A3 during test

4.2.2.2 Energy absorption

Table 4.2 presents the energy absorption values of all specimens. The energy absorption value is obtained by calculating the area under the load-deflection curve. The plain concrete specimen had a sudden failure when the load exceeded its ultimate strength. The plain concrete normally has a number of micro cracks. These micro cracks propagate rapidly with the increasing stresses causing the fracture of specimen. Specimens A1, A2 and A3 could carry higher loads than the plain concrete specimen and deflected at higher values. Observations of specimens after failure revealed that the failure occurred after the rupture of wire mesh-epoxy composite. The percentage increase of energy absorption and flexural capacity of bonded specimens over the control specimen is shown in Figure 4.15. Specimens with different wire mesh-epoxy composite widths had different amounts of energy absorption. Specimens A1 and A3 gained energy absorption of 91% and 65%, respectively, whereas, specimen A2 gained only 31% over the plain concrete specimen. From the results, it can be concluded that the specimen with the large wire mesh-epoxy composite width had the highest improvement in energy absorption. This is due to the fact that the wider composite had more contact area with the concrete surface. This provides more restraint to the micro

cracks in the tension face of specimen and consequently prevents the rapid propagation of micro cracks which cause the specimen failure. In addition, it can be seen from Figure 4.15 that the improvement in energy absorption capabilities of bonded specimens is large compared to the flexural capacity. The increase in flexural capacity and energy absorption of specimen A1, for example, was about 18% and 91% over the control specimen, respectively. This finding is similar to the reported studies for fibre-reinforced concrete (Hassanpour et al., 2012) where the enhancement in energy absorption is much higher than ultimate load.
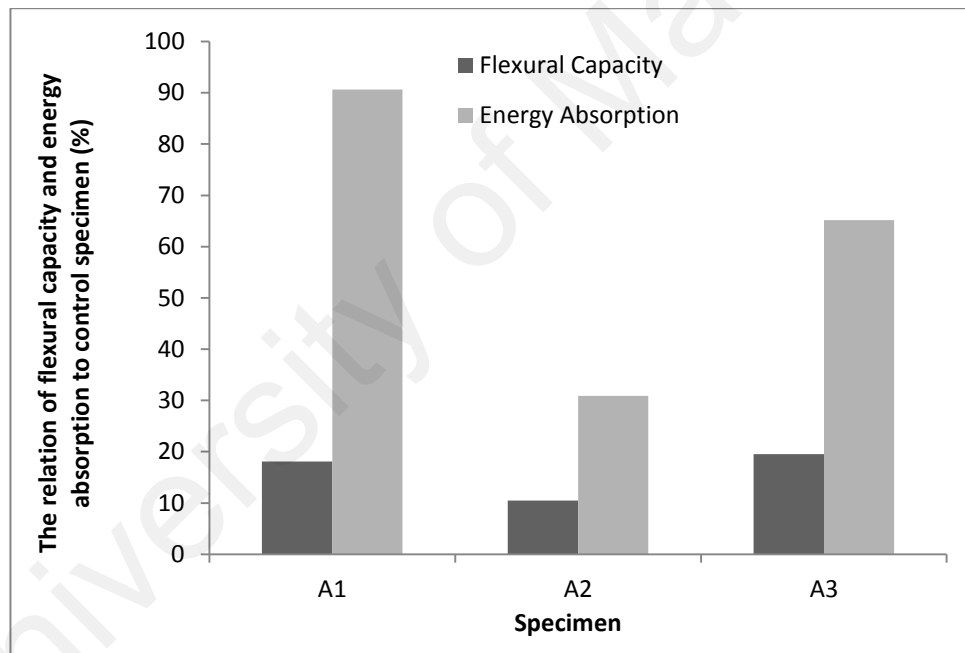

Figure 4.15: Percentage increase in flexural capacity and energy absorption of all specimens

4.3 RC beams

4.3.1 Load-deflection behaviour

The load-deflection response of strengthened beams varies significantly depending on the type of strengthening material (Brena et al., 2003). This variation provides a useful measure of the performance of strengthened beams. The effectiveness of the wire mesh-epoxy composite, CFRP and hybrid wire mesh-epoxy-carbon fibre composite is evaluated and discussed in the following sections.

4.3.1.1 Effect of wire mesh-epoxy composite

The load-deflection relationships of the control specimen (CB) and specimens A1 and A2 are shown in Figure 4.16. Table 4.3 summarizes the load and deflection values at the first crack, yielding and peak for all specimens. It should be mentioned that specimen A1 was strengthened with wire mesh-epoxy composite applied directly on the beam soffit, whereas specimen A2 was strengthened with the wire mesh-epoxy composite in the form of a laminate. The control specimen failed after the yielding of internal steel reinforcement and concrete crushing in the compression zone. Specimens A1 and A2 failed at two different stages, fracture of wire mesh-epoxy composite at yield, followed by concrete crushing after a significant increase in the deflection. The load-deflection curves are trilinear defining three distinct stages: the first stage corresponds to the uncracked section and full elastic behaviour of the beam. The load-deflection curve in this stage is almost a straight vertical line representing the full flexural rigidity of the beam. The second stage starts with the initiation of cracks in the tension zone. In this stage, the maximum tensile stresses in the beam exceed the flexural strength of the concrete. Consequently, the beam has a decrease in its flexural stiffness. This can be observed by the reduction in the slope of the load-deflection curve. The third stage

includes the yielding of the steel reinforcement. The beam at this stage carries a constant amount of load and shows a significant increase in the deflection up to final failure. The load-deflection curve in this stage is almost flat and the beam is considered to have failed. The first crack appeared in the control beam at a load of 10 kN. However, the first crack was observed in beams A1 and A2 at loads of 19 and 18 kN, respectively. This shows an increase of up to 90% over the control beam. The delay in the first crack is mainly attributed to the wire mesh-epoxy composite on the beams soffits. The wire mesh-epoxy composite prevented the initiation of micro-cracks in the vicinity of the beam tension face, and, consequently, prevented the propagation of cracks. The delay of the cracks is of great importance for the serviceability of beams. Maintaining the uncracked section prevents the penetration of water and carbon dioxide from the surrounding environment, which might result in the corrosion of the steel reinforcement. Specimens A1 and A2 showed better stiffness in the post-cracking stage compared to the control specimen. This can be observed from the slope of the load-deflection curve. The load-deflection curves of specimens A1 and A2 are steeper than the control specimen, as shown in Figure 4.16. The improvement in stiffness is due to the contribution of the wire mesh-epoxy composite. The wire mesh-epoxy composite restrained the cracks from widening and the beam could carry higher loads without significant loss in stiffness. The control beam yielded at a load of 54 kN as expected. However, beams A1 and A2 exhibited a significant increase in their yield loads, which were 70 and 68 kN, respectively. This significant increase is important for achieving the required service loads. The wire mesh-epoxy composite ruptured at the mid-span at slightly higher loads than the yield load. The load-deflection curves of specimens A1 and A2 then showed a drop in load to 57 and 55 kN, respectively. These load values are close to that of the control specimen after the yielding load (47 kN). However, the slight increase in load over the control specimen is attributed to the contribution of wire mesh-

epoxy composite at the remaining sections of the beam to the overall rigidity. It should be noted that there was no premature debonding between the wire mesh-epoxy laminate and the concrete surface during all loading stages. The composite continued to contribute to the load carrying capacity and stiffness with a full composite action until rupture. Figure 4.17 shows the failure of the wire mesh-epoxy composite laminate in specimen A2. The specimens then continued to deflect until final failure by concrete crushing followed by rupture of the steel reinforcement.

By comparing the behaviour of specimens A1 and A2, it was found that the wire mesh-epoxy composite could give the same enhancement to the beams behaviour when applied as a laminate. As a result, the wire mesh-epoxy composite can be prepared and delivered to the site in the form of laminate for easier and more practical strengthening process of structures. In practice, the weight of strengthening materials is an important factor. The calculated density of the wire mesh-epoxy composite laminate was found to be 1627 kg/m^3. The density of mild steel is about 7800 kg/m^3 (El-Reedy, 2010). This indicates that the density of steel is about five times the density of the wire mesh-epoxy composite laminate. Hence, the wire mesh-epoxy composite laminate has much lighter weight compared to steel plates. This provides easy handling of the strengthening material on site.

Table 4.3: Results of tested RC beams

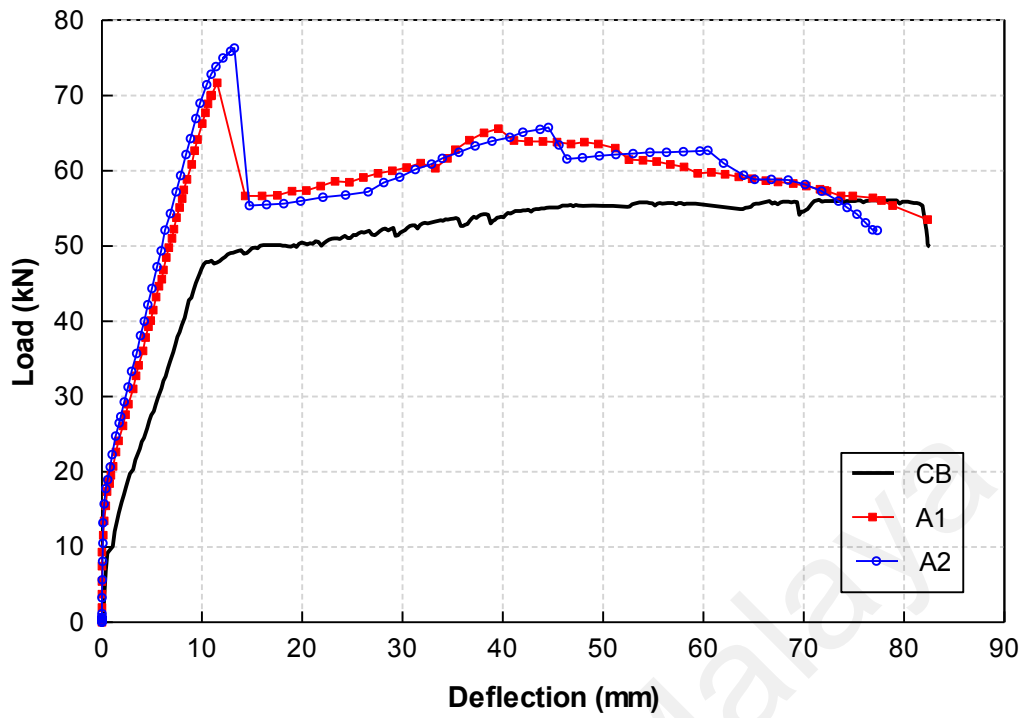| Beam	First crack		Yield		Peak		Mid-span deflection (mm)			
	Load (kN)	% increase	Load (kN)	% increase	Load (kN)	% increase	First crack	Yield	Peak	Failure
CB	10.0	-	47.5	-	56.0	-	1.05	10.1	76.1	82.6
A1	19.0	90.0	70.0	47.4	72.1	29.0	0.73	12.0	12.0	82.4
A2	18.0	80.0	68.0	43.2	75.1	29.0	0.45	12.5	12.5	77.1
B	15.0	50.0	58.4	23.0	77.6	39.0	0.82	9.7	35.0	95.5
HY	16.3	63.0	70.1	47.6	82.3	47.0	1.54	13.4	20.1	74.9

Figure 4.16: Load-deflection relationships of specimens CB, A1 and A2
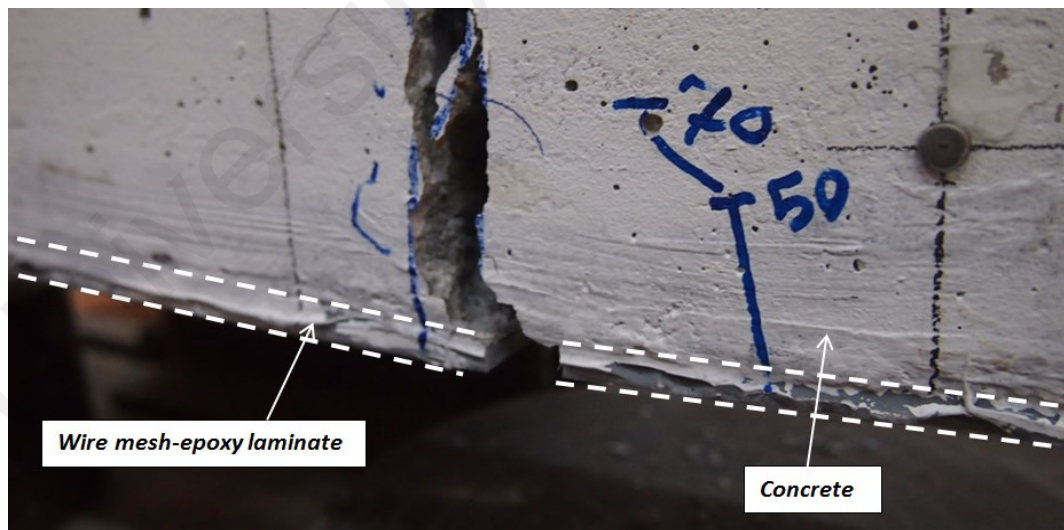

Figure 4.17: Failure of wire mesh-epoxy laminate in specimen A2

4.3.1.2 Comparison between the performance of the wire mesh-epoxy composite and the CFRP

The use of FRP materials for the strengthening and retrofitting of existing RC structures has increased considerably in recent years (Akbarzadeh and Maghsoudi, 2010; Bakis et al., 2002; Meier, 1995). Specimen B was strengthened with a 75 mm wide CFRP sheet. The load-deflection relationships of specimens B, A2 and the control specimen (CB) are shown in Figure 4.18. The first crack occurred in specimen B at a load of 15 kN with an increase of about 50% over the control specimen. The specimen also showed a slight improvement in stiffness after the first crack compared to the control specimen. In addition, the specimen yielded at a load of 58.4 kN. This shows an increase of 23% over the control specimen. A comparison can be made between the behaviour of specimens A1 and A2 and specimen B. Specimens A1 and A2 exhibited an increase in the first crack and yield loads of up to 90% and 47%, respectively. In addition, the maximum load carrying capacity was achieved at the yielding of the steel reinforcement in specimens A1 and A2. This indicates that a significant enhancement in the behaviour of specimens strengthened with wire mesh-epoxy composite is gained in the pre-yielding stages. This is of great importance for achieving the required increase in load and the delay of cracking for beams under service load. In RC design, the beam is considered structurally failed after the yielding of the steel reinforcement (Nawy, 2005). Therefore, the effectiveness of the strengthening material is always evaluated based on the amount of increase in load prior to the yielding of the steel reinforcement. Specimen B showed a higher ultimate or peak load than specimens A1 and A2. However, this increase in load only occurred after the yielding of the steel reinforcement. This is mainly attributed to the properties of the FRP material. FRP is a brittle material that shows a linear stress-strain behaviour until failure. In addition, the failure strain of CFRP in specimen B is 21000 microstrains, whereas the yield strain of the tension steel reinforcement is 2700

microstrains. Therefore, the tension steel in specimen B yielded before the CFRP sheet strains, and shows a measurable increase in load. Consequently, CFRP only showed a considerable contribution to the load carrying capacity after yielding. Specimen B continued to deflect significantly after yielding with an increase in load values until reaching the maximum load (77.6 kN). A sudden drop in load to 55.9 kN was then observed at a deflection of 34.5 mm. This drop is due to the debonding of the CFRP sheet. Debonding is a common failure mode in beams strengthened with FRP materials (Buyukozturk et al., 2004; Büyüköztürk and Yu, 2006; Teng and Chen, 2007). Debonding of FRP occurs due to the high stress concentrations at certain regions in the interface between the FRP and the concrete. The stress concentrations are initiated due to the discontinuities of materials and the occurrence of cracks. As a result, a separation propagation path is initiated at the regions of high stress concentration depending on the properties of the strengthening materials and the surface conditions of the concrete. Figure 4.19 shows specimen B after the debonding of the CFRP sheet. Debonding is an undesirable failure mode in the structural strengthening, as the FRP material, which has a relatively high cost, cannot be utilized effectively. The specimen continued to deflect after debonding at almost constant load values until final failure. It can be concluded that the wire mesh-epoxy is more efficient in increasing the load-carrying capacity of beams under service compared to CFRP. In addition, the wire mesh-epoxy composite failed by fracture. This indicates that the material was fully utilized for achieving the targeted improvement in the structure load carrying capacity unlike the CFRP, which failed by premature debonding.
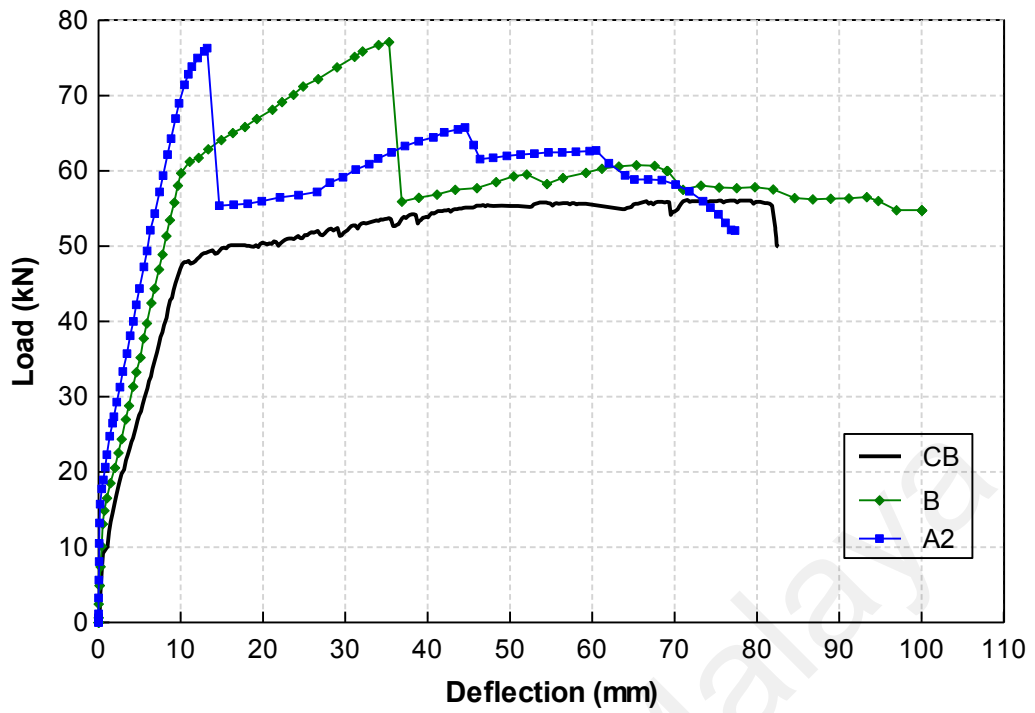
Figure 4.18: Load-deflection relationships of specimens B, A2 and CB

Figure 4.19: Debonding of CFRP sheet in specimen B

4.3.1.3 Performance of hybrid of wire mesh-epoxy composite and CFRP for strengthening

Specimen HY was strengthened with a hybrid of strengthening materials, namely, a wire mesh-epoxy-carbon fibre composite. Recently, hybrid composite materials have been increasingly used for the strengthening and retrofitting of RC structures (Grace et al., 2004; Hosny et al., 2006; Wu et al., 2006; Yi and Cho, 2012). The load-deflection relationships of specimens HY and CB are presented in Figure 4.20. It was shown in the previous sections that the specimens bonded with wire mesh-epoxy composite exhibited a drop in load after yielding due to the fracture of the wire mesh-epoxy composite. Despite the significant increase in yield load, the specimen did not show a significant enhancement in the load carrying capacity after yielding. In addition, specimen B showed a considerable increase in load carrying capacity only after yielding. The main aim for using the hybrid wire mesh-epoxy-carbon fibre composite is to investigate the enhancement of behaviour of strengthened specimens at the overall loading process, i.e. pre-yield and post-yield stages. The results of plain concrete specimens showed that the use of hybrid wire mesh-epoxy with carbon fibre produces progressive failure due to the sequential rupture of materials with different failure strains. Similar to the other strengthened specimens, specimen HY exhibited an increase in the first crack load of up to 16.3 kN. The specimen also showed a slight increase in stiffness after the occurrence of the first crack compared to the control specimen. The yield load was increased up to 70 kN. This indicates an increase in the first crack and yield loads of 63% and 47.6% over the control specimen, respectively.

In comparison with the specimens bonded with wire mesh-epoxy and CFRP alone, specimen HY exhibited a similar enhancement in yield load. After yielding, the specimen continued carrying increasing loads until 80 kN. The wire mesh-epoxy composite then ruptured and a drop in load to 72 kN was observed. This drop in load is

more gradual compared to that in the specimens with the wire mesh-epoxy composite alone, which is due to the existence of CFRP sheet. After the rupture of the wire mesh-epoxy composite, the load was totally transferred to the CFRP sheet. As the specimen started to deflect at larger values, the CFRP sheet strained remarkably. Hence, the CFRP sheet started to contribute significantly to the specimen load carrying capacity in the post-yielding stage. It should be noted that small debonding at the mid-span in the wire mesh-epoxy laminate was observed after the rupture, as seen in Figure 4.21. The debonding at mid-span is attributed to the loss in composite action between the wire mesh-epoxy laminate and the CFRP sheet. After the rupture of the wire mesh-epoxy composite at yielding, a small slippage at the interface of the wire mesh-epoxy composite and CFRP sheet occurred. This slippage occurred due to the material relaxation after fracture. Hence, a debonding propagation path started to initiate. However, the propagation did not extend, which was largely due to the strong bonding between the laminate and concrete surface at the sections that are away from the mid-span. Specimen HY carried a load up to 82.3 kN. This increase in load is the largest compared to the A1, A2 and B specimens. The CFRP sheet then started to rupture while maintaining higher load values compared to control beam. In addition, The CFRP sheet in specimen HY did not debond like in the case of specimen B. This is attributed to the clamping effect provided by the wire mesh-epoxy laminate. Therefore, the CFRP sheet could be fully utilized for improving the performance of the strengthened specimen. It can be concluded that the use of a hybrid wire mesh-epoxy-carbon fibre composite can significantly provide a better performance of the strengthened specimens at all loading stages compared to the use of wire mesh-epoxy and CFRP alone.
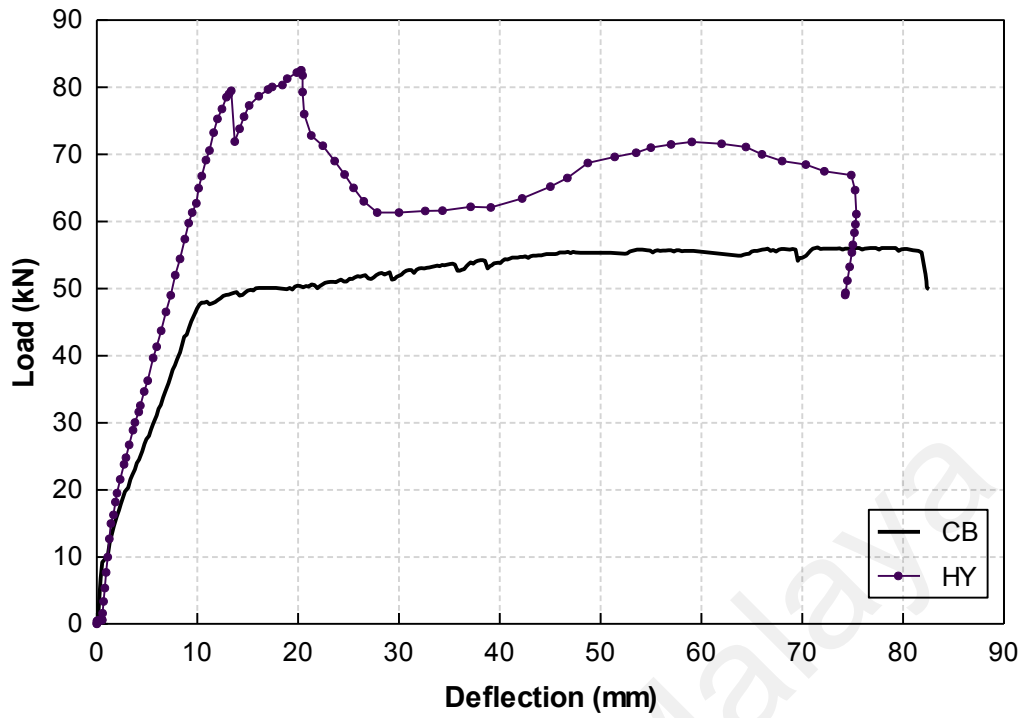
Figure 4.20: Load-deflection relationships of specimens HY and CB
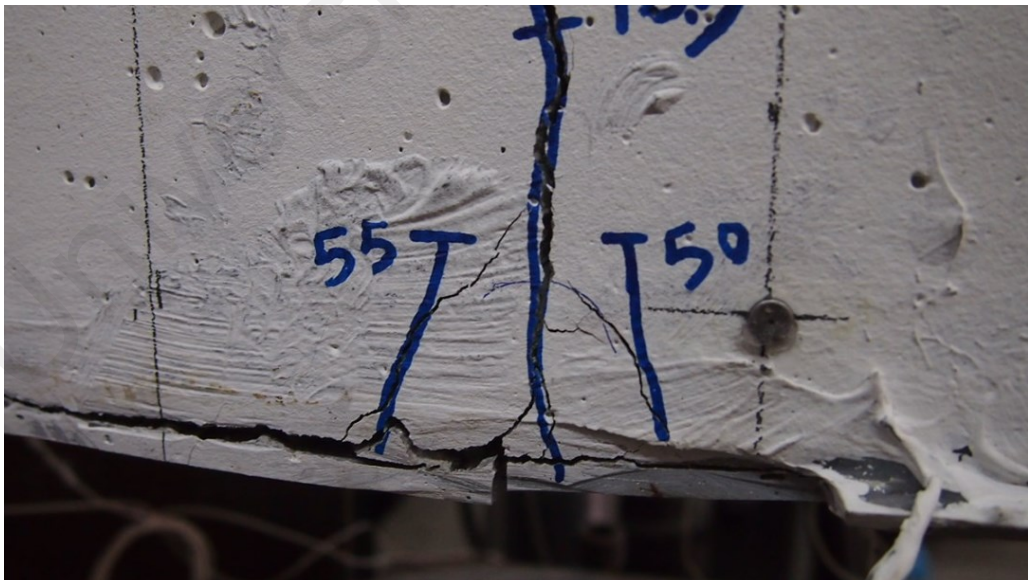

Figure 4.21: Debodning of wire mesh-epoxy composite at mid-span after rupture in specimen HY

4.3.2 Stiffness of the beams

Stiffness is an essential concern when considering the serviceability behaviour of the RC structures. The stiffness values of all the specimens are presented in Table 4.4. All the strengthened beams showed significantly more stiffness than the control specimen. However, all the specimens showed a reduction in stiffness after the occurrence of the first crack. Most beams that carry service loads are usually at this stage (Nawy, 2005). Hence, it is important to evaluate the increase in the stiffness of the strengthened specimens at the working load range. The working load range is defined in the load-deflection curve as the point of deflection that is equal to the span/480. This ratio is provided by the ACI Committee 318 (2008) for roofs or floors constructed supporting or attached to non-structural elements that are likely to be damaged by large deflections. The working load deflection (span/480) for all beams was found to be 5.2083 mm. As seen in Table 4, all the strengthened specimens exhibited an increase in stiffness at a service load of up to 59.5% over the control specimen, CB. In normal RC unstrengthened beams, the internal steel reinforcement affects the stiffness of the beam by controlling the growth of the cracks. However, the external bonded material provides restraint to the initiation and growth of the cracks. Specimens A1 and A2, bonded with wire mesh-epoxy composite, showed the largest increase in stiffness compared to the other two specimens (B and HY). In strengthened RC beams, the overall stiffness is dependent on the concrete, steel and epoxy used for bonding the external reinforcement. The steel used for the beam specimens has an elastic modulus of about 200 GPa, which is five times the elastic modulus of concrete (39 GPa). Whereas, the elastic modulus of epoxy used in this study (4.5 GPa) is a small fraction compared to concrete and steel. Specimens A1 and A2 gained enhancement in stiffness of 48.4% and 59.5%, respectively, while specimen B showed the lowest increase in stiffness with only a 27.7% increase over specimen CB. A study by Swamy et al. (1987) showed that the

flexural stiffness and rigidity of strengthened specimens depends greatly on the degree of cracking, loading level, thickness of bonded material and adhesive. This explains the variation in stiffness throughout the specimens. The total thickness of epoxy used in the composite laminate reached approximately 5 mm. This value is large compared to that used for the CFRP sheet. In addition, the CFRP sheet used in specimen B has a thickness of 0.17 mm. This thickness is too small compared to the composite laminate. Specimen HY did not show a considerable increase in stiffness compared to specimens A1 and A2 even though the wire mesh-epoxy composite was attached to the tension face of the specimen. The wire mesh-epoxy composite laminate in specimen HY was not in full contact with the concrete surface as in specimens A1 and A2 due to the existence of the CFRP sheet in the hybrid composite.

Table 4.4: Effect of strengthening on stiffness and energy absorption

Beam	Stiffness at service moment (kN.m/m)	% increase	Energy absorption (N.m)	% increase
CB	2439	0	4335	0
A1	3620	48.4	4777	10.2
A2	3890	59.5	4693	8.3
B	3114	27.7	5873	35.5
HY	3222	32.1	4812	11.0

4.3.3 Energy absorption values

The energy absorption values for all specimens are shown in Table 4.4. Energy absorption is a paramount characteristic for the evaluation of the fracture work of the overall structural element. The energy absorption is estimated by the area under the load-deflection curve. All the strengthened specimens showed higher energy absorption

values compared to the control specimen. Specimens A1 and A2 exhibited an increase in energy absorption of about 10.2% and 8.3%, respectively. In the control beam, the steel started to yield when the applied load reached the yield strength, and the cracks propagated significantly throughout the specimen section. However, a considerable delay in the cracks and enhancement of the yield load was achieved in the wire mesh-epoxy bonded specimens. In addition, both specimens, A1 and A2, showed a close amount of energy absorption capability. Hence, it can be concluded that the use of the laminate of wire mesh-epoxy composite gives a similar enhancement to the beams energy absorption and overall ductility compared to the wire mesh-epoxy applied directly to the beam, as in the case of specimen A1. Specimen HY with the hybrid of wire mesh-epoxy-carbon fibre composite showed a slightly better enhancement in energy absorption than specimens A1 and A2. The increase in energy absorption in specimen HY was found to be about 11% over that of the control beam. This enhancement is attributed to the sequential failure of the wire mesh-epoxy and CFRP. However, the small enhancement in the energy absorption capability is attributed to the rapid rupture of the CFRP sheet after the failure of the wire mesh-epoxy at a relatively high load. Hence, further studies are needed to investigate the effect of different amounts of CFRP in the hybrid on the energy absorption and ductility of the strengthened specimens. Specimen B showed an increase in energy absorption of about 35% over the control beam. The large increase in the energy absorption is related to the increase in the load and improvement in stiffness after yielding. In addition, due to the relatively low reinforcement ratio and high concrete compressive strength of the beam specimens, the contribution of the CFRP to the overall deformability of the specimen in the post-yield stage delayed the concrete crushing. As a result, the specimen showed higher deflection at failure compared to the other specimens.

4.3.4 Measured strains

The measured strain values at the mid-span of the steel, wire mesh-epoxy and CFRP for all specimens are presented in Table 4.5. The strain of the steel at failure could not be recorded during the test due to the damage of strain gauges after yielding. Figure 4.22 shows the mid-span strains of steel and wire mesh-epoxy in specimen A2. The strains of both the steel and wire mesh-epoxy showed the same values up to the cracking stage. However, the strains of the wire mesh-epoxy increased at values larger than the steel after the first crack. This is attributed to the fact that the strain was measured in the strengthening materials using the strain gauges, which were located at a greater distance than the steel from the neutral axis. The strengthened specimens showed a reduction in the steel strain at yielding of about 17% to 21% compared to the control specimen. The strain readings showed that the steel yielding could be clearly observed in the control specimen and specimen B by the bend in the shape of the load-deflection curve. However, this could not be observed in the specimens bonded with the wire mesh-epoxy laminate. A rapid increase in load occurred after the yielding of the steel and prior to the fracture of the wire mesh-epoxy composite in specimens A1, A2 and HY. In addition, the wire mesh-epoxy composite showed a variation in strain values among the specimens. The variation in strain is related to some factors, such as, the mixing of epoxy under laboratory conditions and the alignment of the wire mesh layers in the composite.

The typical strain distribution of the wire mesh-epoxy and CFRP throughout the beam span is shown in Figures 4.23 and 4.24, respectively. The strains for both materials showed a gradual increase in the locations closer and within the constant moment region as expected. Furthermore, the strains for both materials increased remarkably after yielding up to the point of failure. As can be seen in Figure 4.23, the strains in the wire mesh-epoxy composite reached a higher value at the mid-span compared to the adjacent

points due to the rupture failure. Whereas, the strains showed a more even distribution in the CFRP sheet as it failed prematurely by debonding. Figure 4.25 compares the mid-span strains of the CFRP sheet in specimens B and HY. As can be seen in the figure, the strains in specimen HY increased in lower values than specimen B after cracking. This reduction in strain is due to the load sharing mechanism with the wire mesh-epoxy in the hybrid in specimen HY. However, after the fracture of wire mesh-epoxy at 80 kN, a rapid increase in strain occurred until failure. The CFRP in specimen B showed an increase in the load with strain after yielding until final failure by debonding. It should be mentioned that the strain at failure of CFRP in specimen B was 72.5% of the ultimate strain, which is provided by the manufacturer, while it was 93% for specimen HY. This is because the wire mesh-epoxy laminate in specimen HY prevented the premature debonding of CFRP and allowed the sheet to stretch until reaching its theoretical failure strain. The other strains plots of steel, wire mesh-epoxy composite and CFRP are presented in Appendix C chapter.

Table 4.5: Summary of measured strains (Microstrain)

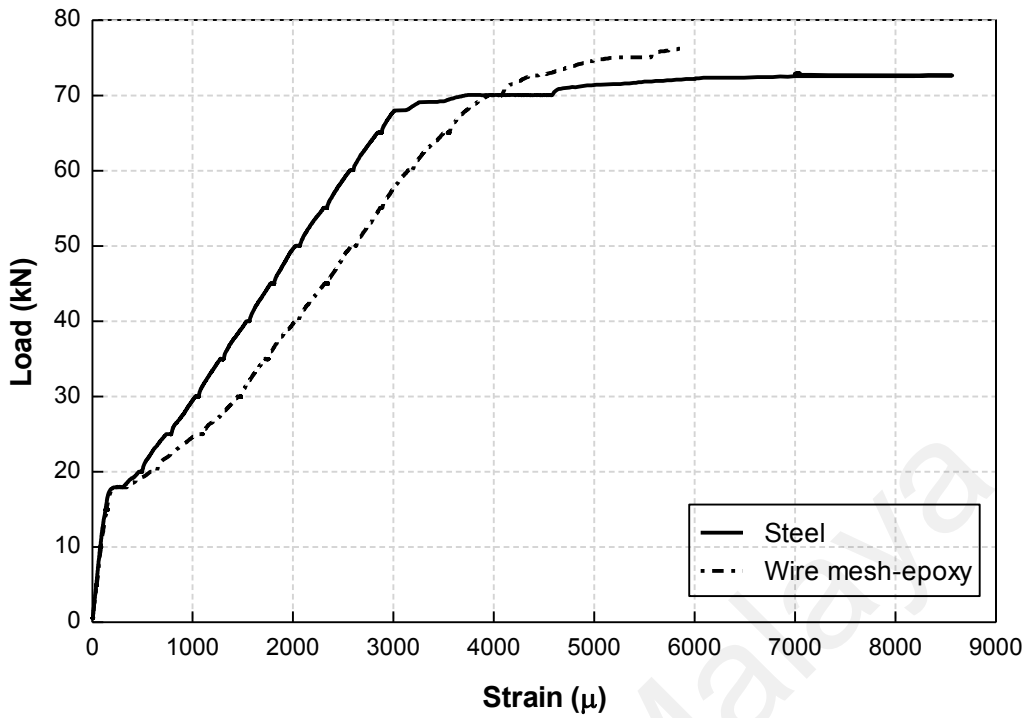| Beam	Steel strain		Wire mesh-epoxy strain			CFRP strain		
	First crack	Yield	First crack	Yield	Failure	First crack	Yield	Failure
CB	151	3549	-	-	-	-	-	-
A1	237	3028	238	2510	3664	-	-	-
A2	202	3009	191	3934	5863	-	-	-
B	109	2814	-	-	-	171	4377	15233
HY	198	2895	173	3288	4611	221	3545	19528

Figure 4.22: Comparison of mid-span strains of steel and wire mesh-epoxy in specimen A2
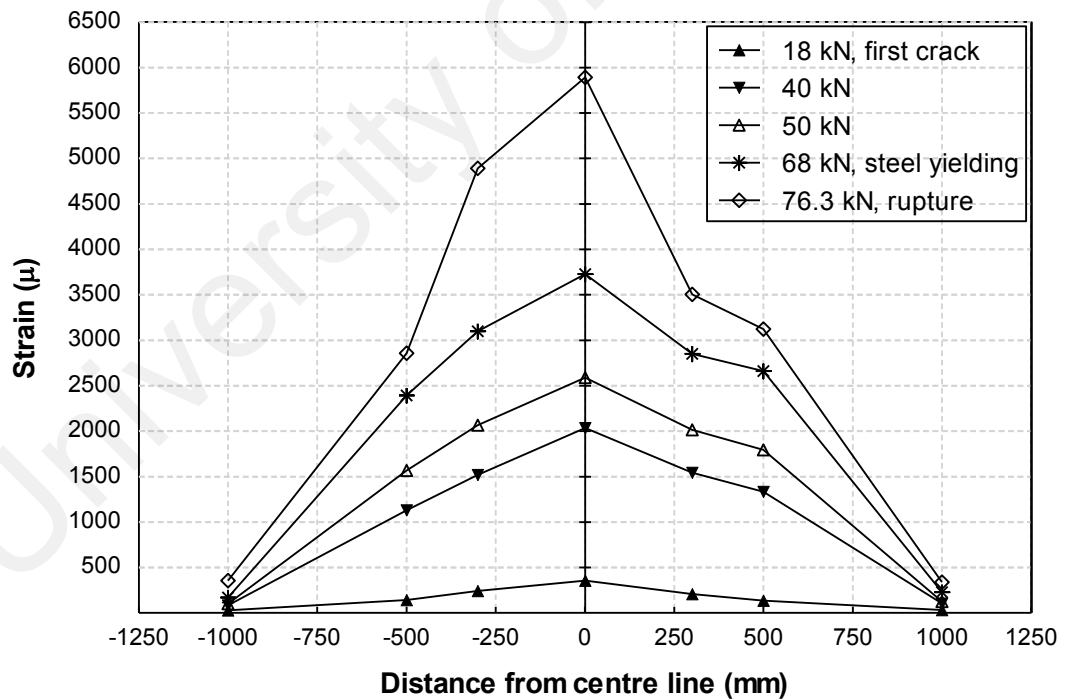

Figure 4.23: Strain distributions in the wire mesh-epoxy laminate at different loading stages for specimen A2
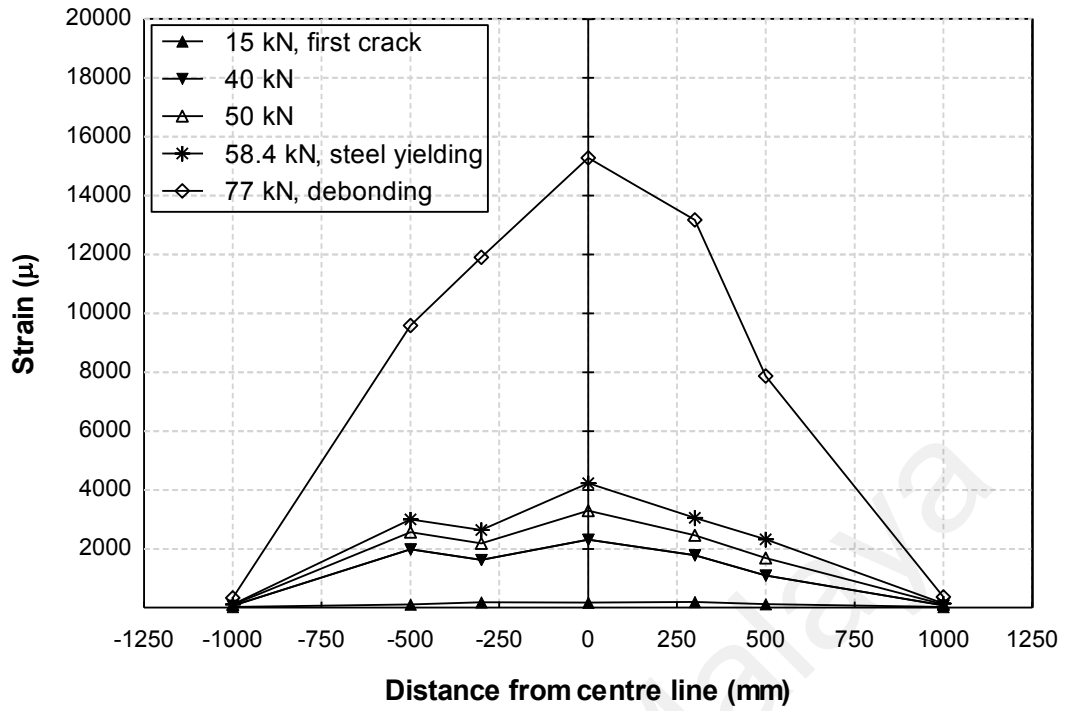
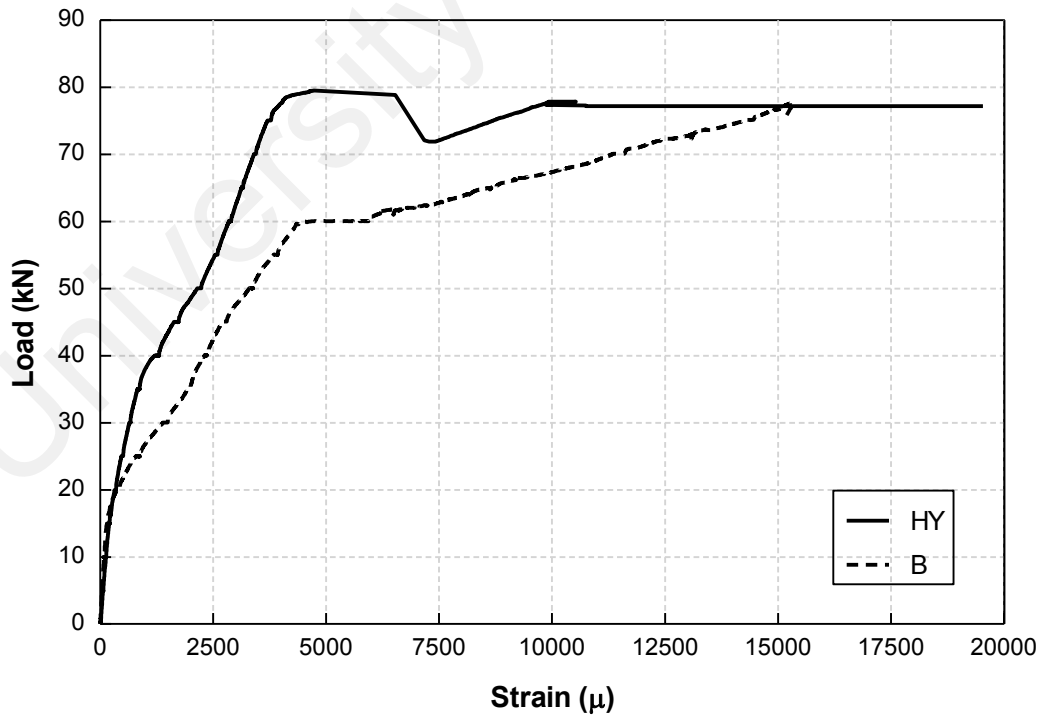Figure 4.24: Strain distributions in the CFRP sheet at different loading stages for specimen B

Figure 4.25: CFRP sheet mid-span strain for specimens HY and B

98

4.3.5 Crack patterns

Cracking behaviour is one of the most important aspects for the determination of the serviceability of RC structures (Nawy, 2005). The first crack in the control specimen appeared at a load of 10 kN. As the load increased, vertical flexural cracks started to grow deeper from the beam soffit to the top. The degree of cracking varied throughout the specimen span depending on the deflection and stresses values. The cracks were more concentrated at areas close to the mid-span and reduced gradually at areas near the support. Specimens A1 and A2 had similar cracking behaviour. The first crack in specimens A1 and A2 were observed at loads of 19 and 18 kN, respectively. However, the first cracks in specimens B and HY appeared at loads of 15 and 16.3 kN, respectively. A critical crack with a relatively large width was observed at the section where the wire mesh-epoxy composite fractured near the mid-span of specimens A1, A2 and HY (Figures 4.17 and 4.21). The number of vertical flexural cracks was more for the specimens strengthened with wire mesh-epoxy composites compared to control specimen CB and specimen B. In addition, the cracks were closely spaced, narrow and uniformly distributed compared to specimens CB and B. Figure 4.26 shows the measured crack width at different load levels. The crack width readings with load for specimens A1 and A2 were almost similar. Hence, only specimen A2 crack width values are presented in the figure. For the sake of comparison, the regression line was drawn to show the overall trend of the increased crack width. The slope of the line was taken as a measure of the degree of the control of cracks widening by the strengthening material. As can be seen from the figure, the slope of the regression line of specimens A2 and HY is lower than specimens CB and B. The lower slope means that the specimen could carry higher load values with lower average crack opening. This shows that the wire mesh-epoxy composite in specimens A1, A2 and HY restricted the cracks opening with the increasing loads. Hence, it can be concluded that the use of wire mesh-

epoxy composite is effective for controlling the crack widths and distribution in RC strengthened beams.
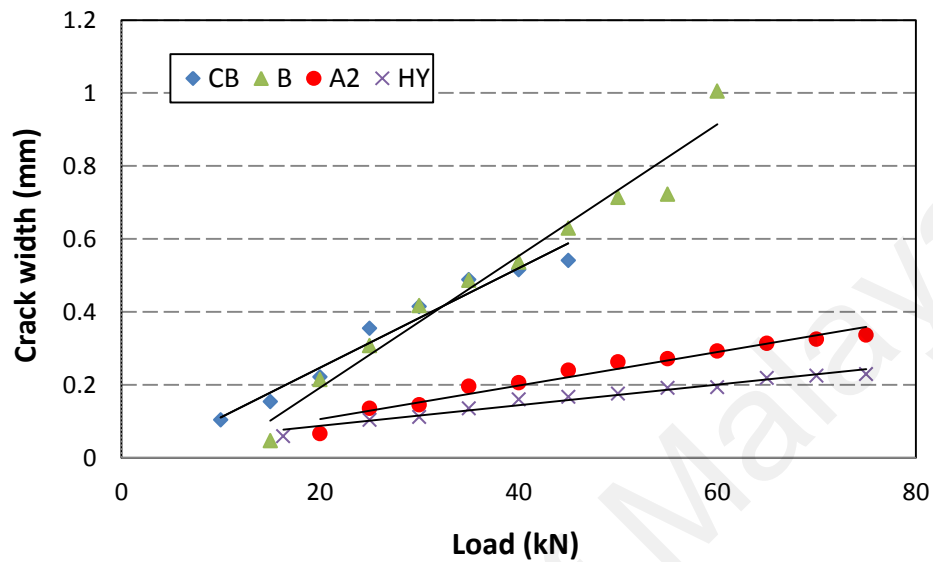

Figure 4.26: Relationship between average crack width and load

CHAPTER 5

CONCLUSION AND RECOMMENDATIONS

5.1 General

The selection criteria of strengthening materials depend greatly on certain factors, such as, the durability of material, ease of handling on the site, satisfactory performance and cost-effectiveness. A number of strengthening materials has been investigated in the last three decades. However, research on the development of optimum strengthening materials is still needed. A composite of wire mesh and epoxy resin was proposed and investigated in this research. The experimental programme consisted of studying the flexural behaviour of plain concrete beam specimens as well as RC beams bonded with wire mesh-epoxy composites. The results reported in this research provide an indication of the flexural performance of beams strengthened with the wire mesh-epoxy composite. The conclusion of this study and recommendations for future research are presented in this chapter.

5.2 Conclusion

5.2.1 Plain concrete beams

(1) The use of wire mesh-epoxy composite constitutes a new technique to significantly enhance the performance of concrete in flexure. An increase in flexural strength up to about 123% over the plain concrete control specimen could be achieved.

(2) All specimens bonded with wire mesh exhibited an increase in first crack load. This increase is associated with the increase in the number of wire mesh layers.

(3) Compared to the control beam specimen, the energy absorption capability improved significantly. The increase in the number of wire mesh layers increased the energy absorption. However, the energy absorption of specimens with four and five layers of wire mesh was more significant.

(4) Using four layers of wire mesh was found to be optimum with an increase in ultimate flexural load capacity and energy absorption of about 88% and 470%, respectively.

(5) A remarkable increase in the energy absorption in specimens bonded with a hybrid wire mesh-epoxy-carbon fibre composite was achieved. Compared to the control concrete specimen, specimens bonded with a hybrid composite could achieve an enhancement in the flexural load capacity and energy absorption of about 64% and 356%, respectively. This enhancement is attributed to the sequential failure of the wire mesh and the delayed separation of the carbon fibre.

(6) The use of a wider wire mesh-epoxy composite was found to improve the energy absorption capability better than narrower composites with an increase of up to 91% over the plain concrete specimen.

5.2.2 RC beams

(1) The wire mesh-epoxy composite can be fabricated and applied to beams in the form of laminates. The fabrication of the composite as a laminate provides easier handling and application during the strengthening work on site.

(2) The wire mesh-epoxy composite significantly enhanced the yield strength of beam specimens. An increase of yield load of up to 47% over the control specimen was achieved.

(3) The use of wire mesh-epoxy composite as a strengthening material could significantly increase the first crack load. An increase in first crack load up to 90% was observed in this study. In addition, beams strengthened with wire mesh-epoxy composite showed a significant improvement in restraining the formation of cracks.

(4) Specimens strengthened with wire mesh-epoxy composite showed a significant increase in the stiffness under service loads.

(5) The use of hybrid wire mesh-epoxy-carbon fibre composite showed an improvement in both the pre-yield and post-yield loading stages due to the sequential failure of the wire mesh-epoxy laminate and CFRP sheet. In addition, the presence of wire mesh-epoxy laminate in the hybrid prevented the premature debonding of the CFRP.

5.3 Recommendations for future research

(1) Further studies are required to develop this new strengthening method, such as long-term behaviour of the composite to assess the protection provided by the epoxy of the wire mesh.

(2) The mechanical properties of the wire mesh-epoxy composite, such as, tensile, compressive and flexural behaviour need to be investigated in order to provide a better understanding of the characteristics of the material and the strengthened beams.

(3) Further research is needed to investigate the use of different amounts of CFRP in the hybrid of the wire mesh-epoxy-carbon fibre composite in order to achieve better performance with respect to the ultimate load carrying capacity and ductility.

(4) Modification of epoxy with other relatively low cost materials (such as, ultra-fine sand or clay) can be used to provide better properties of the composite (e.g. fire resistance) and reduce the cost of epoxy resin.

(5) Analytical and numerical studies for wire mesh-epoxy strengthened RC beams are recommended for predicting their flexural behaviour and design equations.

(6) The investigation of the use of the wire mesh-epoxy and hybrid wire mesh-epoxy-carbon fibre composites for shear strengthening is recommended.

REFERENCES

ACI Committee 440. (2008). "Guide for the design and construction of externally bonded FRP systems for strengthening concrete structures". *ACI 440.2R-08*, ACI, Farmington Hills, MI, www.concrete.org.

ACI Committee 549. (1988). "Guide for the design, construction, and repair of Ferrocement". *ACI Structural Journal*, 85(3): p. 325-351.

ACI Committee 318. (2008). "Building code requirements for structural concrete and commentary". *ACI 318R-08*, ACI, Farmington Hills, MI, www.concrete.org.

Adhikary, B. B., and Mutsuyoshi, H. (2002). "Numerical simulation of steel-plate strengthened concrete beam by a non-linear finite element method model". *Construction and Building Materials*, 16(5), 291-301.

Ahmed, H. I., and Robles-Austriaco, L. (1991). "State-of-the-art report on rehabilitation and restrengthening of structures using ferrocement". *Journal of ferrocement*, 21(3), 243-258.

Akbarzadeh, H., and Maghsoudi, A. (2010). "Experimental and analytical investigation of reinforced high strength concrete continuous beams strengthened with fiber reinforced polymer". *Materials & Design*, 31(3), 1130-1147.

Al-Kubaisy, M. A., and Jumaat, M. Z. (2000). "Ferrocement laminate strengthens RC beams". *Concrete International*, 22(10), 37-43.

Almusallam, T. H., Elsanadedy, H. M., Al-Salloum, Y. A., and Alsayed, S. H. (2013). "Experimental and numerical investigation for the flexural strengthening of RC beams using near-surface mounted steel or GFRP bars". *Construction and Building Materials*, 40, 145-161.

Arduini, M., and Nanni, A. (1997). "Parametric study of beams with externally bonded FRP reinforcement". *ACI Structural Journal*, 94(5), 493-500.

Arslan, G., Sevuk, F., and Ekiz, I. (2008). "Steel plate contribution to load-carrying capacity of retrofitted RC beams". *Construction and Building Materials*, 22(3), 143-153.

ASTM A370 – 13, "Standard Test Methods and Definitions for Mechanical Testing of Steel Products" *ASTM International*, West Conshohocken, PA, 2013, DOI: 10.1520/A0370, www.astm.org.

ASTM C469 / C469M - 14, "Standard Test Method for Static Modulus of Elasticity and Poisson's Ratio of Concrete in Compression" *ASTM International*, West Conshohocken, PA, 2014, DOI: 10.1520/C0469_C0469M, www.astm.org.

ASTM C496 / C496M - 11, "Standard Test Method for Splitting Tensile Strength of Cylindrical Concrete Specimens" *ASTM International*, West Conshohocken, PA, 2011, DOI: 10.1520/C0496_C0496M-11, www.astm.org.

ASTM D638 - 10, "Standard Test Method for Tensile Properties of Plastics" *ASTM International*, West Conshohocken, PA, 2010, DOI: 10.1520/D0638-10, www.astm.org.

ASTM D3039/D3039M-08, "Standard Test Method for Tensile Properties of Polymer Matrix Composite Materials" *ASTM International*, West Conshohocken, PA, 2008, DOI: 10.1520/D3039_D3039M-08, www.astm.org.

ASTM D7565/D7565M-10, "Standard Test Method for Determining Tensile Properties of Fiber Reinforced Polymer Matrix Composites Used for Strengthening of Civil Structures" *ASTM International*, West Conshohocken, PA, 2010, DOI: 10.1520/D7565_D7565M-10, www.astm.org.

Attari, N., Amziane, S., and Chemrouk, M. (2012). "Flexural strengthening of concrete beams using CFRP, GFRP and hybrid FRP sheets". *Construction and Building Materials*, 37, 746-757.

Bakis, C., Bank, L. C., Brown, V., Cosenza, E., Davalos, J., Lesko, J., . . . Triantafillou, T. (2002). "Fiber-reinforced polymer composites for construction-state-of-the-art review". *Journal of Composites for Construction*, 6(2), 73-87.

Balaguru, P. (1989). "Use of ferrocement for confinement of concrete". *Journal of ferrocement*, 19(2), 135-140.

Balaguru, P., Narahari, R., and Patel, M. (1992). "Flexural toughness of steel fiber reinforced concrete". *ACI materials Journal*, 89(6), 541-546.

Balamuralikrishnan, R., and Jeyasehar, C. (2009). Flexural Behavior of RC Beams Strengthened with Carbon Fiber Reinforced Polymer(CFRP) Fabrics. Open Civil Engineering Journal, 3, 102-109.

Bank, L. C. (2013). "Progressive failure and ductility of FRP composites for construction: review". *Journal of Composites for Construction*, 17(3), 406-419.

Bansal, P. P., Kumar, M., and Kaushik, S. (2008). "Effect Of Wire Mesh Orientation On Strength Of Beams Retrofitted Using Ferrocement Jackets". *Int. J. Eng*, 2(1), 8-19.

Banthia, N., Nandakumar, N., and Boyd, A. (2002). "Sprayed fiber-reinforced polymers: From laboratory to a real bridge". *Concrete international*, 24(11), 47-52.

Basunbul, I., Gubati, A., Al-Sulaimani, G., and Baluch, M. (1990). "Repaired reinforced concrete beams". *ACI Materials Journal*, 87(4), 348-354.

Bonacci, J., and Maalej, M. (2001). "Behavioral trends of RC beams strengthened with externally bonded FRP". *Journal of Composites for Construction*, 5(2), 102-113.

Brena, S. F., Bramblett, R. M., Wood, S. L., and Kreger, M. E. (2003). "Increasing flexural capacity of reinforced concrete beams using carbon fiber-reinforced polymer composites". *ACI Structural Journal*, 100(1), 36-46.

British Standards Institution (2009). "Testing Hardened Concrete — Compressive strength of test specimens". *BS EN 12390–3*, Milton Keynes, UK.

British Standards Institution (2009). "Testing Hardened Concrete — Flexural Strength of Test Specimens". *BS EN 12390–5*, Milton Keynes, UK.

British Standards Institution (2004). "Eurocode 2: Design of Concrete Structures: Part 1-1: General Rules and Rules for Buildings". *British Standards Institution*.

Bunsell, A., and Harris, B. (1974). "Hybrid carbon and glass fibre composites". *Composites*, 5(4), 157-164.

Buyukozturk, O., Gunes, O., and Karaca, E. (2004). "Progress on understanding debonding problems in reinforced concrete and steel members strengthened using FRP composites". *Construction and Building Materials*, 18(1), 9-19.

Büyüköztürk, O., and Yu, T.-Y. (2006). "Understanding and assessment of debonding failures in FRP–concrete systems". *Paper presented at the Seventh International Congress on Advances in Civil Engineering*, Yildiz Technical University, Istanbul, Turkey.

Campbell, F. C. (2010). "Structural Composite Materials". Materials Park, Ohio: ASM International.

Chiew, S.-P., Sun, Q., and Yu, Y. (2007). "Flexural strength of RC Beams with GFRP Laminates". *Journal of composites for Construction*, 11(5), 497-506.

Diab, Y. (1998). "Strengthening of RC beams by using sprayed concrete: experimental approach". *Engineering structures*, 20(7), 631-643.

El-Reedy, M. (2010). "Steel-reinforced concrete structures: Assessment and repair of corrosion". CRC press.

Esfahani, M. R., Kianoush, M., and Tajari, A. (2007). "Flexural behaviour of reinforced concrete beams strengthened by CFRP sheets". *Engineering structures*, 29(10), 2428-2444.

Fahmy, E. H., Shaheen, Y. B., and Korany, Y. S. (1997). "Use of ferrocement laminates for repairing reinforced concrete slabs". *Journal of ferrocement*, 27(3), 219-232.

Fukuda, H., and Chou, T.-W. (1982). "Monte Carlo simulation of the strength of hybrid composites". *Journal of Composite Materials*, 16(5), 371-385.

GangaRao, H. V. S., Taly, N., and Vijay, P. V. (2007). "Reinforced Concrete Design with FRP Composites". Boca Raton: Taylor & Francis Group, LLC.

Garden, H., and Hollaway, L. (1998). "An experimental study of the influence of plate end anchorage of carbon fibre composite plates used to strengthen reinforced concrete beams". *Composite Structures*, 42(2), 175-188.

Grace, N. F., Abdel-Sayed, G., and Ragheb, W. F. (2002). "Strengthening of concrete beams using innovative ductile fiber-reinforced polymer fabric". *ACI Structural Journal*, 99(5), 692-700.

Grace, N. F., Ragheb, W. F., and Abdel-Sayed, G. (2003). "Flexural and shear strengthening of concrete beams using new triaxially braided ductile fabric". *ACI Structural Journal*, 100(6), 804-814.

Grace, N. F., Ragheb, W. F., and Abdel-Sayed, G. (2004). "Development and application of innovative triaxially braided ductile FRP fabric for strengthening concrete beams". *Composite Structures*, 64(3), 521-530.

Grace, N. F., Sayed, G., Soliman, A., and Saleh, K. (1999). "Strengthening reinforced concrete beams using fiber reinforced polymer (FRP) laminates". *ACI Structural Journal*, 96, 865-874.

Guan, Y., Jiang, B., and Song, X. (2012). "Experimental study and numerical simulation on bonding behavior of the new HB-FRP strengthening technology". *Journal of Performance of Constructed Facilities*, 26(2), 220-227.

Harris, H. G., Somboonsong, W., and Ko, F. K. (1998). "New ductile hybrid FRP reinforcing bar for concrete structures". *Journal of Composites for Construction*, 2(1), 28-37.

Hassanpour, M., Shafigh, P., and Mahmud, H. B. (2012). "Lightweight aggregate concrete fiber reinforcement–A review". *Construction and Building Materials*, 37, 452-461.

Hawileh, R. A., Rasheed, H. A., Abdalla, J. A., and Al-Tamimi, A. K. (2014). "Behavior of reinforced concrete beams strengthened with externally bonded hybrid fiber reinforced polymer systems". *Materials & Design*, 53, 972-982.

Hayashi, T. (1972). "On the improvement of mechanical properties of composites by hybrid composition". *Paper presented at the Eighth International Reinforced Plastics Conference.*

Hinton, M. J., Kaddour, A. S., and Soden, P. D. (2004). "Failure criteria in fibre reinforced polymer composites: the world-wide failure exercise". Elsevier.

Hosny, A., Shaheen, H., Abdelrahman, A., and Elafandy, T. (2006). "Performance of reinforced concrete beams strengthened by hybrid FRP laminates". *Cement and Concrete Composites*, 28(10), 906-913.

Iorns, M. (1987). "Laminated ferrocement for better repair". *Concrete International: Design and Construction*, 9(9), 34-38.

ISIS Canada Educational Module No. 2. (2006). "An Introduction to FRP Composites for Construction". *ISIS Canada: A Canadian Network of Centres of Excellence*. University of Manitoba, Winnipeg, Manitoba, Canada, www.isiscanada.com.

Jones, R., Swamy, R., and Bloxham, J. (1986). "Crack control of reinforced concrete beams through epoxy bonded steel plates". *Adhesion between polymers and concrete*, 542-555.

Jones, R., Swamy, R., and Charif, A. (1988). "Plate separation and anchorage of reinforced concrete beams strengthened by epoxy-bonded steel plates". *Structural Engineer*, 66(5), 85-94.

Jumaat, M. Z., and Alam, M. A. (2009). "Strengthening of RC beams using externally bonded plates and anchorages". *Australian Journal of Basic and Applied Sciences*, 3(3), 2207-2211.

Jumaat, M. Z., and Alam, M. A. (2010). "Experimental and numerical analysis of end anchored steel plate and CFRP laminate flexurally strengthened reinforced concrete (rc) beams". *International Journal of the Physical Sciences*, 5(2), 132-144.

Kajfasz, S. (1967). "Concrete beams with external reinforcement bonded by gluing". *RILEM International Symposium, Synthetic Resins in Building Construction, Part 2*, Paris, 142-151.

Khalifa, A., Alkhrdaji, T., Nanni, A., and Lansburg, S. (1999). "Anchorage of surface mounted FRP reinforcement". *Concrete International*, 21, 49-54.

Kim, H. S., and Shin, Y. S. (2011). "Flexural behavior of reinforced concrete (RC) beams retrofitted with hybrid fiber reinforced polymers (FRPs) under sustaining loads". *Composite Structures*, 93(2), 802-811.

Lee, H. (2004). "Effectiveness of anchorage in concrete beams retrofitted with sprayed fiber-reinforced polymers". *Journal of reinforced plastics and composites*, 23(12), 1285-1300.

Lee, H., Avila, G., and Montanez, C. (2005). "Numerical study on retrofit and strengthening performance of sprayed fiber reinforced polymer". *Engineering structures*, 27(10), 1476-1487.

Lee, H., and Hausmann, L. (2004). "Structural repair and strengthening of damaged RC beams with sprayed FRP". *Composite Structures*, 63(2), 201-209.

Lee, H., Hausmann, R., and Seaman, W. (2008). "Effectiveness of retrofitting damaged concrete beams with sprayed fiber-reinforced polymer coating". *Journal of Reinforced Plastics and Composites*, 27(12), 1269-1286.

Lerchental, H. (1967). "Bonded sheet metal reinforcement for concrete slabs". *RILEM International Symposium, Resins in Building Construction*, Paris, 165-173.

Lu, G., and Yu, T. Y. (2003). "Energy absorption of structures and materials". United Kingdom: Woodhead Publishing Limited.

Maalej, M., and Bian, Y. (2001). "Interfacial shear stress concentration in FRP-strengthened beams". *Composite Structures*, 54(4), 417-426.

Maalej, M., and Leong, K. (2005). "Effect of beam size and FRP thickness on interfacial shear stress concentration and failure mode of FRP-strengthened beams". *Composites science and technology*, 65(7), 1148-1158.

MacDonald, M., and Calder, A. (1982). "Bonded steel plating for strengthening concrete structures". *International Journal of Adhesion and Adhesives*, 2(2), 119-127.

Malek, A. M., Saadatmanesh, H., and Ehsani, M. R. (1998). "Prediction of failure load of R/C beams strengthened with FRP plate due to stress concentration at the plate end". *ACI Structural Journal*, 95, 142-152.

Manders, P., and Bader, M. (1981a). "The strength of hybrid glass/carbon fibre composites- Part 2 A statistical model". *Journal of Materials Science*, 16(8), 2233-2245.

Manders, P., and Bader, M. (1981b). "The strength of hybrid glass/carbon fibre composites -Part 1 Failure strain enhancement and failure mode". *Journal of Materials Science*, 16(8), 2233-2245.

Mehta, P. K., and Monteiro, P. J. M. (2006). "Concrete (Microstructure, Properties, and Materials) (3rd ed.)". New York: MacGraw-Hill.

Meier, U. (1995). "Strengthening of structures using carbon fibre/epoxy composites". *Construction and Building Materials*, 9(6), 341-351.

Mosley, B., Bungey, J., and Hulse, R. (2007). "Reinforced Concrete Design to Eurocode 2 (6th ed.)". New York: Palgrave Macmillan.

Nawy, E. G. (2005). "Reinforced Concrete: A Fundamental Approach (6th ed.)". New Jersey, United States: Prentice Hall.

Neville, A. M., and Brooks, J. J. (2008). "Concrete Technology". England: Pearson Education Limited.

Obaidat, Y. T., Heyden, S., and Dahlblom, O. (2010). "The effect of CFRP and CFRP/concrete interface models when modelling retrofitted RC beams with FEM". *Composite Structures*, 92(6), 1391-1398.

Obaidat, Y. T., Heyden, S., Dahlblom, O., Abu-Farsakh, G., and Abdel-Jawad, Y. (2011). "Retrofitting of reinforced concrete beams using composite laminates". *Construction and Building Materials*, 25(2), 591-597.

Oh, H.-S., and Sim, J. (2004). "Interface debonding failure in beams strengthened with externally bonded GFRP". *Composite Interfaces*, 11(1), 25-42.

Oudah, F., and El-Hacha, R. (2012). "A new ductility model of reinforced concrete beams strengthened using fiber reinforced polymer reinforcement". *Composites Part B: Engineering*, 43(8), 3338-3347.

Padron, I., and Zollo, R. F. (1990). "Effect of synthetic fibers on volume stability and cracking of portland cement concrete and mortar". *ACI Materials Journal*, 87(4), 327-332.

Paramasivam, P., Lim, C., and Ong, K. (1998). "Strengthening of RC beams with ferrocement laminates". *Cement and Concrete Composites*, 20(1), 53-65.

Paramasivam, P., Ong, K., and Lim, C. (1994). "Ferrocement laminates for strengthening RC T-beams". *Cement and Concrete Composites*, 16(2), 143-152.

Park, R., and Paulay, T. (1975). "Reinforced Concrete Structures". Canada: John Wiley & Sons, Inc.

Phillips, L. (1976). "The hybrid effect—Does it Exist?". *Composites*, 7(1), 7-8.

Quattlebaum, J. B., Harries, K. A., and Petrou, M. F. (2005). "Comparison of three flexural retrofit systems under monotonic and fatigue loads". *Journal of Bridge Engineering*, 10(6), 731-740.

Raithby, K. (1982). "Strengthening of concrete bridge decks with epoxy-bonded steel plates". *International Journal of Adhesion and Adhesives*, 2(2), 115-118.

Rasheed, H. A., Nassajy, M., Al Subaie, S., Abrishamchian, S. M., and Al Tamimi, A. (2011). "Suppressing delamination failure mode in concrete beams strengthened with short CFRP laminates". *Mechanics of Advanced Materials and Structures*, 18(3), 194-200.

Razaqpur, A., and Ali, M. M. (1996). "A new concept for achieving ductility in FRP-reinforced concrete". *Paper presented at the First International Conference on Composites in Infrastructure*, Tucson, Arizona, 401-413.

Reinhorn, A., and Prawel, S. (1985). "Ferrocement for seismic retrofit of structures". *Paper presented at the Second International Symposium on Ferrocement*, Roorkee, India, 157-172.

Ritchie, P. A., Thomas, D. A., Lu, L.-W., and Conelly, G. M. (1991). "External reinforcement of concrete beams using fiber reinforced plastics". *ACI Structural Journal*, 88(4), 490-500.

Roads & Maritime- New South Wales (2014). "Strengthening steel plate epoxy glued and bolted to soffit of headstock", Retrieved June 14, 2014, from: <http://www.rms.nsw.gov.au/environment/heritage/heritageconservreg/data_file s/4309518.html>.

Roberts, T. (1989). "Approximate analysis of shear and normal stress concentrations in the adhesive layer of plated RC beams". *The Structural Engineer*, 67(12), 229-233.

Romualdi, J. (1987). "Ferrocement for infrastructurerehabilitation". *Concrete International: Design and Construction*, 9(9), 24-28.

Saadatmanesh, H., and Ehsani, M. R. (1991). "RC beams strengthened with GFRP plates. I: Experimental study". *Journal of Structural Engineering*, 117(11), 3417-3433.

Shahawy, M., Arockiasamy, M., Beitelman, T., and Sowrirajan, R. (1996). "Reinforced concrete rectangular beams strengthened with CFRP laminates". *Composites Part B: Engineering*, 27(3), 225-233.

Shannag, M., and Mourad, S. (2012). "Flowable high strength cementitious matrices for ferrocement applications". *Construction and Building Materials*, 36, 933-939.

Sharif, A., Al-Sulaimani, G., Basunbul, I., Baluch, M., and Ghaleb, B. (1994). "Strengthening of initially loaded reinforced concrete beams using FRP plates". *ACI Structural Journal*, 91(2), 160-168.

Siddiqui, N. A. (2010). "Experimental investigation of RC beams strengthened with externally bonded FRP composites". *Latin American Journal of Solids and Structures*, 6(4), 343-362.

Sika (2012). "Sikadur®-330", product data sheet, 2-part epoxy impregnation resin [Edition 2012-05_1], Retrieved December 05, 2013, from:http://mys.sika.com/en/solutions_products-old/02/02a013/02a013sa06/02a013sa06100/02a013sa06105.html.

Sika (2010). "SikaWrap®-301 C" , product data sheet,unidirectional woven carbon fibre fabric for structural strengthening [Edition 2010-12_1], Retrieved December 02, 2013, from:http://mys.sika.com/en/solutions_products-old/02/02a013/02a013sa06/02a013sa06100/02a013sa06103.html.

Smith, S. T., and Teng, J. (2002a). "FRP-strengthened RC beams. I: review of debonding strength models". *Engineering Structures*, 24(4), 385-395.

Smith, S. T., and Teng, J. (2002b). "FRP-strengthened RC beams. II: Assessment of debonding strength models". *Engineering structures*, 24(4), 397-417.

Sobuz, H. R., Ahmed, E., Hasan, N. M. S., and Uddin, M. A. (2011). "Use of carbon fiber laminates for strengthening reinforced concrete beams in bending". *International Journal of Civil and Structural Engineering*, 2(1), 67-84.

Soroushian, P., and Tlili, A. (1993). "Development and characterization of hybrid polyethylene fiber reinforced cement composites". *ACI Materials Journal*, 90(2), 182-190.

Soulioti, D., Barkoula, N., Paipetis, A., and Matikas, T. (2011). "Effects of Fibre Geometry and Volume Fraction on the Flexural Behaviour of Steel-Fibre Reinforced Concrete". *Strain*, 47(s1), e535-e541.

Swamy, R., Jones, R., and Bloxham, J. (1987). "Structural behaviour of reinforced concrete beams strengthened by epoxy-bonded steel plates". *Structural Engineer*. Part A, 65, 59-68.

Takiguchi, K. (2003). "An investigation into the behavior and strength of reinforced concrete columns strengthened with ferrocement jackets". *Cement and Concrete Composites*, 25(2), 233-242.

Teng, J., and Chen, J. (2007). "Debonding failures of RC beams strengthened with externally bonded FRP reinforcement: behaviour and modelling". *Paper presented at the Proceedings of the First Asia-Pacific Conference on FRP in Structures (APFIS 2007)*, Hong Kong, 33-42.

Teng, J. G., Chen, J. F., Smith, S. T., and Lam, L. (2002). "FRP: strengthened RC structures". England: John Wiley & Sons, Ltd.

Thanoon, W. A., Jaafar, M. S., A Kadir, M. R., and Noorzaei, J. (2005). "Repair and structural performance of initially cracked reinforced concrete slabs". *Construction and Building Materials*, 19(8), 595-603.

Toutanji, H., Zhao, L., and Zhang, Y. (2006). "Flexural behavior of reinforced concrete beams externally strengthened with CFRP sheets bonded with an inorganic matrix". *Engineering Structures*, 28(4), 557-566.

Triantafillou, T. C., and Plevris, N. (1992). "Strengthening of RC beams with epoxy-bonded fibre-composite materials". *Materials and Structures*, 25(4), 201-211.

Wang, P., Huang, Z., Jiang, J., and Wu, Y. (2012). "Performance of Hybrid Fiber Reinforced Concrete with Steel Fibers and Polypropylene Fibers". *Paper presented at the Civil Engineering and Urban Planning 2012*, Yantai, China, 458-461.

Wu, Z., Li, W., and Sakuma, N. (2006). "Innovative externally bonded FRP/concrete hybrid flexural members". *Composite structures*, 72(3), 289-300.

Wu, Z., Shao, Y., Iwashita, K., and Sakamoto, K. (2007). "Strengthening of preloaded RC beams using hybrid carbon sheets". *Journal of Composites for Construction*, 11(3), 299-307.

Xing, G., Wu, T., Liu, B., Huang, H., and Gu, S. (2010). "Experimental investigation of reinforced concrete T-beams strengthened with steel wire mesh embedded in polymer mortar overlay". *Advances in Structural Engineering*, 13(1), 69-80.

Xiong, G., Wu, X., Li, F., and Yan, Z. (2011). "Load carrying capacity and ductility of circular concrete columns confined by ferrocement including steel bars". *Construction and Building Materials*, 25(5), 2263-2268.

Yap, S. P., Bu, C. H., Alengaram, U. J., Mo, K. H., and Jumaat, M. Z. (2014). "Flexural toughness characteristics of steel-polypropylene hybrid fibre-reinforced oil palm shell concrete". *Materials & Design*, 57, 652–659.

Yap, S. P., Johnson Alengaram, U., and Jumaat, M. Z. (2013). "Enhancement of mechanical properties in polypropylene-and nylon-fibre reinforced oil palm shell concrete". *Materials & Design*, 49, 1034–1041.

Yi, S.-T., and Cho, S. G. (2012). "Effect of hybrid fibre reinforcement on capacity of reinforced concrete beams". *Paper presented at the Proceedings of the ICE - Structures and Buildings*.

Yost, J. R., Gross, S. P., and Deitch, M. J. (2007). "Fatigue behavior of concrete beams strengthened in flexure with near surface mounted CFRP". *Paper presented at the 8th International symposium on fiber reinforced polymer reinforcement for reinforced concrete structures (FRPRCS-8)*, University of Patras, Patras, Greece.

Zhou, Y., Gou, M., Zhang, F., Zhang, S., and Wang, D. (2013). "Reinforced concrete beams strengthened with carbon fiber reinforced polymer by friction hybrid bond technique: Experimental investigation". *Materials & Design*, 50, 130-139.

APPENDIX A

DESIGN OF RC BEAMS

A.1 Section analysis and design

A.1.1 ACI committee 318 (2008)
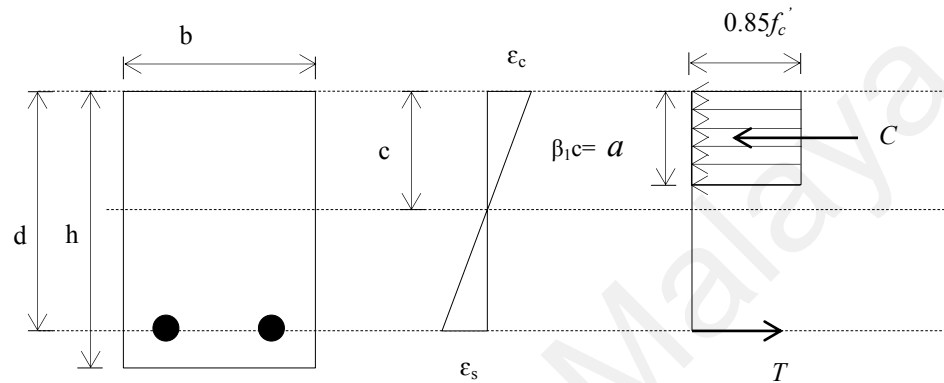
Section details

b = 150 mm (5.85 in)

h = 250 mm (9.7 in)

$d = h - \dfrac{\phi}{2} = 250 - 25 - \dfrac{12}{2} = 219$ mm (8.541 in)

$A_s = 2 \times \pi \times (6)^2 = 226.19$ mm^2 (0.344 in)

$f_c^{'} = 52.88$ N/mm^2 (7669.59 psi)

$f_y = 529$ N/mm^2 (76724.9 psi)

$E_s = 199.948$ kN/mm^2 (29×10^6 psi)

<u>Calculation</u>

$$\rho = \frac{A_s}{bd} = \frac{0.344}{5.85 \times 8.541} = 0.0068$$

$$\rho_{min} = \frac{3\sqrt{f_c'}}{f_y} = \frac{3 \times \sqrt{7669.59}}{76724.9} = 0.00342 \text{ or } \frac{200}{f_y} = \frac{200}{76724.9} = 0.002607$$

$$\rho > \rho_{min}$$

$\therefore$ Section is satisfactory

$$\beta_1 = 0.85 - 0.05(\frac{f_c' - 4000}{1000}) = 0.85 - 0.05(\frac{7669.59 - 4000}{1000}) = 0.667$$

$$\overline{\rho_b} = \beta_1 \frac{0.85 f_c'}{f_y} \frac{87000}{87000 + f_y}$$

$$= (0.667)\frac{0.85(7669.59)}{76724.9} \frac{87000}{87000 + 76724.9} = 0.05667\,(0.53138) = 0.0301$$

$$0.75\,\overline{\rho_b} = 0.75 \times 0.0301 = 0.0226$$

$$\rho = 0.00688$$

$$\rho < 0.75\,\overline{\rho_b}$$

$\therefore$ Section is under-reinforced

$$a = \frac{A_s f_y}{0.85 f_c' b} = \frac{0.344 \times 76724.9}{0.85 \times 7669.59 \times 5.85} = 0.692$$

$$M_n = A_s f_y (d - \frac{a}{2})$$

$$= (0.344)(76724.9)(8.541 - \frac{0.692}{2}) = 216293.63 \text{ in-lb } (24.4 \text{ kN.m})$$

A.1.2 Eurocode 2 (2004)
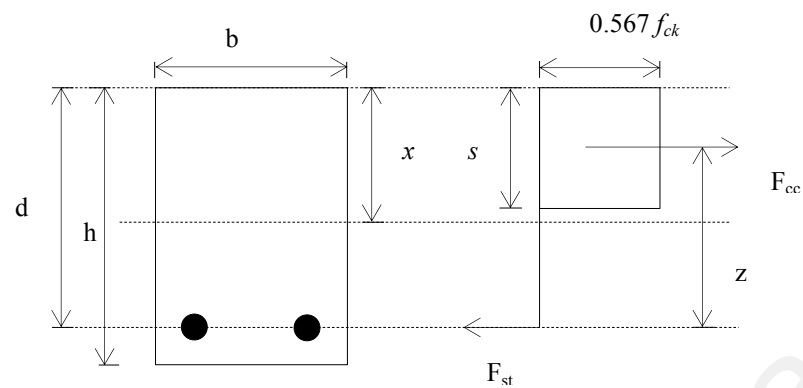
For equilibrium:

$F_{cc} = F_{st}$

$0.567 f_{ck}$ b $s = 0.87 f_{yk}$ A_s

$0.567 \times 52.88 \times 150 \times s = 0.87 \times 529 \times 226.19$

$s = 23.146$ mm

$x = \dfrac{s}{0.8} = \dfrac{23.146}{0.8} = 28.93$ mm

0.617 d $= 0.617 \times 219 = 135.123$ mm

$x < 0.617$ d

∴ The steel has yielded.

$F_{st} \approx 0.87 f_{yk}$

∴ M = $F_{st} \times z$

M = $0.87 f_{yk}$ A_s (d - $\dfrac{s}{2}$)

$$= 0.87 \times 529 \times 226.19\ (219 - \frac{23.146}{2}) \times 10^{-6}$$

$$= 21.59 \text{ kN.m}$$

A.2 Shear reinforcement

In order to ensure that the beam will not fail by shear after adding the external strengthening material, the beam was designed in shear under the condition of maximum applied load of 200 kN. The shear force diagram is shown below.
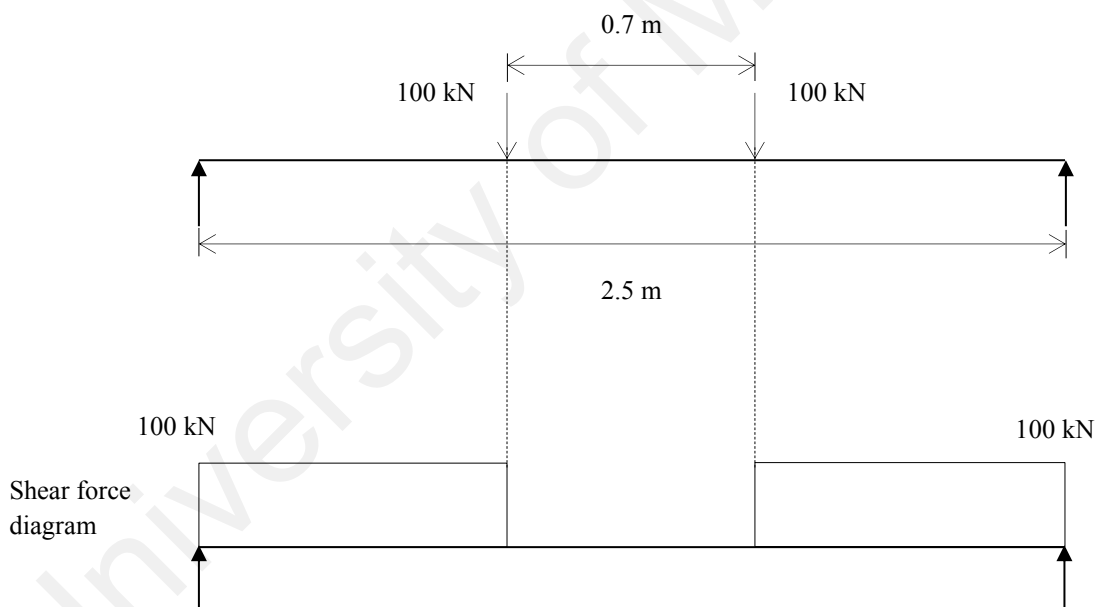
A.2.1 ACI committee 318 (2008)

V_u = 100 kN (22471.91 lb)

At the first critical section at a distance d from the face of support, V_u = 100 kN (Constant shear diagram).

ϕ = 0.85 (shear)

$$V_c = 2\lambda\sqrt{f_c'}\,b_w\,d \quad (\lambda=1, \text{ normal concrete})$$

$$= 2\times1\times\sqrt{7669.59}\times5.85\times8.541$$

$$= 8751.46 \text{ lb}$$

$$8\sqrt{f_c'}\,b_w\,d = 8\times\sqrt{7669.59}\times5.85\times8.541$$

$$= 35005.85 \text{ lb}$$

$$\frac{V_u}{\phi} - V_c = \frac{22471.91}{0.85} - 8751.46$$

$$= 17686.08 \text{ lb}$$

$$8\sqrt{f_c'}\,b_w\,d > \frac{V_u}{\phi} - V_c$$

$\therefore$ Cross section is satisfactory.

$$\frac{\phi V_c}{2} = \frac{0.85\times8751.46}{2} = 3719.37 \text{ lb}$$

$$V_u > \frac{\phi V_c}{2}$$

Shear reinforcement is required.

$$\phi V_c = 0.85\times8751.46$$

$$= 7438.741 \text{ lb}$$

$$V_u > \phi V_c$$

$$A_v = \frac{(\frac{V_u}{\phi}-V_c)s}{f_{yv}d}$$

For 8 mm (0.315 in) diameter mild steel bar,

$$A_v = 2 \times \pi \times (0.156)^2$$

$$= 0.1529 \text{ in}^2$$

$$0.1529 = \frac{(\dfrac{22471.91}{0.85} - 8751.46)\,s}{45976.95 \times 8.541}$$

s = 3.39 in (86.1 mm)

$\therefore$ 8 mm diameter mild steel is provided for shear reinforcement with spacing of 75 mm center to center throughout the shear span.

A.2.2 Eurocode 2 (2004)

Design shear force V_{Ef} at the face of support = 100 kN

Design shear force V_{Ed} at distance d from the face of support = 100 kN

Checking the crushing strength $V_{Rd, max}$ of the concrete diagonal strut at the face of beam support,

For most cases, the angle of inclination of the strut is θ = 22º, with cot θ = 2.5 and tan θ = 0.4.

Hence, $V_{Rd, max(22)} = \dfrac{0.36 b_w d (1 - \dfrac{f_{ck}}{250}) f_{ck}}{(\cot \theta + \tan \theta)}$

$$= \frac{(0.36 \times 150 \times 219)(1 - \dfrac{52.88}{250}) \times 52.88}{(2.5 + 0.4)}$$

$$= 170.03 \text{ kN}$$

$$V_{Rd, max} > V_{Ef}$$

$$\frac{A_{sw}}{s} = \frac{V_{Ed}}{0.78 d f_{yk} \cot \theta}$$

$$A_{sw} = 2 \times \pi \times (4)^2$$

$$= 100.53 \text{ mm}^2$$

$$\frac{100.53}{s} = \frac{100 \times 10^3}{0.78 \times 219 \times 317 \times 2.5}$$

$$s = 136.09 \text{ mm}$$

$\therefore$ 8 mm diameter mild steel is provided for shear reinforcement with spacing of 75 mm

center to center throughout the shear span.

APPENDIX B

ANCILLARY TEST RESULTS

B.1 General

The different tests preparation and results of the materials used in this study are presented and discussed in this chapter. The tests involved the compressive, splitting tensile and flexural tests of concrete. In addition, the tensile tests of steel, CFRP, epoxy and wire mesh are presented.

B.2 Concrete

Three different batches of concrete were used in this study. First batch was for the first group of plain concrete beams. The second batch was for the second group of plain concrete beams. The third batch was for the RC beams. The plain concrete beams mix was made in the laboratory while a ready mix concrete was used for RC beams.

The curing process of plain concrete was different from the RC beams. Plain concrete beam specimens were placed in water curing tank for 28 days, whereas, the RC beams were cured by covering the beam with wet sponges or fabric. The sponges were kept wet by applying water for 28 days. All curing processes were performed under laboratory temperature of 28±3°C. The compressive strength of concrete was determined in accordance with BS EN 12390–3 (2009). Concrete cubes with dimensions of 100×100×100 mm were tested, Figure B.1 (a). Splitting tensile strength test was conducted in accordance with ASTM C496 / C496M (2011). A cylinder of 10 mm diameter and 20 mm length was used, Figure B.1 (b). The flexural strength of concrete was determined based on the guidelines presented in BS EN 12390–5 (2009). A plain concrete beam with dimensions of 100×100×500 mm was tested in four-point

bending until failure, Figure 3.1 (c). In addition, the elastic modulus of concrete was determined in accordance with ASTM C469 / C469M (2014). A concrete cylinder with dimensions of 150×300 mm was used. Figure B.2 shows the compressive stress-strain relationship of concrete up a stress of 11.3 MPa of concrete third batch used for RC beams. The concrete elastic modulus for RC beams batch was found 39 GPa. All tests were performed after 28 days. Tables B.1, B.2 and B.3 present the compressive, splitting tensile and flexural strengths of concrete mixes.

Table B.1: Concrete compressive, splitting tensile and flexural strength test results of first concrete batch (First group of plain concrete beams)

Concrete properties	28-day strength (MPa)
Compressive	44.0
Splitting tensile	3.4
Flexural	5.1

Table B.2: Concrete compressive, splitting tensile and flexural strength test results of second concrete batch (Second group of plain concrete beams)

Concrete properties	28-day strength (MPa)
Compressive	56.0
Flexural	6.8

Table B.3: Concrete compressive, splitting tensile and flexural strength test results of third concrete batch (RC beams)

Concrete properties	28-day strength (MPa)
Compressive	52.88
Splitting tensile	4.25
Flexural	5.30

(a) Compressive Test

(b) Splitting tensile test
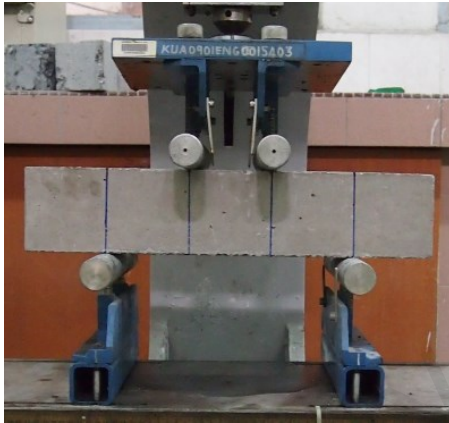
(c) Flexural test

Figure B.1: Different tests for obtaining the properties of concrete mixes
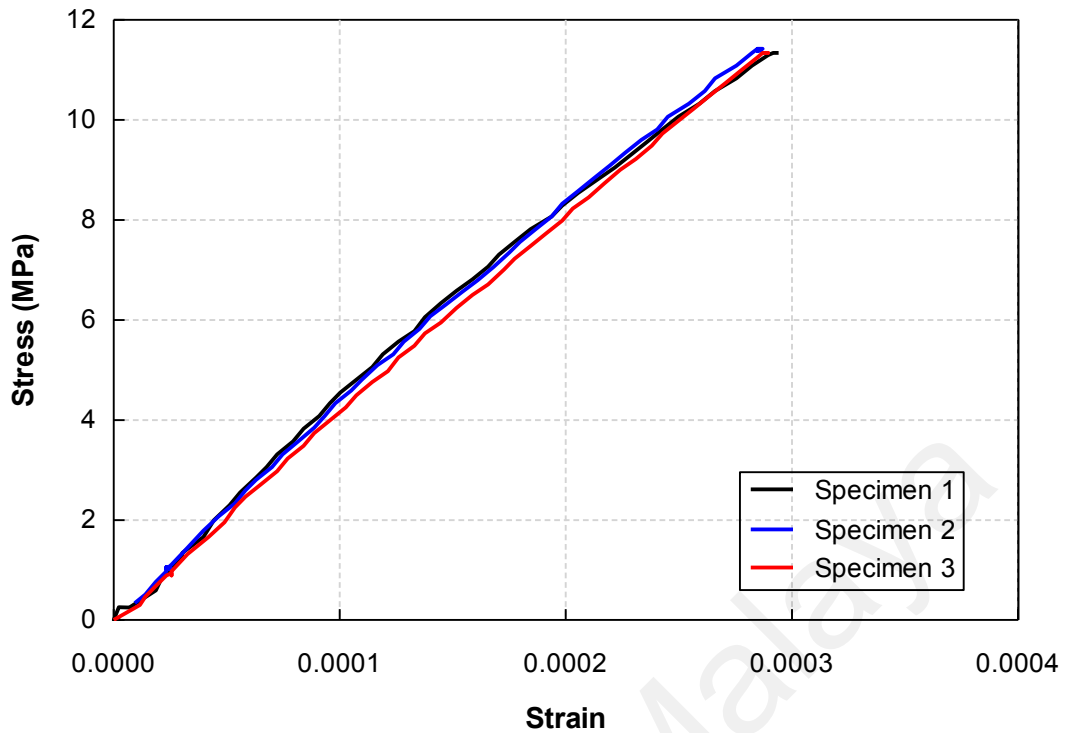
Figure B.2: Concrete compressive stress-strain relationship up to stress of 11.3 MPa for the determination of elastic modulus for the third concrete batch (RC beams)

B.3 Steel reinforcement

The tensile test of 12 mm diameter steel bars was done in accordance with ASTM A370 (2013). The specimen length and cross-sectional area were 600 mm and 113.1 mm^2, respectively. A strain gage was attached to the center of specimen for monitoring the strain during the test. Figure B.3 shows the specimen during the test. A total of three specimens were tested. In addition, Figure B.4 shows the stress-strain relationship of steel. The yield strength and strain were recorded at the point where there is no increase in the stress with the increase in strain. The average yield strength and strain are 493 MPa and 2769 micro-strain, respectively. The average elastic modulus was found 178 GPa. It should be noted that no strain values could be recorded at the ultimate stress due to the damage of strain gage after yielding. Therefore, Figure B.4 shows the stress-strain relationship up to yielding stage only.
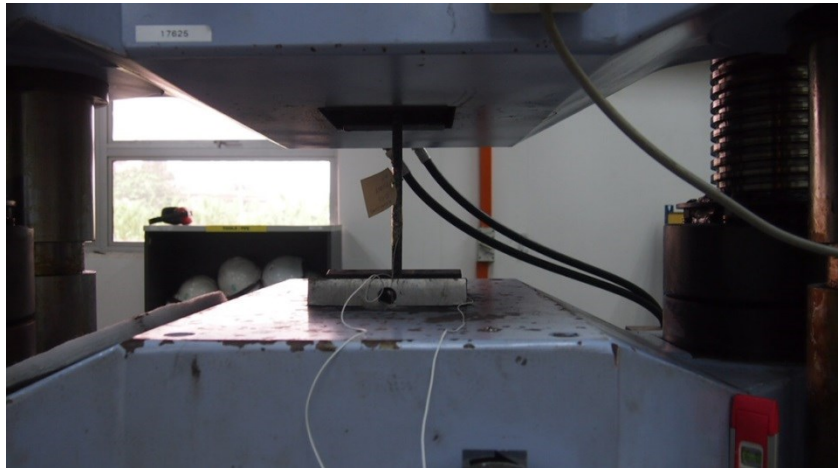
Figure B.3: Tensile test of steel bar
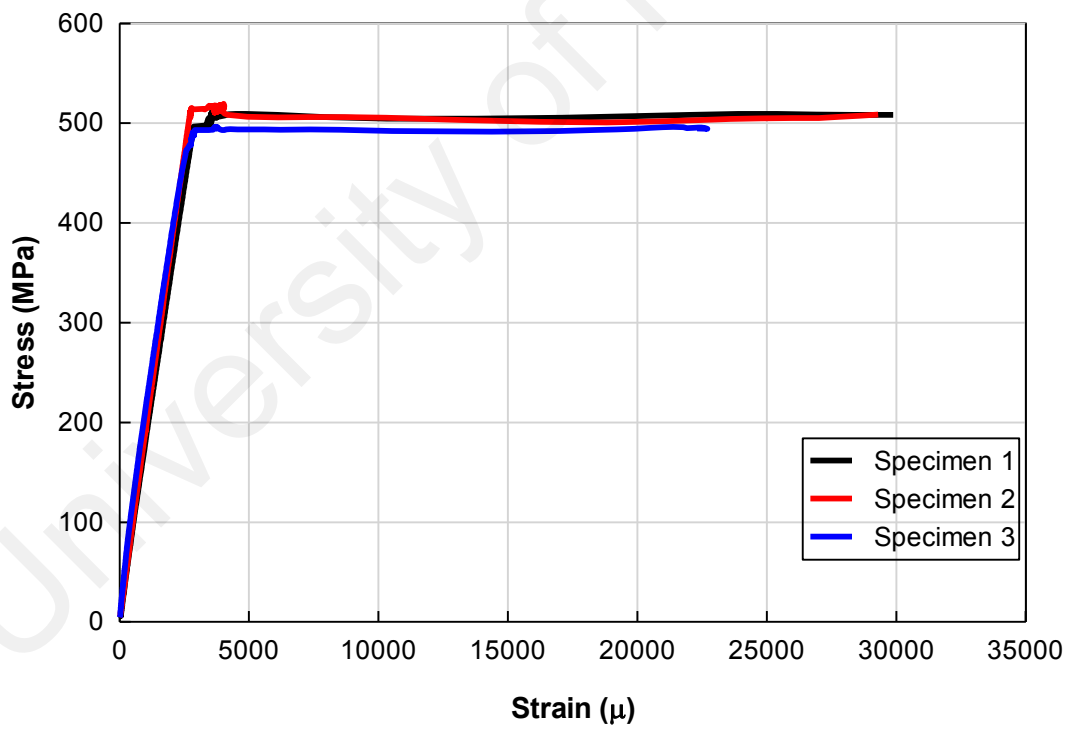
Figure B.4: Stress-strain relationship of steel bar

B.4 Welded wire mesh

Two types of wire mesh from two different suppliers were used in this study. The first type was used for the plain concrete specimens whereas the second type was used for RC beams. The wire mesh tension specimens were prepared and tested in accordance with ACI Committee 549 (1988). The specimen is a rectangular mesh with width and length of 50 and 150 mm, respectively. The gripping pads were prepared by embedding both ends in gypsum. The length of pads was 90 mm at each end of the specimen. The free portion of the wire mesh (70 mm) representing the gage length. Two LVDTs were attached on an aluminum bridge mount to record the elongation. The strain readings were obtained by dividing the recorded elongation by the gage length (70 mm) while the stresses were calculated by dividing the total load by the cross-sectional area of the wires. Figure B.5 shows the wire mesh sample during test. Three specimens were tested for each sample of wire mesh. One specimen in the first wire mesh sample failed prematurely at a location close to the gypsum pad. The average properties of the two samples of wire mesh are presented in Table B.4. Figures B. 6 and B.7 show the stress-strain relationships of wire mesh samples.

Table B.4: Mechanical properties of wire mesh

Wire mesh sample	Ultimate strength (MPa)	Yield strength (at 0.2% offset) (MPa)	Ultimate strain	Elastic modulus (GPa)
First sample	572.0	440.0	0.015	119.7
Second sample	665.0	270.4	0.012	114.2
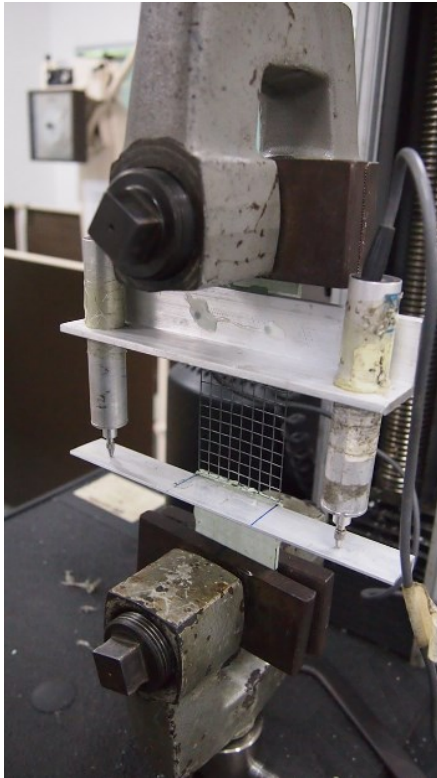
Figure B.5: Tensile test of wire mesh
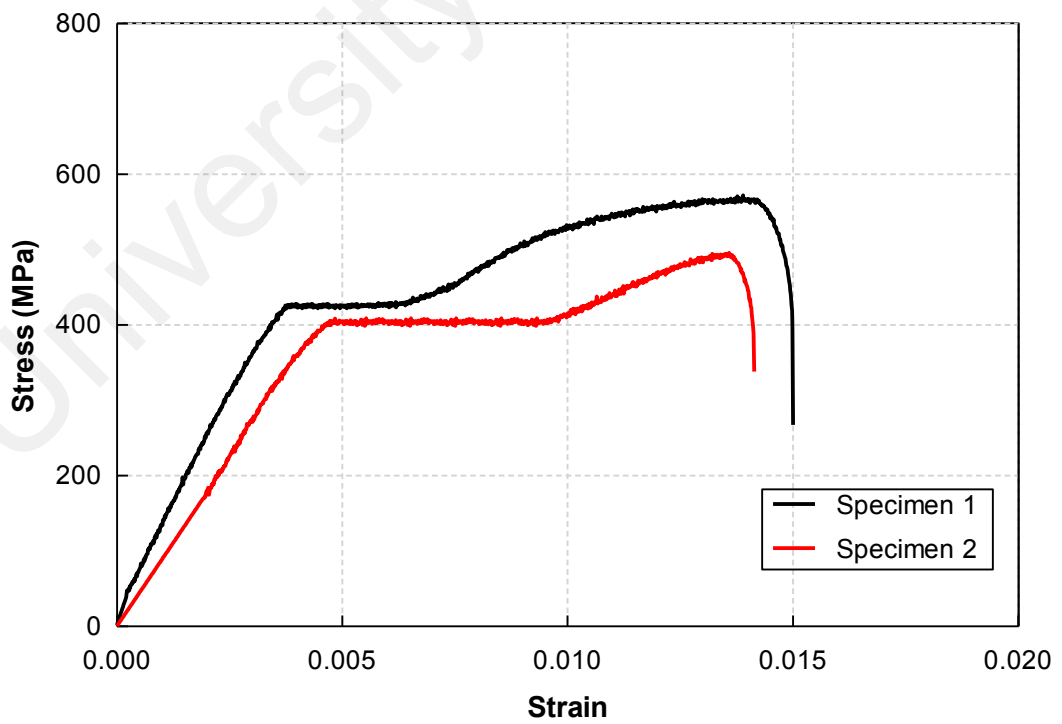
Figure B.6: Stress-strain relationship of the first sample of wire mesh
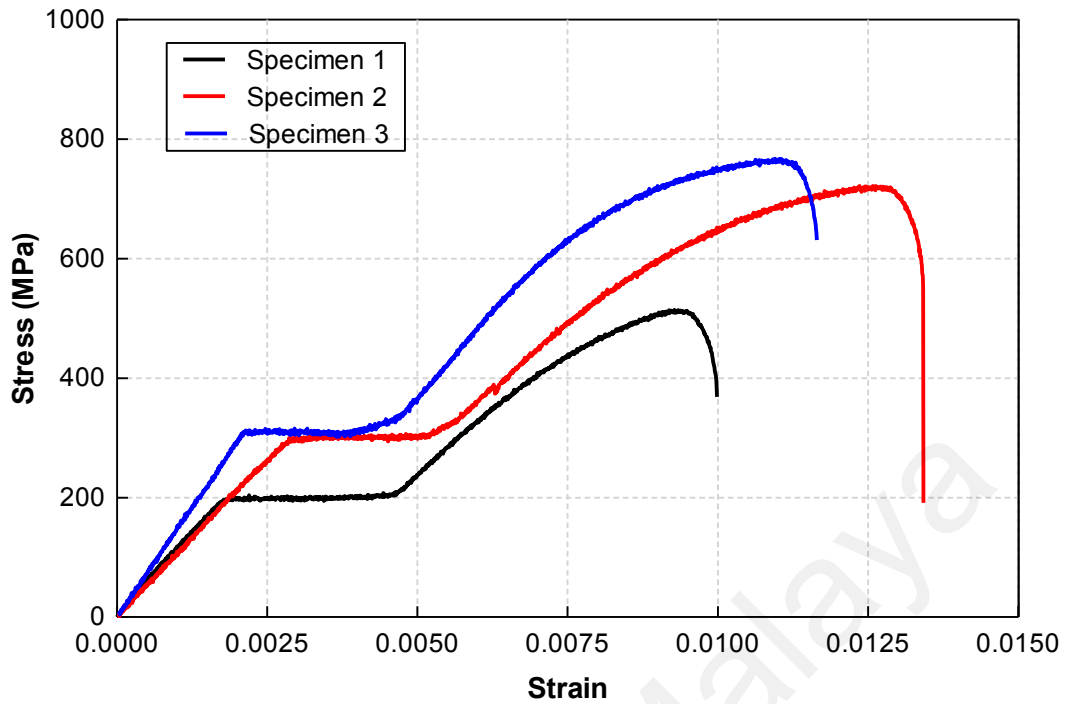
Figure B.7: Stress-strain relationship of the second sample of wire mesh

B.5 CFRP sheets

Tension test specimens were prepared and tested in accordance with ASTM D3039/D3039M (2008) and ASTM D7565/D7565M (2010). The dry CFRP sheets were cured in resin (Sikadure®-330, 2012) with an amount of 0.75 kg/m² for each layer. Two specimens were fabricated and loaded until failure. The specimens have a total length of 250 mm and width of 15 mm. The average thickness was about 0.48 mm. In order to avoid failure at grips, steel tabs were fabricated and placed at the specimens edges. The steel tabs had a thickness and length of 1.5 and 56 mm, respectively. The tabs were bonded to the sheets with the same epoxy adhesive used to cure the CFRP sheets (Sikadure®-330, 2012). The steel tabs help to introduce the load successfully through the specimen and prevent premature failure at grips due to discontinuity. A strain gage was placed at the center of specimens to record the strain in material during the test. Figure B.8 shows the CFRP specimen during the test. Slippage of steel tab was

observed in one specimen during test. Figure B.9 shows the stress-strain relationship of CFRP. In addition, the average test results of CFRP specimens and the properties of dry carbon fibres provided by the manufacturer (SikaWrap®-301 C, 2010) are presented in Table B.5. The results of specimen which had slippage of steel tabs during test were discarded. The properties of laminates were found close to the properties of dry fibres reported by the manufacturer.

Table B.5: Comparison between the test results of CFRP sheets and dry fibre mechanical properties specified by the manufacturer (SikaWrap®-301 C, 2010)

Mechanical Properties	Test	Dry fibre properties according to manufacturer
Tensile strength (MPa)	4647.2	4900
Tensile elastic modulus (GPa)	227.96	230
Ultimate strain	0.0202	0.0210

Figure B.8: Tensile test of CFRP sheet
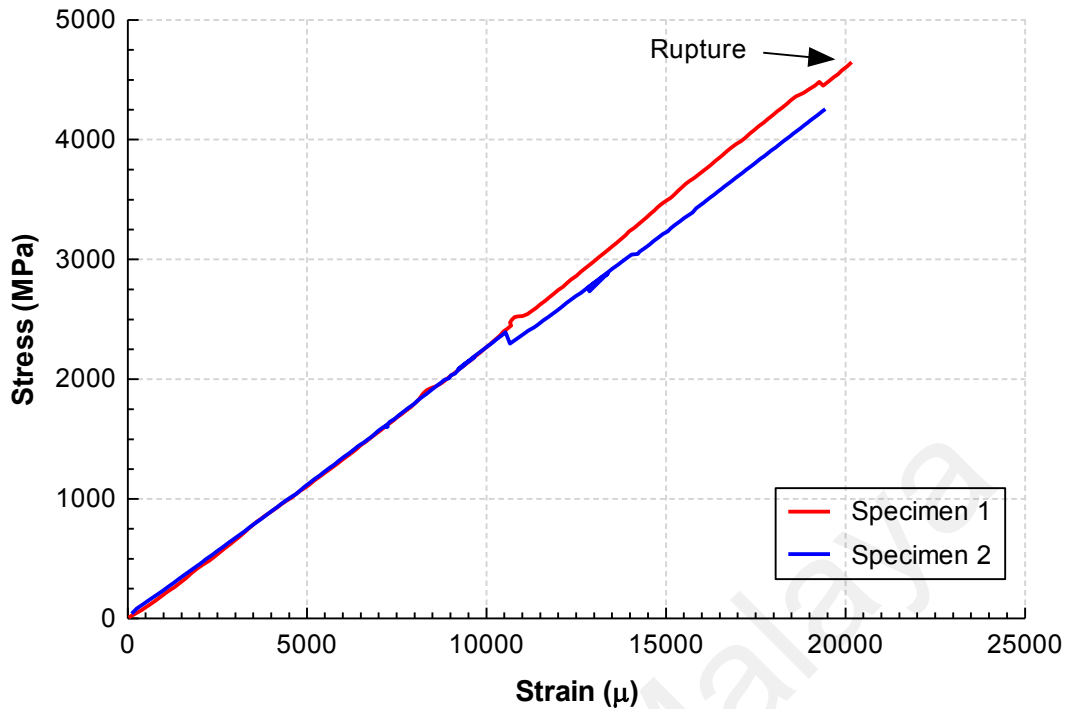
Figure B.9: Stress-strain relationship of CFRP sheet

B.6 Epoxy resin

The epoxy adhesive tension specimens were prepared in accordance with ASTM D 638 (2010). The dumbbell-shaped specimens had an overall size of 19×165 mm. The width of narrow section was 13 mm. The thickness and gage length of specimens were 7 and 57 mm, respectively. Figure B.10 shows the epoxy specimen during the test. The strain was measured by a strain gage placed at the center of the specimen. Three specimens were prepared and tested. One specimen failed at lower load due to the existence of void in the epoxy. The stress-strain relationship of epoxy is shown in Figure B.11. Table B.6 compares between the mechanical properties of epoxy obtained by test and the properties reported by the manufacturer (Sikadure®-330, 2012).

Table B.6: Comparison between the test results of epoxy resin and the properties reported by the manufacturer (Sikadure®-330, 2012)

Mechanical Properties	Test	Dry fibre properties according to manufacturer
Tensile strength (MPa)	33.5	30
Tensile elastic modulus (MPa)	4446.17	4500
Ultimate strain	0.0098	0.009

Figure B.10: Tensile test of epoxy resin
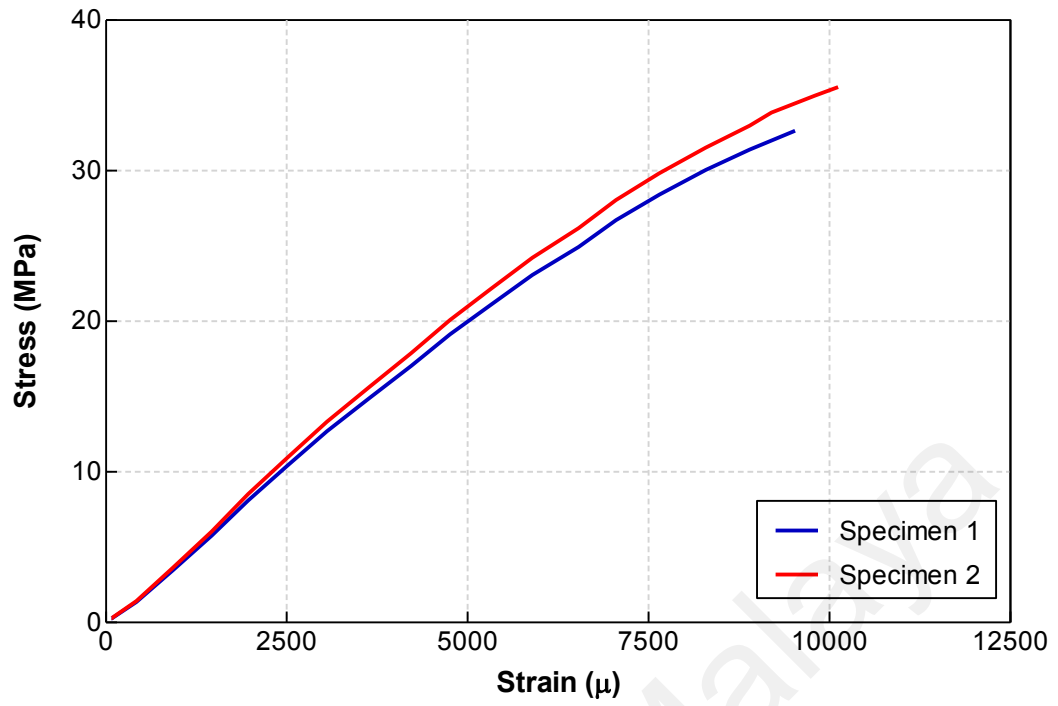
Figure B.11: Stress-strain relationship of epoxy resin

APPENDIX C

STRAINS IN STEEL, WIRE MESH-EPOXY AND CFRP OF RC BEAMS

C.1 Control beam (CB)

C.1.1 Steel
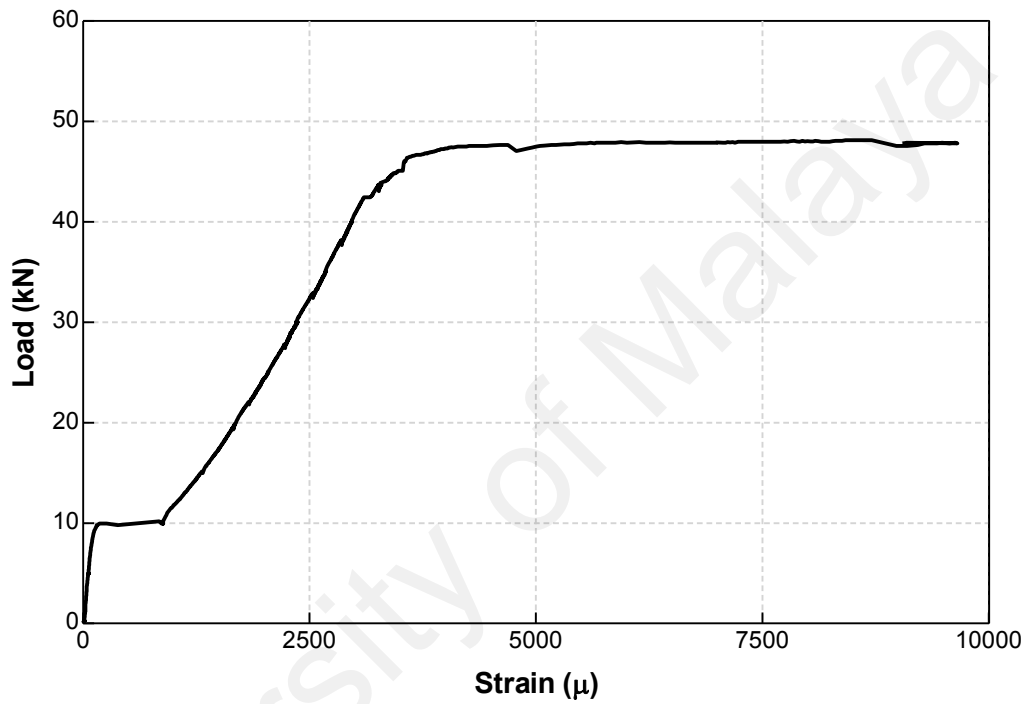
Figure C.1: Mid-span strain of steel reinforcement in control beam (CB)

C.2 Beam A1

C.2.1 Steel
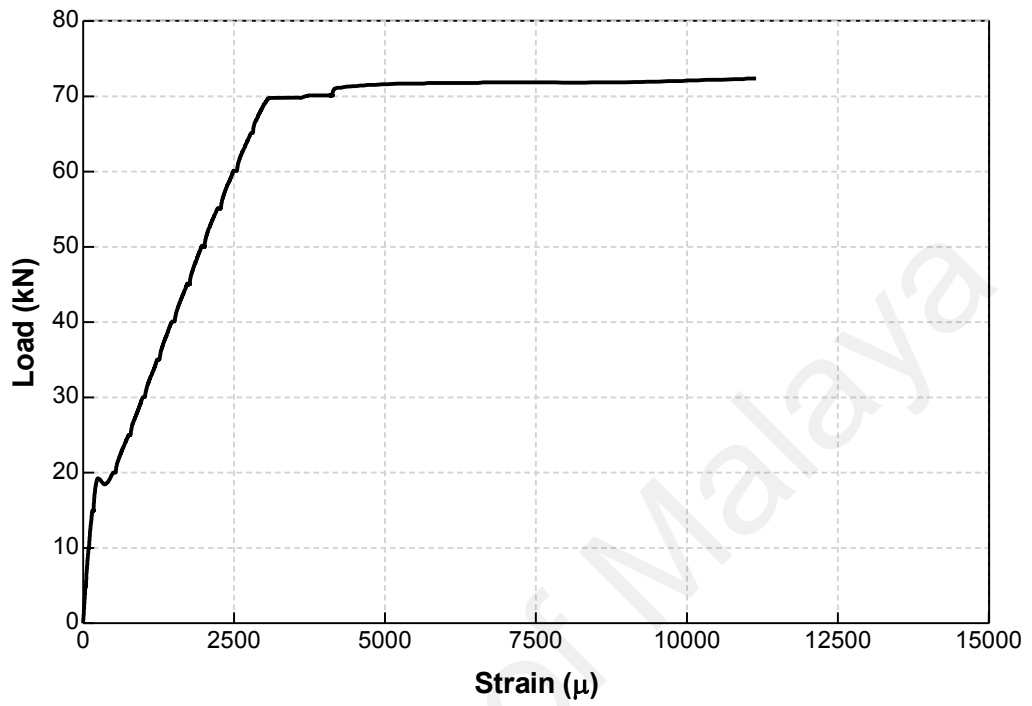
Figure C.2: Mid-span strain of steel reinforcement in beam A1

C.2.2 Wire mesh-epoxy
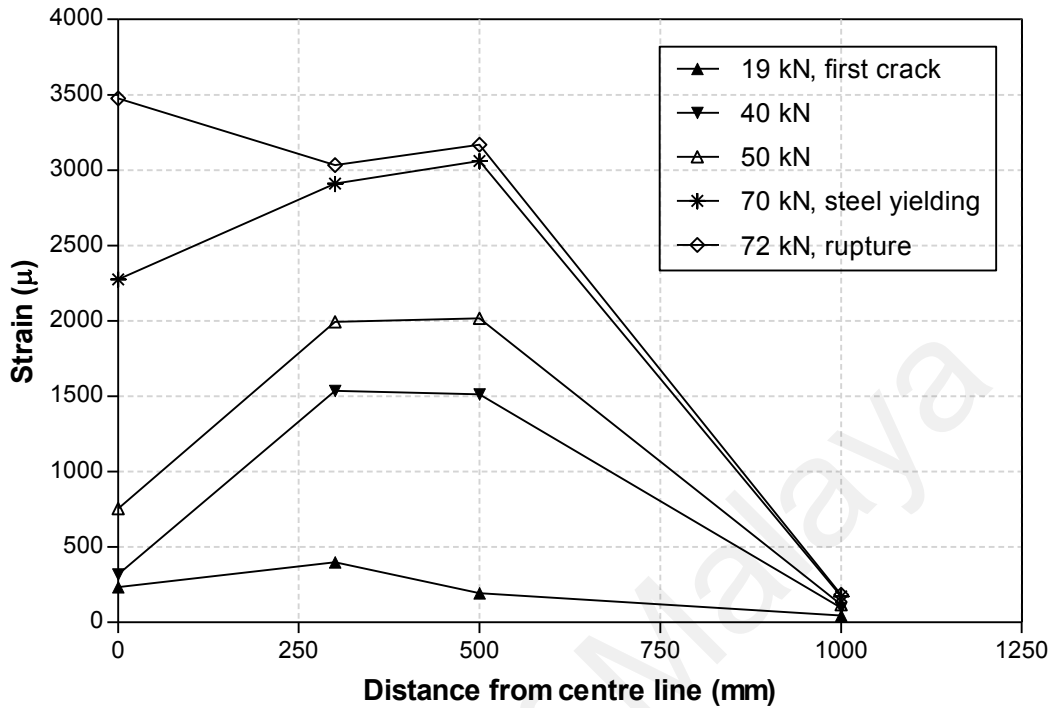
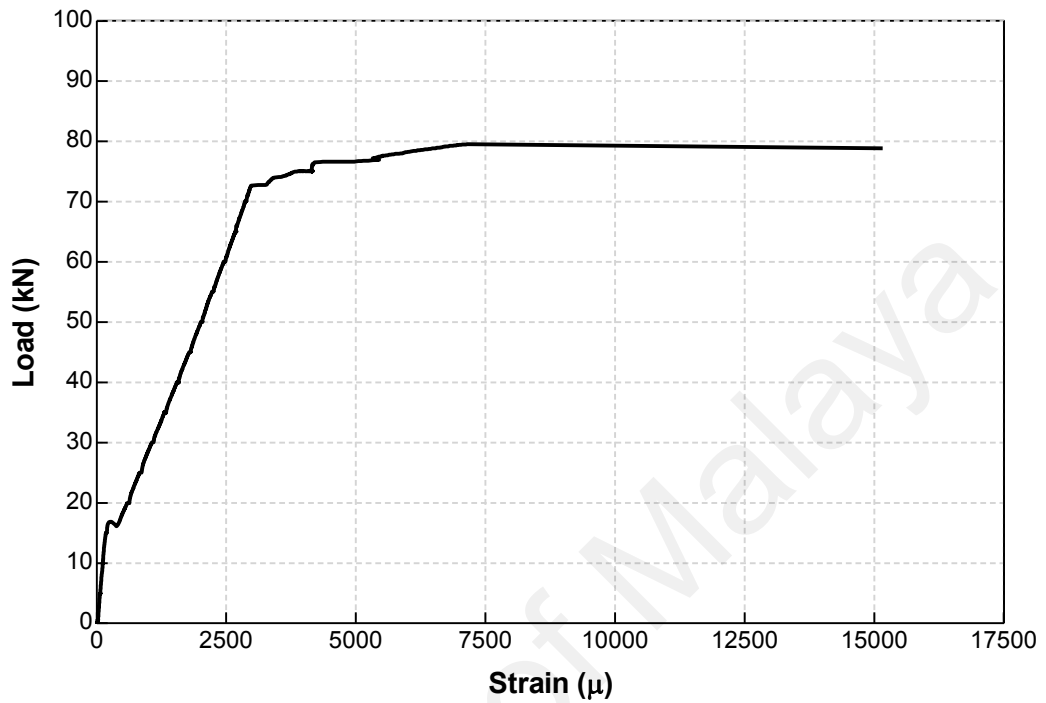Figure C.3: Strain distributions in the wire mesh-epoxy laminate at different loading stages for beam A1 (Note: Strains at the other side of beam could not be recorded due to the damage of strain gages)
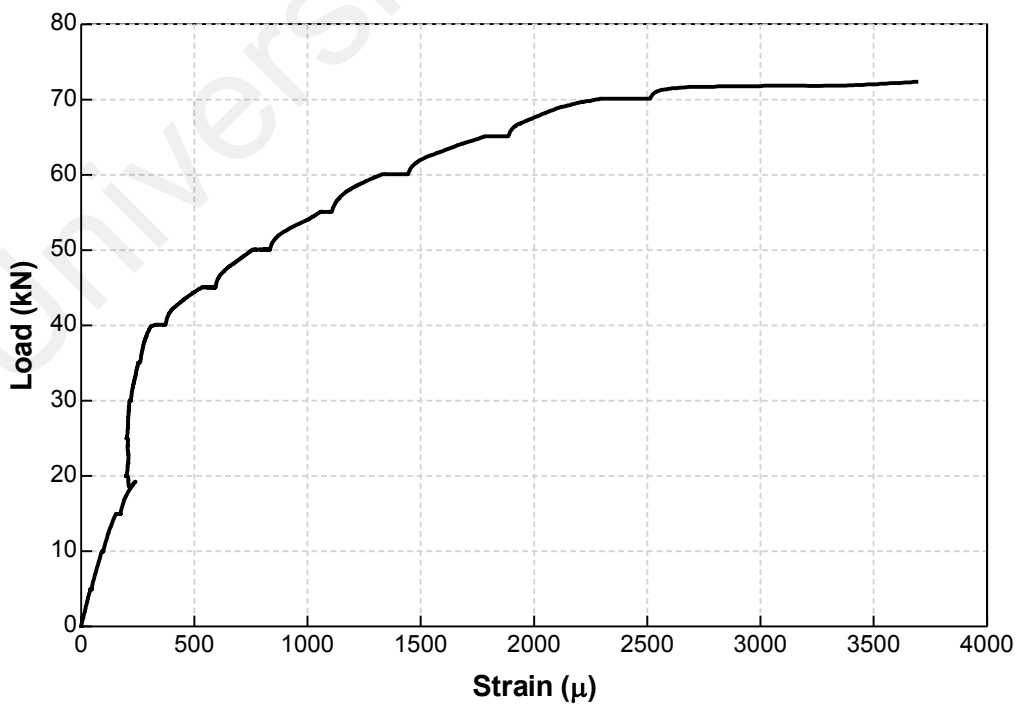
Figure C.4: Mid-span strain of wire mesh-epoxy laminate in beam A1

C.3 Beam A2

C.3.1 Steel
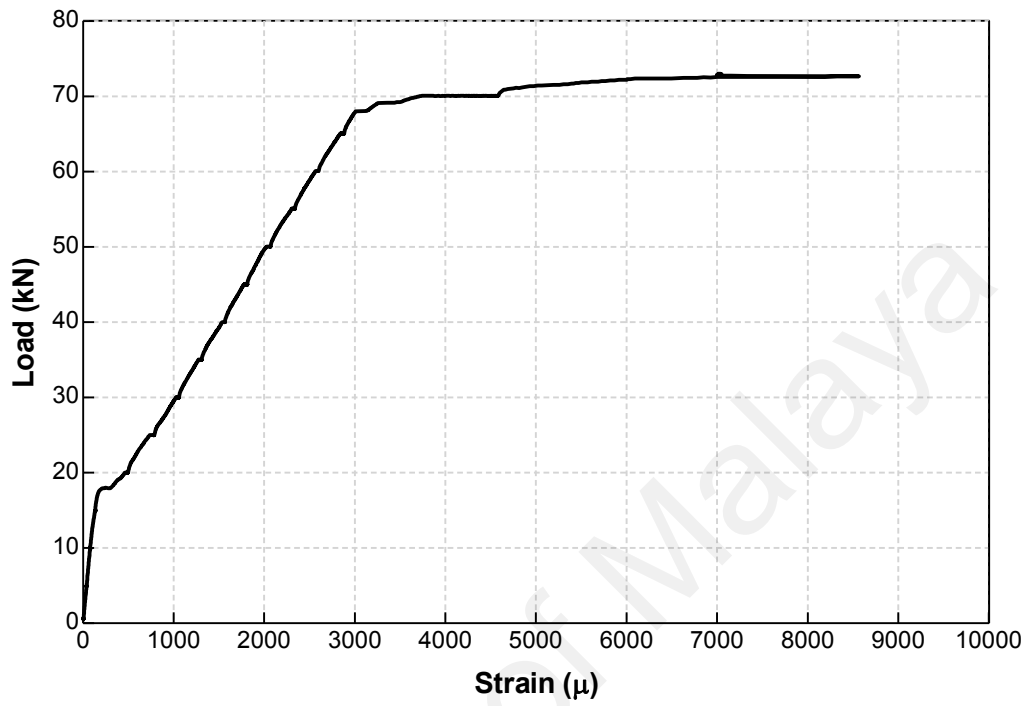
Figure C.5: Mid-span strain of steel reinforcement in beam A2

C.3.2 Wire mesh-epoxy
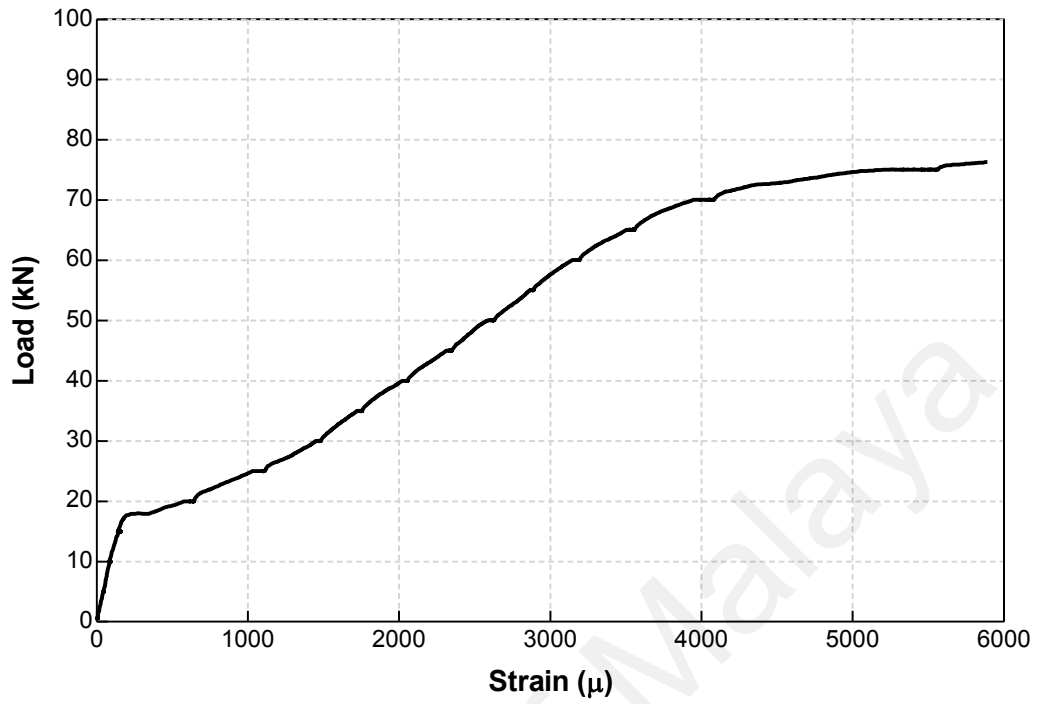
Figure C.6: Mid-span strain of wire mesh-epoxy laminate in beam A2

C.4 Beam B

C.4.1 Steel
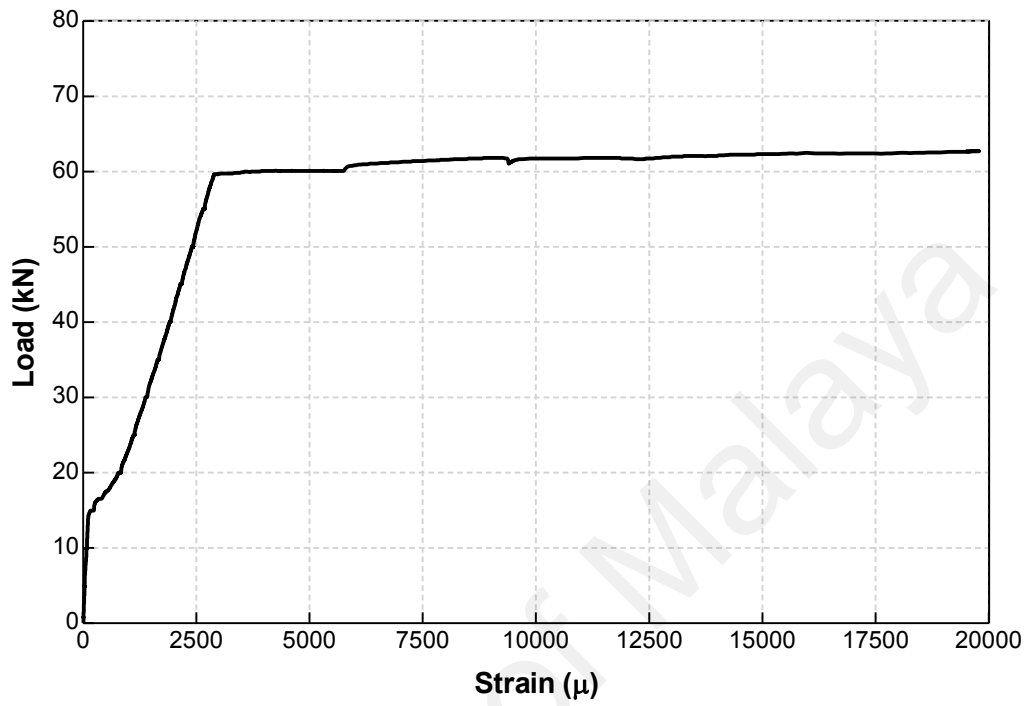
Figure C.7: Mid-span strain of steel reinforcement in beam B

C.4.2 CFRP
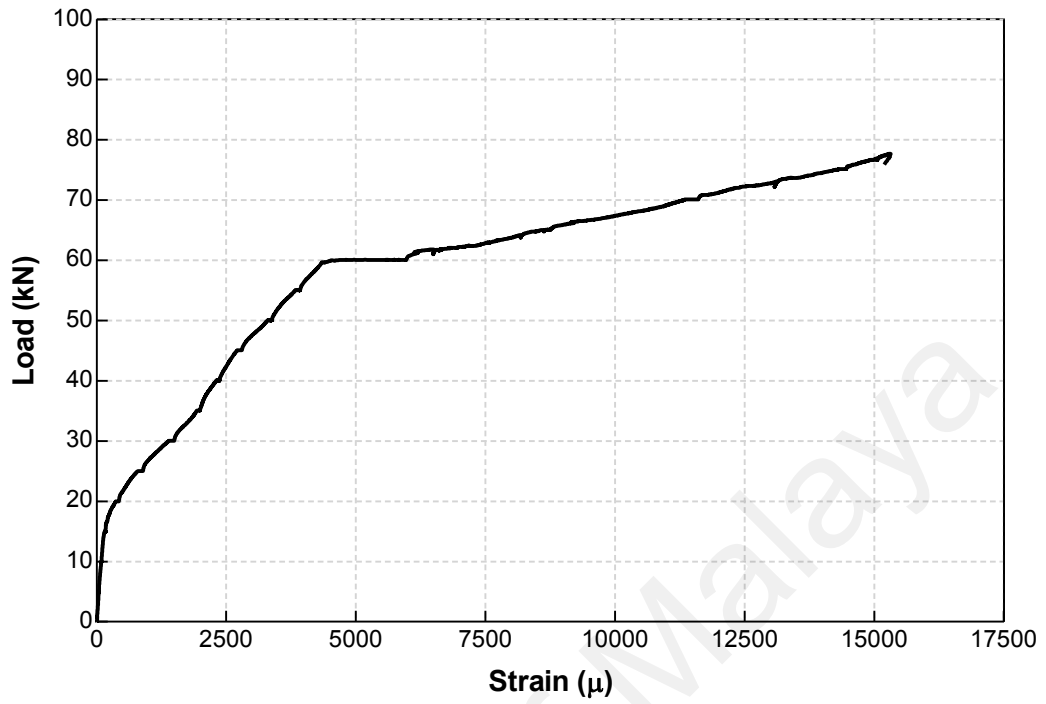
Figure C.8: Mid-span strain of CFRP sheet in beam B

C.5 Beam HY

C.5.1 Steel

Figure C.9: Mid-span strain of steel reinforcement in beam HY
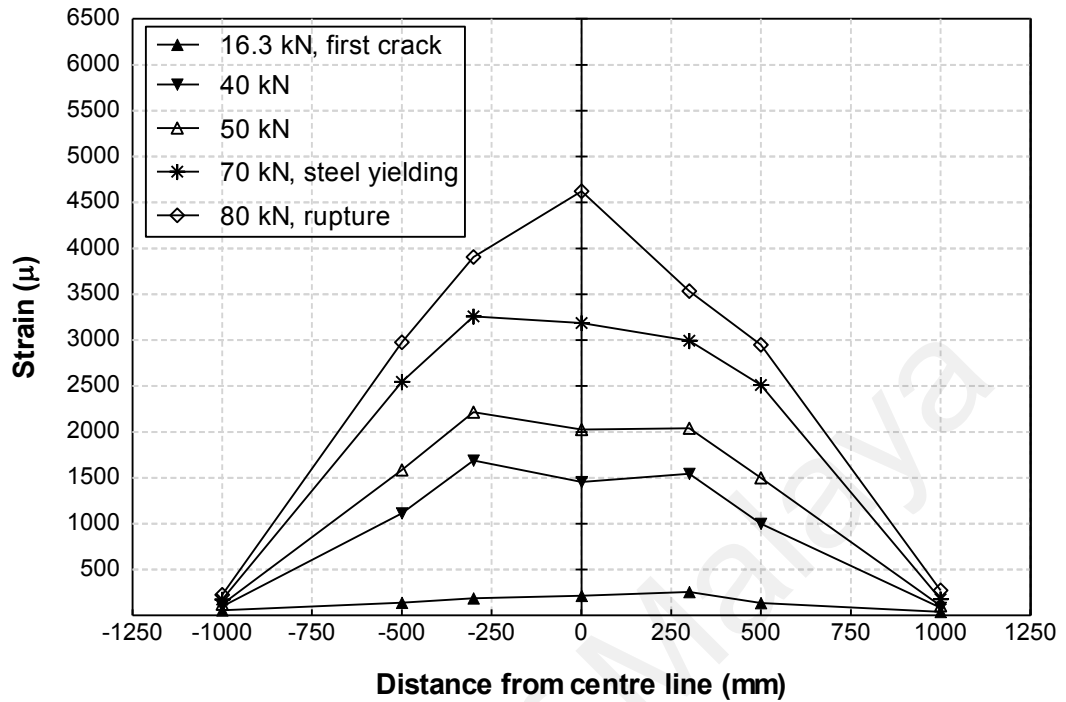
C.5.2 Wire mesh-epoxy

Figure C.10: Strain distributions in the wire mesh-epoxy laminate at different loading stages for beam HY
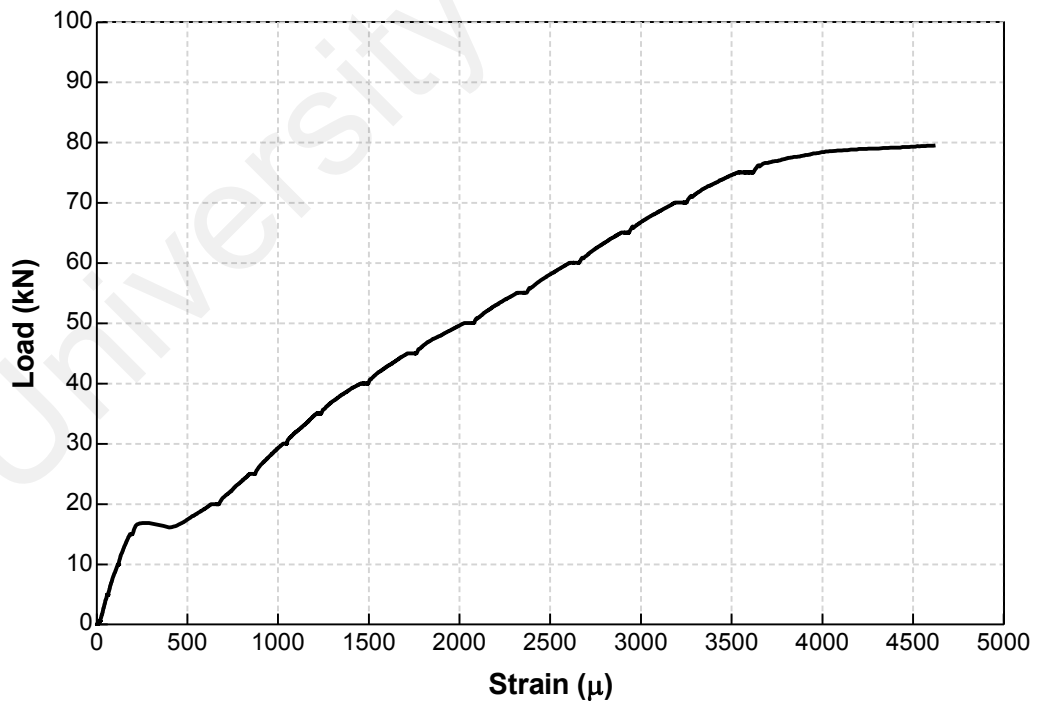

Figure C.11: Mid-span strain of wire mesh-epoxy laminate in beam HY
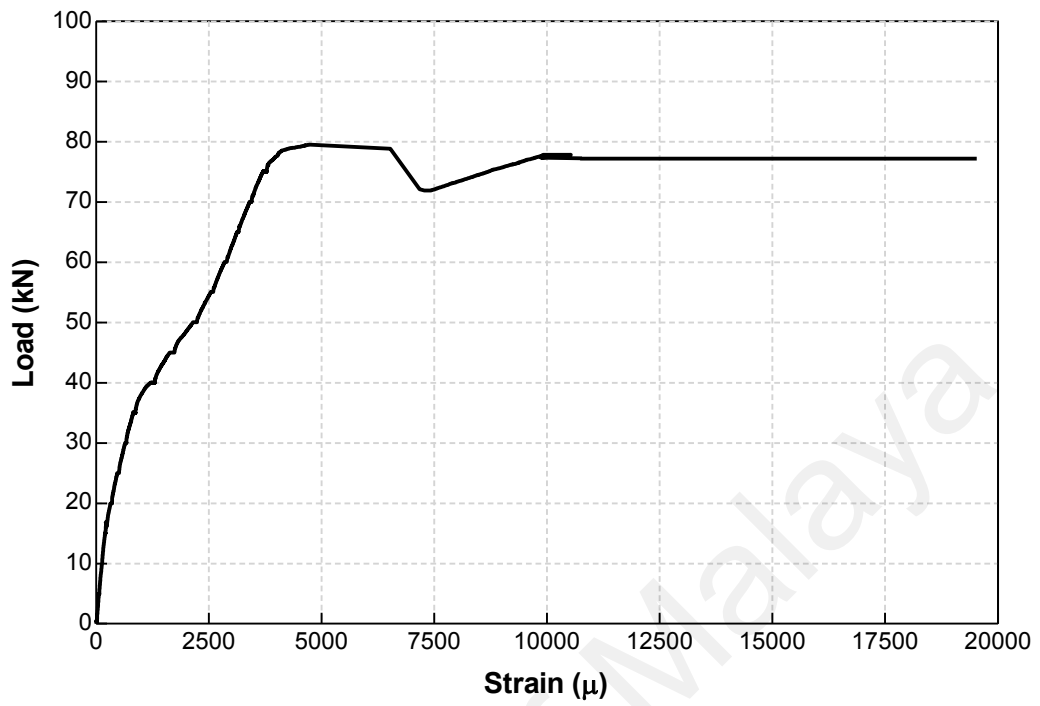
C.5.3 CFRP

Figure C.12: Mid-span strain of CFRP in beam HY